Helsinki University of Technology Publications in Materials Science and Metallurgy
Teknillisen korkeakoulun materiaalitekniikan ja metallurgian julkaisuja
Espoo 2005 TKK-MK-163

MASS SPECTROMETRIC STUDY OF VOLATILE COMPONENTS IN MOULD POWDERS

Doctoral Thesis

Andrei Chilov

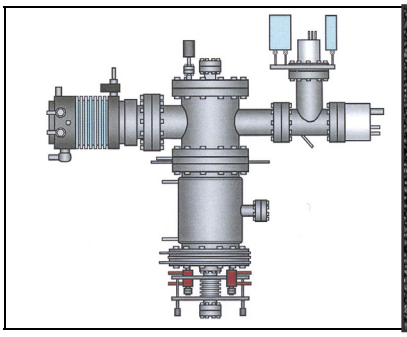
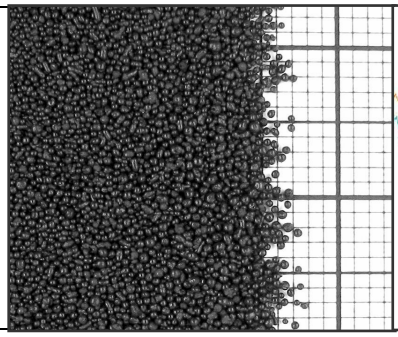
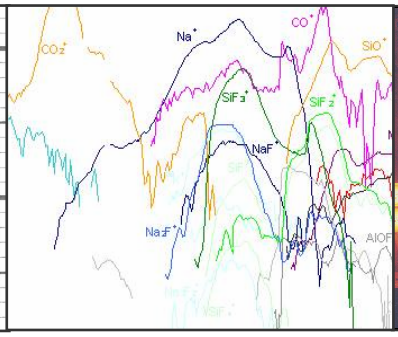

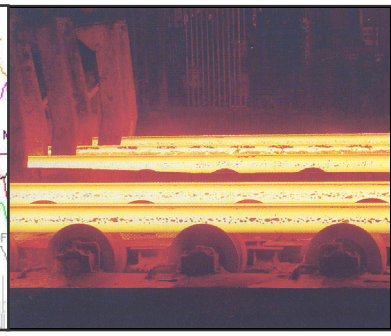

TEKNILLINEN KORKEAKOULU
TEKNISKA HÖGSKOLAN
HELSINKI UNIVERSITY OF TECHNOLOGY
TECHNISCHE UNIVERSITÄT HELSINKI
UNIVERSITE DE TECHNOLOGIE D'HELSINKI

Helsinki University of Technology Publications in Materials Science and Metallurgy

Teknillisen korkeakoulun materiaalitekniikan ja metallurgian julkaisuja

Espoo 2005 TKK-MK-163

MASS SPECTROMETRIC STUDY OF VOLATILE COMPONENTS IN MOULD POWDERS

Andrei Chilov

Dissertation for the degree of Doctor of Science in Technology to be presented with due permission of the Department of Materials Science and Engineering for public examination and debate in Auditorium V1 at Helsinki University of Technology (Espoo, Finland) on the 28th of January, 2005, at 12 noon.

Helsinki University of Technology

Department of Materials Science and Engineering

Laboratory of Metallurgy

Teknillinen korkeakoulu

Materiaalitekniikan osasto

Metallurgian laboratorio

Helsinki University of Technology
Laboratory of Metallurgy
P.O. Box 6200
FIN-02015 TKK, Finland

Available in pdf-format at http://lib.hut.fi/Diss/

Cover: Fig. 1: Vacuum system of the apparatus, Fig. 2: Mould granules on a millimiter scale, Fig. 3: Vaporisation curves of a mould powder, Fig. 4: Steel strands cooling down.

ISBN 951-22-7311-X
ISBN 951-22-7327-6 (electronic)
ISSN 1455-2329

Picaset Oy
Helsinki 2005

ABSTRACT

The mass spectrometric Knudsen effusion method was applied for the study of vaporization processes of mould powders. All measurements were performed in vacuum conditions in the temperature range between 100 and 1550°C, the standard rate of temperature elevation being 100°C/hour. Mould powders were selected from those used in continuous casting at Saarstahl AG (Völklingen, Germany) to represent the variety of types and compositions. In addition to SiO_2, CaO, Al_2O_3 and MgO they contained 0.4-14.3 wt% Na_2O, 0.3-1.0 wt% K_2O, 0.1-3.6 wt% Fe_2O_3, 2.6-7.6 wt% fluorine and 3.4-9.1 wt% carbon.

With such complex mixtures as mould powders only a half-quantitative analysis of vaporization curves could be carried out. Mass spectra were interpreted with the help of isotopic abundance ratios and equilibrium constants for the gas phase components. Hence, they were not deciphered in full and the main results are given as time/temperature dependences of ion currents.

The results confirm that fluorides dominate in the gas phase. Vaporization (sublimation) occurs mainly in the form of NaF, Na_2F_2, KF, SiF_4 and CaF_2, while gaseous AlF_3, MgF_2, AlOF are generated in smaller amounts and depend on the slag composition. Yet, in the given experimental conditions, the gas phase was found to be richer in molecular species than found previously. Analysis of the NaF/Na_2F_2 ratio proved the existence of Na(g). Some components of the mass spectra indicate the presence of significant amounts of SiF_2 and SiO in the vapour. The relative intensities of Mg^+ and MgF^+ ion currents suggest that Mg in vapour is present in the form of Mg(g) and its fluorides. The extra gaseous components observed in this study could be explained by the presence of carbon in the samples. This was confirmed by comparison with the vapour phase composition of the decarburised sample of a mould powder. CO could be registered in the vapour up to temperatures 1400-1500°C. In the temperature interval between 100 and 600°C, the gas phase was formed by H_2O and CO_2. In addition, numerous ion currents of small intensities were recorded between 100 and 450°C but their origin remained unclear. They were attributed to impurities, though some of them may have included components of the assay, such as K_2O or Na_2O. HF(g) could not be detected in the vapour.

The thesis is partly based on the work done within the European Coal and Steel Community Project concerning emissions of hazardous substances (the data related to pre-melted slags, fluorine free mixtures, Li_2O substituted compositions).

Keywords: mould powders, continuous casting, gaseous emissions, mass spectrometry, Knudsen method.

PREFACE

The work was carried out in the Laboratory of Metallurgy, Helsinki University of Technology, during the years 1998-2004. This has been, for the most part, within the framework of the European Coal and Steel Community Project.

I would like to express my sincere gratitude to my supervisor, Professor Lauri Holappa, for giving me an opportunity to work under his expert guidance, always encouraging, for his endless patience and confidence in my success.

I am deeply thankful to Dr. Erkki Heikinheimo whose profound expertise in various hardware matters and constant readiness to promote and speedup any innovation, have guaranteed that the present - purely experimental - work has been successfully concluded.

It is also my pleasure to thank all the staff of the Laboratory of Metallurgy for their co-operation. The working atmosphere has always been a comfortable combination of friendly help, with a wide discretion to act.

The study was initiated as a part of the project coordinated by the ECSC. Its financial support is gratefully acknowledged herein. Special thanks go to the project partners. Our meetings and discussions took place throughout the course of the work programme and the partners' results are repeatedly cited in this thesis.

Finally, I must pay tribute to Dr. V.L. Stolyarova, my former supervisor, under whose guidance I mastered the basics of mass spectrometry and the experimental method of thermodynamics, which served as the foundation of the present study.

The full range of problems related to the subject of this study is limitless indeed. However, at some point a limiting line had to be drawn. Hopefully, the work will contribute to the better understanding of the chemistry of processes in the mould slag layer and will be of use and interest to other researchers and practitioners in this field.

Espoo, 30th December 2004

Andrei Chilov

CONTENTS

1 INTRODUCTION

1.1 Mould fluxes in continuous casting and their development

Continuous casting is based on quite simple ideas, yet decades had to pass until it started to dominate in industrial practice. It took time to formulate the requirements to the key elements of the technology in order to make a caster work smoothly, yielding high-quality product. In earlier years, its development relied essentially on practical experience, but as continuous casting attained a degree of perfection, further progress demanded deeper understanding of the mechanisms underlying the process. Phenomena occurring in the mould of a caster are among the most intricate and interrelated ones, so it is no surprise that a lot of reported studies /1-24/, especially by Japanese workers, are devoted to the role and characteristics of mould fluxes or widely refer to their properties. Achievements of the last twenty years of extensive research were cautiously summarised by Mills /17/: from 'black magic' to the scientific approach. The knowledge hitherto accumulated provides a rational background for the selection and improvement of mould fluxes, and suggests some criteria for assessment of innovative ideas.

Fluxes serve to lubricate the mould, protect the meniscus from oxidation, provide its thermal insulation, moderate heat transfer to the mould and absorb inclusions. Accordingly, manufacturers and researchers are interested primarily in the properties directly related to these five functions, that is, viscosity, melting behaviour, crystallisation etc., and their correlation with the operational parameters: casting speed, strand size, steel grade and oscillation pattern. Other factors are less important and have a somewhat subordinate role. One such secondary issue is the transition of the mould powder components to the gas phase during heating. No general scheme of this process has been proposed yet, though some aspects of the gas emission problem were investigated in detail. Decomposition of carbonates and carbon oxidation, formation of gaseous fluorides and modification of flux composition through evaporation are either skipped or regarded in separate contexts. In a comprehensive review of mould fluxes by Pinheiro, Samarasekera and Brimacombe /8/, for example, effects of vaporisation are not discussed at all. Nevertheless, gas formation is an indispensable feature of the operation of mould powders and obviously needs more thorough understanding.

Typical commercial mould fluxes are composed of CaO, SiO_2 and Al_2O_3 with additions of alkali oxides, fluorides and carbon. A major part of R&D deals with these 'standard' fluxes, but efforts to devise other, more radical, innovations are also found in the literature. An example are non-oxidizing fluxes for cleaner steel production proposed by Hammerschmidt and Janke /25/. By comparing free energies of formation of different metal oxides, the authors pointed out and eliminated those, which could promote reoxidation in steel (SiO_2 and alkali oxides). By addition of some extra constituents (SrO and some fluorides), in appropriate concentrations, the properties of such fluxes could be adjusted to satisfy the principal requirements of continuous casting. However, the content of fluorides in these compositions, including the very poisonous NaF and LiF, was about twice that of standard fluxes. Thus, referring again to the broad expertise of Mills /17/, great care must be taken with any crucial breach of standards: existing conventional mould fluxes are rather well balanced compositions.

1.2 Reduction of fluorine content

Fluorides have the best performance as fluxing agents in slags, but are undesirable from the environmental point of view: (i) they are easily evaporated from slags, producing health-injurious gaseous substances; (ii) they cause increased wear of refractories and corrosion of machinery; (iii) they create problems of storage and utilization of the solid waste. Typical compositions of mould powders at present include 4-10% fluorine, motivating steady interest in the methods and the implications of reduction of fluorine content.

As a development of the ideas put forward in /25/, D. Janke *et al* /26/ tried to solve this problem by introducing 'non-oxidizing' oxides into fluxes. It was assumed that Li_2O or SrO could effectively regulate viscosity and melting behaviour, so that their complete or partial substitution for CaF_2 and Na_2O retains mould flux performance within acceptable limits. At the same time, contamination of the atmosphere by fluorides would be noticeably lower, first of all as a result of the elimination of sodium fluoride emissions. This is particularly important because NaF evolves first and is more environmentally hazardous compared to other fluorides.

The wide-ranging study devoted to this problem was performed within the European Steel and Coal Community project (Report EUR 20645 EN) in 1998-2001 /26/. A large part of the work dealt with the properties of commercial powders because some reference background for further investigations had to be created. The research programme included the experimental determination of viscosity, the melting behaviour and volatile properties of several industrial powders, fluorine free mixtures, mixtures with partial substitution of fluorspar (CaF_2) by lithium oxide and tests of the effect of pre-melting on the volatility of mould powders. The closely related problem of cutting down fluorine content in tundish slags was also worked out. The results were promising concerning the evaporation of fluorides. It was concluded, that the proposed scheme of substitution allows to reduce it considerably, though the impact of this dramatic compositional change on other mould flux characteristics was found to be too strong to allow any immediate industrial trials.

Experiments confirmed that fluorine evolves from the condensed phase mainly in the form of gaseous NaF, SiF_4, AlF_3 and CaF_2. New significant features were also established. It was found, for example, that Na may be present in the vapour in atomic form, while in earlier reports /28-30/ sodium was attributed wholly to NaF(g), that SiF_2 dominates over SiF_4 at high temperatures, and that carbon and carbonates must be taken into consideration. And yet, quantitative assessment of mass loss is not well proven with the presently available data, even for the idealized case of laboratory experiments. It is clear, that better understanding of the sublimation processes and more accurate data are needed.

Application of the mass spectrometric Knudsen effusion method, despite its obvious limitations and drawbacks, provides the most detailed information. It should be mentioned, that the part of the project /26/ concerning the gas phase studies was not just a matter of routine measurements. The specific character of the experimental method demanded investigations on a rather broad basis, because the simple inspection of several selected vapour species did not suffice. Consequently, the results are not limited to fluoride emissions and in some aspects may have general interest, irrespective of the project purpose.

Gas phase studies reported in /26/ were then re-evaluated and summarized in the following general conclusions: (i) the mass spectrometric effusion method has only a limited applicability for direct evaluation of gaseous emissions in the caster, but

can improve significantly the understanding of vaporisation processes of mould powders; (ii) the collected data are not full; (iii) the employed experimental facilities placed limits on further advance in data acquisition. With these considerations the work was continued.

1.3 The aim of the study

The aims were:

- To evaluate the existing data related to vaporisation of mould powders and the potential of mass spectrometric effusion method for further advance of these studies
- To modify the existing experimental equipment in a way most beneficial for the investigation of the volatility of mould powders
- To obtain a consistent and complete set of experimental data representing the gas phase components above mould powders at high temperatures
- To verify the idea of reduction of emission of gaseous fluorides by partial substitution of fluorine-containing components of mould powders by lithium oxide
- To establish the effect of preliminary melting of mould powders on their volatility and evolution of gaseous fluorides
- Taking as a basis the acquired data to characterize the emission of fluorides by mould powders observed in the laboratory experiments and the possibilities of their reduction.

2 GAS EVOLUTION IN MOULD

Mould fluxes undergo certain changes that are accompanied by the generation of gaseous products through the whole operation cycle in a caster. Gas emissions may be a result of heating and reaction with oxygen and moisture in the air. The greater part of gaseous emissions is produced above the meniscus during mould powder melting. Direct investigation of gas phase above or inside the powder layer in the mould is a difficult problem that has not been solved to date. The results found in the literature refer to separate features of the process such as carbon oxidation, decomposition of carbonates and formation of gaseous fluorides. Some papers on thermodynamic properties of oxide-fluoride systems also contain data referring to the sublimation process of mould fluxes.

2.1 Mould powders composition

Mould powders (MP) are the solid materials added to continuous casting moulds; mould fluxes are liquid and the result of melting of a mould powder. Confusion in terminology often occurs /10/, but in the present work it is not very important because the formation of the glass phase in the melt is not discussed. For simplicity both will be generally referred to hereafter as ‘mould powders’ or ‘mould granules’ (the powders shaped into globular particles typically 0.2-0.7 mm in diameter).

The functions of mould powders in a continuous caster are:

- Lubrication between the strand and the mould
- Moderation of heat transfer from strand to mould
- Thermal insulation of the flux pool
- Protection of liquid steel from reoxidation
- Absorption of inclusions from the metal.

Mould powders must firstly comply with these basic functions and also to meet additional requirements, such as easy feed, low costs and environmental safety. Optimal mould powder properties depend on a particular steel grade and set of operational variables of a caster and this is the reason why so many types of powders have been designed. Composition of presently used commercial mould powders are given in Table 2.1 and Fig. 2.1.

Table 2.1 Typical composition ranges for mould fluxes, wt% /8/.

CaO	SiO_2	Al_2O_3	TiO_2	Na_2O	K_2O	FeO	MgO	MnO	BaO	Li_2O	B_2O_3	C	F
25-45	20-50	0-10	0-5	1-20	0-5	0-5	0-10	0-10	0-10	0-4	0-10	1-25	4-10

In most cases the compositions are given by a supplier only in terms of oxides, fluorides, total carbon and free carbon. Mineralogical analysis needs separate research, which provides mostly qualitative results. An example is given in Table 2.2. Before the analysis the powders were decarburised by heating in air for 2h at 700°C. Thus, ‘as received’ samples initially could contain some additional phases, but even the complexity of the composition seen in the table suggests that sublimation processes may differ greatly for different powders. This non-uniformity poses a problem of planning experiments in gas phase studies: what compositions and how many to choose as a typical and representative ones.

The index of basicity CaO/SiO_2, is most commonly used for classification of mould powders. Mills /1/ proposed to represent their compositions as coordinates in a 'SiO_2'-'CaO'-'NaF' triangle. According to their role in the flux as network formers or network breakers oxides were accounted as 'SiO_2' (SiO_2, Al_2O_3, TiO_2) or 'CaO' (CaO, MgO, FeO, MnO). Fluorite and alkali oxides were included, then as products of reaction of NaF formation.

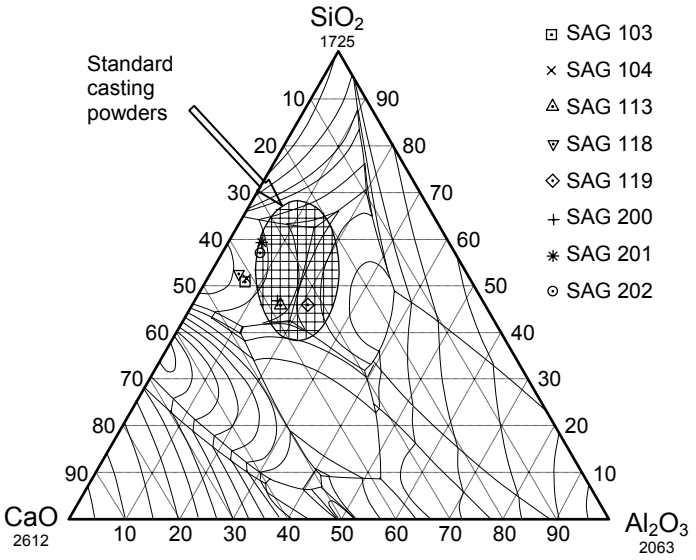

Fig. 2.1 Compositions of investigated mould powders and those typically used

The scheme was found to be well-proven for the characterisation of viscosity of fluxes. It may also be useful for prediction of their vaporization behaviour. In the papers on fluorine emissions /31, 32/ partial pressures of gaseous SiF_4, NaF, AlF_3 and other fluorides are directly correlated to the index of basicity. Strictly speaking, these results refer only to molten fluxes. In the mould of a caster the conditions are not so simple. A lot of gaseous species are already evolved below the melting point of a powder, when it still remains a mixture of solid components. A variety of kinetic effects involving the phases given in Table 2.2 may result in evaporation processes that are not well correlated with the basicity index. The more so, that it is not easy to estimate the change of its value during decomposition of carbonates and formation of alkali oxides and fluorides without additional investigation or assumptions.

Fig. 2.2 illustrates the mould powder performance. A portion of MP fed into the mould at ambient temperature gradually descends to the molten steel surface undergoing different physico-chemical transformations and finally infiltrates into the gap between the mould and the strand. The whole cycle lasts 3-5 min depending on the operational parameters. The processes related to the gas phase are:

- Evaporation of water that may be present in the powder
- Multiplex reactions involving carbon and carbonates
- Reactions between oxide and fluoride components of the powder
- Vaporisation of components of the liquid slag pool

Table 2.2 Chemical and mineralogical composition of mould powders (arbitrary denomination) studied in /2/

Powder	A	C	K	P	Q	T	U	BL	BLA	CB
Chemical composition, wt %										
SiO_2	33.6	35	27.3	35.5	36.7	28	30.6	29.0	28.0	31.5
CaO	35	34	28.7	35.3	35.5	34	34.3	29.0	23.5	33.5
Al_2O_3	2.7	7.5	8.7	6.0	1.6	5	8.1	12.5	13.0	6.5
MgO	4.9	0.6	0.9	0.9	1.1	0.5	0.6	…	…	…
Na_2O	9.7	3.2	14.2	5.1	7.5	6	2.8	4.5	5.0	4.5
K_2O	0.5	0.1	0.7	0.1	0.3	1	1.1	…	…	…
F	5.5	3.6	6.8	5.4	1.4	6	4.3	2.0	5.0	5.3
Fe_2O_3	3.9	0.2	0.9	1.1	0.6	2	0.7	4.8	4.5	0.5
MnO	0.1	0	0	0	0	5	0	…	…	…
Free C	3.9	5.5	…	4.5	4.1	5.4	…	16	18.5	8.2
Phases present in decarburised casting powders *)										
C_3S_2Fl	+	+	+	+		+	+	+	+	+
NAS_2	+		+					+		
CS		+		+	+		+	+		+
C_2AS					?			+		
NC_4S_6H	+			+	+					+
NCS_3	+	+					+			?
NaF			+							
Unknown			1			2		4	6	8

*) $A=Al_2O_3$; C=CaO; $Fl=CaF_2$; $N=Na_2O$; $S=SiO_2$; $H=H_2O$; ? denotes uncertain detection.

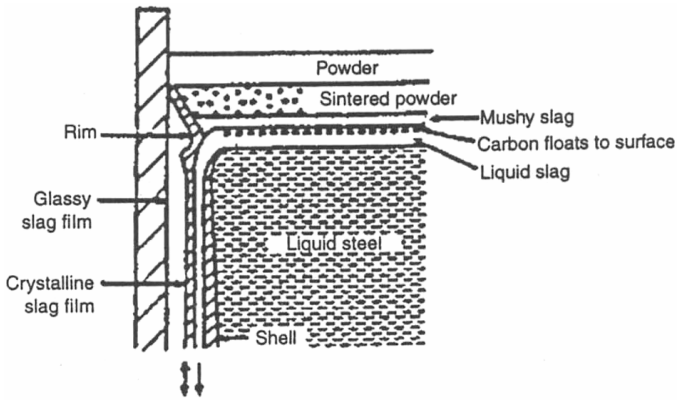

Fig. 2.2 Schematic drawing of the various slag layers formed in the mould /17/

Certainly, in reality the various processes cannot be clearly separated from each other. Formally, argon or nitrogen bubbles occasionally coming through the submerged entry nozzle, may also be accounted for as gaseous components.

Fig. 2.2 is a rather simplified picture. More detailed consideration may include the varying thickness of the powder layer, surface flows and standing wave in liquid steel /18/, and the intermittent character of MP feed. Some of these may also influence gas phase emissions.

2.2 Carbon and carbonates

The principal function of carbon in MP is to control its melting behaviour. Being added to a powder, it can effectively prevent coalescence of particles upon heating, especially in the form of carbon black. The sintered layer formed in this way remains porous and allows gas penetration to ensure carbon burnout by oxygen from the air. Carbon monoxide formed in deeper layers reacts with oxygen diffusing downwards and thus protects steel from oxidation. This is the second and equally important function of carbon.

In a recently published work /33/ the combustion of carbon in MP was studied in conditions closely reproducing those of a casting mould. The scheme of the process considered by the authors is given in Fig. 2.3. Oxygen from the air diffuses through the surface downwards; in the surface region no combustion occurs because the temperature is too low; when the temperature becomes sufficiently high the combustion starts with the formation of CO_2; in the lower region at higher temperatures CO_2 reacts with carbon to form CO; a mixture of carbon dioxide and monoxide transfer to the air. The amount of carbon in the powder and the rates of all processes must be balanced to ensure the full combustion of carbon. Otherwise the remaining carbon can get into the liquid slag pool and carburise steel.

The experimental apparatus consisted of a quartz tube heated at the bottom, containing a 5 cm layer of powder. For a fixed period of time it was exposed to a temperature gradient of 850/150°C and then the profile of the carbon content was measured and compared to the simulated one (the offgas was also analysed).

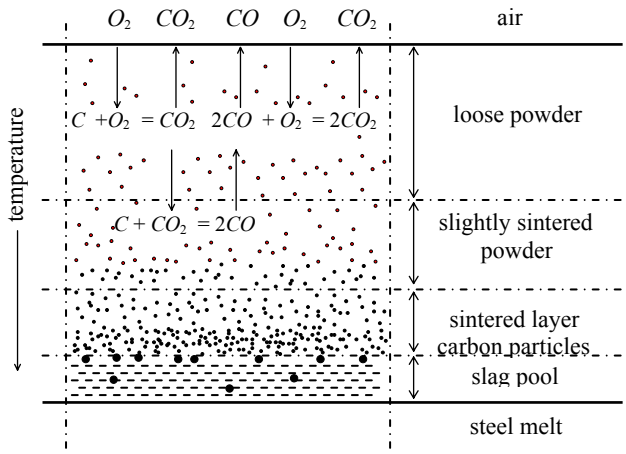

Fig. 2.3 Structure of casting layer in continuous casting mould with carbon combustion reactions /33/

The profiles are given in Fig. 2.4. Two minima of carbon concentration are clearly seen, the minimum at the bottom being quite shallow. This means that with similar conditions in the mould the combustion at the surface of a slag pool would be far from complete.

The plant conditions are essentially different however. The heating was 10-50 times longer while composition was not exactly standard (carbonate-free premelted powder was taken as a basis: 47wt% SiO_2, 37 CaO, 0.3 MgO, 4.5 Al_2O_3, 0.08 TiO_2, 0.15 Fe_2O_3, 10 Na_2O, 4.5 F, 0.27 K_2O; mixed with 5 wt% graphite powder).

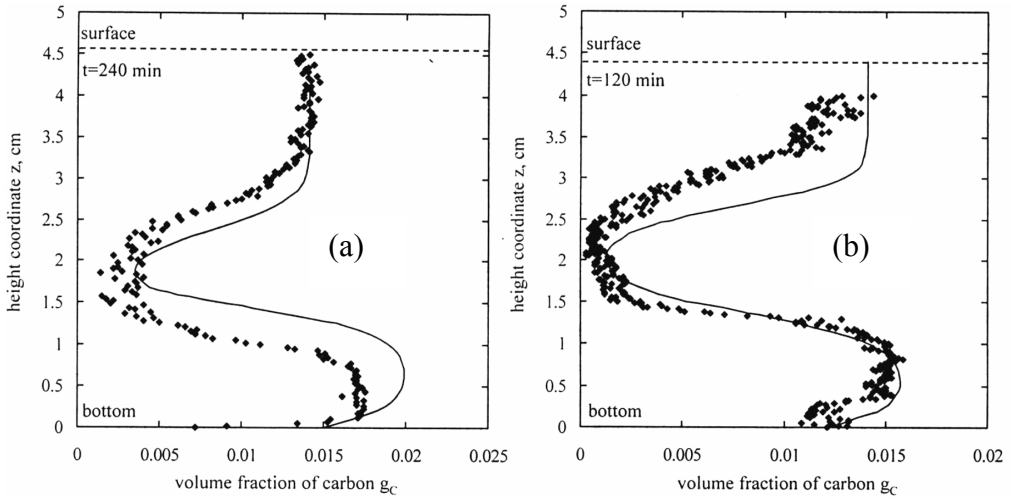

Fig. 2.4 Comparison between experiment and model (a) 4 h of heating time, 885°C at the bottom; (b) 2 h of heating time, 950°C at the bottom /33/

Only the reactions outlined in Fig. 2.3 were considered in the computation. Nevertheless, the resulting simulated curves are in agreement with the experimental data. It can be taken, therefore, as evidence, that combustion of carbon is largely independent from other constituents of mould powders and possible reactions between them, which were totally ignored in theoretical model of /33/. The opposite influence will be discussed later.

Closely related to the combustion of carbon is the decomposition of carbonates. Data essential for the present work are found in several works of Kim *et al* /34-36/. The decomposition mechanism of Na_2CO_3 in the presence of carbon black and SiO_2 was investigated by thermogravimetric (TG) and differential scanning calorimetric (DSC) methods. TG-DSC curves for pure Na_2CO_3 suggested that reaction occurs in two consecutive steps:

$$Na_2CO_3(l) = Na_2O(s) + CO_2(g) \quad (2.1)$$
$$Na_2O(l) = 2Na(g) + ½O_2(g) \quad (2.2)$$

By contrast to the earlier results of Motzfeldt /37/, X-ray diffraction analysis did not reveal any Na_2O in the sample after heating. It was explained by the higher rate of reaction (2.2) compared to (2.1). Addition of carbon black noticeably accelerated the decomposition of Na_2CO_3, Fig. 2.5. Carbothermic decomposition was represented by the overall reaction:

$$Na_2CO_3(l) + 2C(s) = 2Na(g) + 3CO(g) \quad (2.3)$$

Micrographs of samples clarified the mechanisms of carbon performance in powders and the effect of mixing ratios on TG curves. The rate of reaction (2.3) depends on the surface area of Na_2CO_3 particles which tend to decrease as the particles start to melt and agglomerate. Carbon is located on the surface of the particles hindering this process. An increase of carbon density retards coalescence accelerating decomposition.

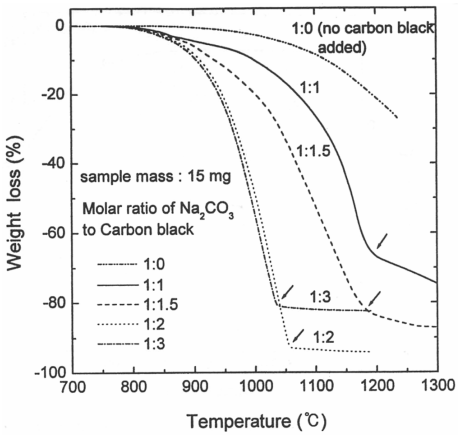

Fig. 2.5 Weight loss of Na_2CO_3-carbon black mixture for different mole ratios. Heating rate 10 K/min. The arrows indicate the points where carbothermic decomposition is complete /34/

Similar curves for Na_2CO_3-SiO_2 mixtures are given in Fig. 2.6, /35/. The curves could be explained by taking into account the results of X-ray diffraction and SEM analyses. The study was summarised as follows:

- The decomposition of Na_2CO_3 is greatly enhanced by the addition of SiO_2
- The governing reaction of decomposition is

$$Na_2CO_3 + SiO_2 = Na_2SiO_3(s) + CO_2(g) \qquad (2.4)$$

- If there is a surplus of Na_2CO_3 after formation of Na_2SiO_3 further decomposition goes partly by the reaction (2.5):

$$Na_2CO_3 + 2Na_2SiO_3 = Na_6Si_2O_7 + CO_2(g). \qquad (2.5)$$

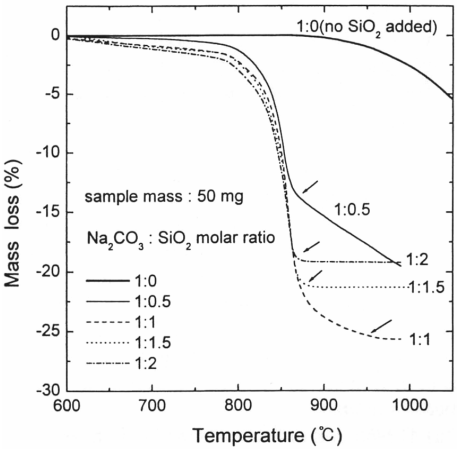

Fig. 2.6 Mass loss of Na_2CO_3-SiO_2 mixtures of different mixing ratios during heating /35/

Fig. 2.7 is also taken from /35/. The mixture Na_2CO_3+$LiAl(SiO_3)_2$+C is closer to practical mould powders, in the authors' opinion. Decomposition starts below 600°C, the lowest temperature among all the studied samples. From general considerations, addition of ingredients to the mixtures should lower this temperature, since additional eutectics may appear. Hence, with multi-component commercial powders even lower temperatures of decomposition may be expected.

In real mould the combustion and decomposition effects mentioned above are combined and to sort them out is a difficult problem. It should also be noted, that actual mineralogical composition is usually unknown. The assumption that Na_2O is added to MP generally as Na_2CO_3 /34/ is probably not fully correct. Half of the phases found in Table 2.2 include Na_2O and obviously not all of them were formed during decarburisation (2h at 700°C).

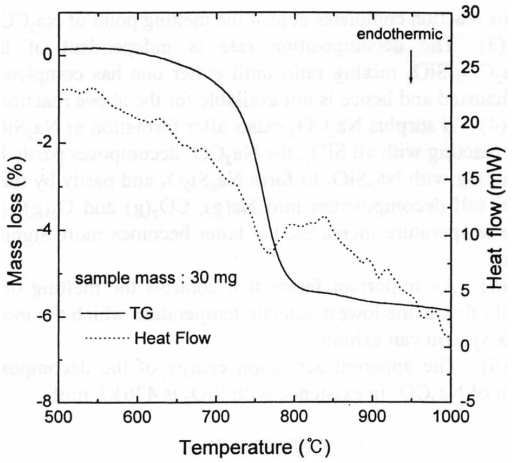

Fig. 2.7 TG-DSC results of Na_2CO_3-SiO_2 decomposition in coexistence with spodumene and carbon black /35/

Data concerning commercial powders, including TG-curves, may be found in /27/. Nine brands of different suppliers were studied. Mass-loss curves for two of them (Table 2.3, Fig. 2.8) are given in the paper. The assumption can be made, that carbon concentration in the first powder was about 1-1.5 %, though it is not quite clear how compositions were normalised.

Table 2.3 Chemical composition of mould powders /27/

	Chemical composition (wt%)								
Commercial name	SiO_2	CaO	MgO	Al_2O_3	Na_2O	Fe_2O_3	MnO	C_{tot}	F
DUXMOL C-2	37.4	37.3	0.56	2.68	6.20	1.10	-	-	2.15
Scorialit M 193 B	33.0	31.5	-	6.3	16.0	2.0	0.1	3.3	9.5

The example shown represents two types of TG-curves. Abrupt drop of the first one, accompanied by intensive exothermic transformations at 650-750°C characterises powders with low carbon content. Gradual melting behaviour seen on the second plot is a result of higher carbon content. This second type of behaviour must be more common judging from the typical carbon concentrations, Table 2.1.

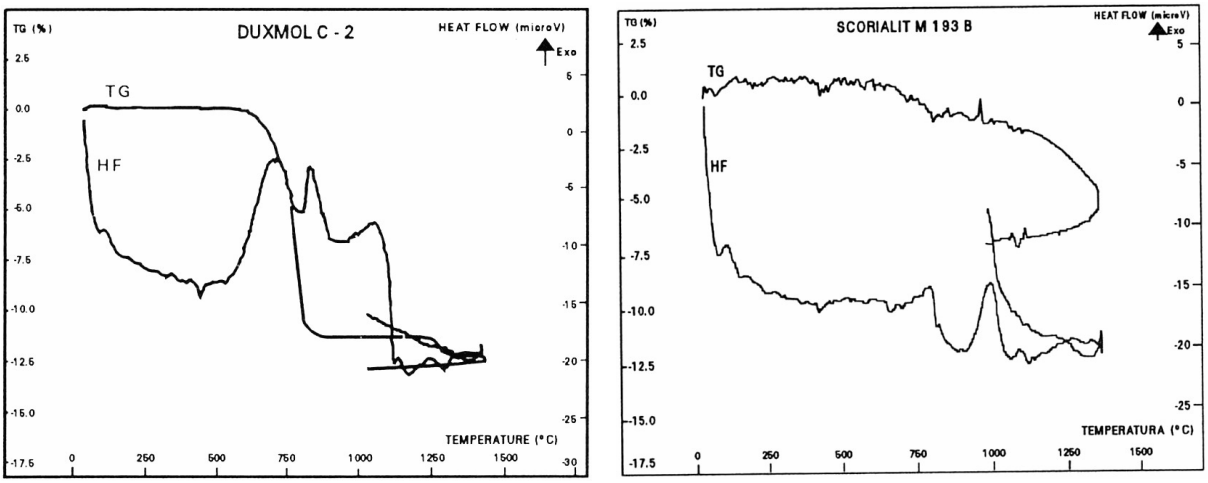

Fig. 2.8 Differential thermal analysis (HF-curves) and thermogravimetric (TG-curves) analysis of mould powders /27/

2.3 Application of mass spectrometry

One of the well-known studies of mould powder volatiles is a work by Zaitsev *et al* /28/. Inasmuch as it was done by the mass spectrometric Knudsen method it must be considered more thoroughly.

The objective of the work /28/ was to establish a mechanism of formation of volatile fluorides and the influence of MP compositions and physical and chemical states of their ingredients on the evolution of fluorides. The work relied essentially on the huge experience of the research group in thermodynamic investigations of oxide-fluoride systems, like CaF_2-Al_2O_3-CaO, CaF_2-Na_2O-SiO_2-CaO and some others /38-45/.

The compositions of mould powders selected for examination in /28/ are given in Table 2.4. As follows from the context, the investigated samples were commercial powders, not subjected to calcination, decarburisation or premelting, MP No.6 probably contained cryolite.

Partial vapour pressures of components were measured by comparison of ion currents (the method will be described later in part 3). The samples, along with the standard substance, were charged into a double effusion block and evacuated to high vacuum. Mass spectra recorded at various temperatures were decoded primarily collating them with previous results /38-43/ obtained for simpler slag systems. The results of decoding are outlined in Table 2.5. The origin of ion currents of FeF^+, MnF^+, MgF^+, TiF_2^+ and TiF^+, which were also mentioned, was not discussed.

By mould powder volatiles' the authors meant either evaporated fluorides or fluorides formed by exchange reactions of oxides with fluorite/cryolite, Table 2.6. Reactions involving Na_2AlF_6 are not included in the table because vaporization processes of MP containing cryolite are more complex and were not studied in details. Some reactions are added for further discussion.

Table 2.4 Basic chemical compositions (mass %) of mould powders studied in /28/

No.	C	CaO	SiO_2	Al_2O_3	F	Na_2O+K_2O
1	8	30	30	8	7	6
2	8	32	32	8	8	6
3	8	34	34	10	8	6
4	6	36	32	5	8	8
5	18	30	37	13	4	6
6	20	20	30	13	10	6
7	4	30	40	7	5.5	6.5
8	5	27	23	10	6.5	12
9	12	22	38	15	4.5	8

Table 2.5 Ions of mass spectra and their molecular precursors /28/

Ions	Na^+ NaF^+	K^+ KF^+	SiF_3^+ SiF_2^+ SiF^+	AlF_2^+ AlF^+ Al^+	$NaAlF_3^+$ Na^+ NaF^+ AlF_2^+ AlF^+ Al^+	$Na_2AlF_4^+$ Na^+ NaF^+ AlF_2^+ AlF^+ Al^+	$AlOF^+$ AlF^+ Al^+	CaF^+ Ca^+	BF_2^+ BF^+
Molecule	Na F	KF	SiF_4	AlF_3	$NaAlF_4$	Na_2AlF_5	AlOF	CaF_2	BF_3

All the observed vapour species except, $CaF_2(g)$, are formed in a similar way according to the table, by reaction of an oxide with CaF_2, one of the products being CaO. The mass spectrometric results in /28/ are given mainly as a description of a variety of vapour species observed in the experiments in isothermal conditions or at a constant rate of temperature elevation. They were summarised in the following scheme:

- At lower temperatures NaF and KF dominate in the vapour
- As the temperature rises SiF_4 and AlF_3 start to evaporate
- At further heating (T>900°C) SiF_4 becomes the principal component, while the concentration of alkali fluorides drops as a result of effusion
- At still higher temperatures other fluoride species appear in the vapour; their concentrations follow the sequence: $AlF_3 > CaF_2 > BF_3 > AlOF$

Vaporisation curves recorded at a constant heating rate were given only for one sample of mould powder. In Fig. 2.9 they are presented on a widened temperature scale corresponding to the whole temperature range of mould powder performance in a caster.

The practical aim of the study was the determination of atmospheric pollution by a caster. Two additional trials were performed to facilitate the practical interpretation of mass spectrometric data. Weight loss of samples was measured in vacuum conditions (0.5 h exposure at 1262°C) and in inert argon atmosphere (5 min at 1527°C). The results were in satisfactory agreement with the values of weight loss calculated from the vaporisation curves by the Hertz-Knudsen formula.

Dependence of weight loss on carbon content in the samples was hardly detectable. Mould powders with and without amorphous graphite were characterised by almost the same weight loss. The authors concluded that the interaction of carbon with silicon and calcium oxides, which should lead to the formation of carbides and carbon oxides, does not proceed to any significant degree.

Table 2.6 Primary reactions of the formation of volatile fluorides and their equilibrium constants /28/

	K_p		
	727°C	1227°C	1527°C
Reaction			
$Na_2O(s)+ CaF_2(s) = 2NaF(g)+CaO(s)$	3.69e-6	8.69	376.9
$K_2O(s)+ CaF_2(s) = 2KF(g)+CaO(s)$	2.11	2.22e4	1.30e5
$SiO_2(s) + 2CaF_2(s) = SiF_4(g)+2CaO(s)$	4.37e-15	2.24e-9	3.82e-7
$Al_2O_3(s) +3CaF_2(s) = 2AlF_3(g)+3CaO(s)$	1.94e-34	1.97e-17	2.45e-12
$Al_2O_3(s) +CaF_2(s) = 2AlOF(g)+CaO(s)$	2,33e-39	2.41e-20	3.01e-14
$MgO(s)+CaF_2(s) = Mg_2F(s)+CaO(s)$	4.07e-15	1.69e-7	3.72e-5
$CaF_2(s) \Rightarrow CaF_2(g)$	2.25e-13	3.25e-6	4.88e-4
$AlF_3(s) \Rightarrow AlF_3(g)$	5.82e-6	0.448	16.7
$NaF(s) \Rightarrow NaF(g)$	3.60e-7	8.16e-3	0.145
$2NaF(g) = Na_2F_2(g)$	1.76e-06	2.39e-2	0.550
$3NaF(g) = Na_3F_3(g)$	1.03e-10	5.98e-3	2.09
$Li_2O(s)+ CaF_2(s) = 2LiF(g)+CaO(s)$	4.67e-10	9.22e-3	3.02
$LiF(s) = LiF(g)$	5.27e-7	8.54e-3	1.66e-1
$2LiF(g) = Li_2F_2(g)$	7.08e-7	1.43e-3	0.37
$3LiF(g) = Li_3F_3(g)$	1.65e-12	4.76e-4	0.284
$2NaF(g)+H_2O(g) = Na_2O(s)+2HF(g)$	9.17e-4	2.56e-5	1.59e-5

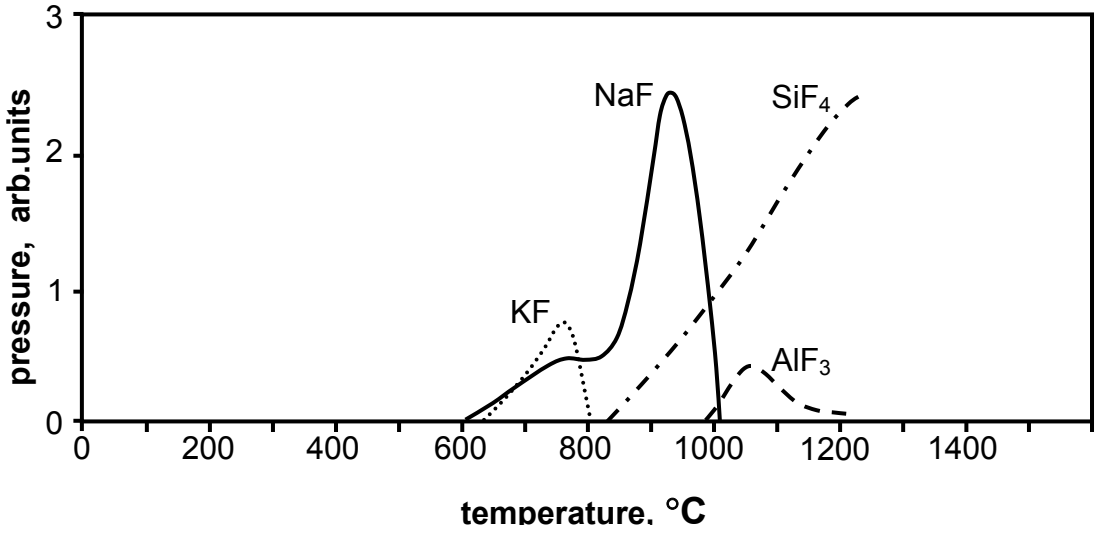

Fig. 2.9 Evolution of fluorides from MP No.2 (arbitrary units) found from mass-spectral experiments /28/ as a function of temperature; heating rate 250°C/h

The most environmentally hazardous gaseous emission of a caster is HF, formed by hydrolysis of fluorides. A substantial part of the paper is allotted to this separate problem, but it includes no new experimental results, conclusions were founded mainly on thermodynamic evaluation. In short, the results may be rendered as follows:

- Atmospheric water: greater part of AlF_3 and small part of SiF_4 and CaF_2 are hydrolysed; no hydrolysis of NaF and KF takes place.
- Physically absorbed water is vaporised during heating and does not react with fluorides.

- Chemically bound water greatly enhances evolution of HF; concentration of AlF_3, SiF_4 and CaF_2 is diminished; that of NaF and KF remains about the same.

A problem of general interest is to find how gaseous emissions are related to the chemical composition of mould powder. The basicity of slags and concentration of CaF_2 were pointed out as the primary factors governing evolution of fluorides. Regularities of gas phase formation were established by analysis of the results of previous studies of CaF_2-SiO_2-CaO, CaF_2-Al_2O_3-CaO and CaF_2-SiO_2-Al_2O_3-CaO systems, Fig. 2.10 and Fig. 2.11.

As can be seen in Fig. 2.10 (a), an increase in the basicity (CaO/SiO_2) from 0.5 to 1.2 in a slag with 0.15 mole fraction of CaF_2, makes the partial pressure and, therefore, the evolution of SiF_4 20-100 times lower. The effect of CaF_2 content on partial pressures is not so strong, but also quite obvious, Fig. 2.11. Introduction of Al_2O_3 into the slag does not change the presented picture, with the exception that AlF_3 and negligible amounts of AlOF appear in the gaseous phase. Evolution of fluorides of aluminium, sodium, potassium and other elements as a function of slag basicity and CaF_2 content obeys the same pattern.

Also one experimental test illustrating the effect of 'preliminary smelting' of MP (other authors use also the words 'premelting' or 'prefusing') on the reduction of fluorides emission was performed. The benefit of premelting is substantiated by comparison of activities of fluorite and oxides in their mixture and in their melt. The activity of CaF_2 in slags does not greatly depend on other oxides, while the mutual influence of oxides on their activities is essential (references were given in /28/). As a result, the activity of oxides responsible for the evolution of fluorides will drop dramatically upon melting, if oxide mixtures have high index of basicity. To obtain experimental proof the weight loss of CaF_2-SiO_2-CaO mixtures was measured when exposed to 1300°C in a furnace for 20 min. When CaF_2 was added to preliminary melted oxides, mass reduction was 2-3 times smaller than for mixtures of individual oxides. Additionally, an increment in the basicity index from 0.65 to 1.0 resulted in a 3-4 times lower mass loss for both types of mixture.

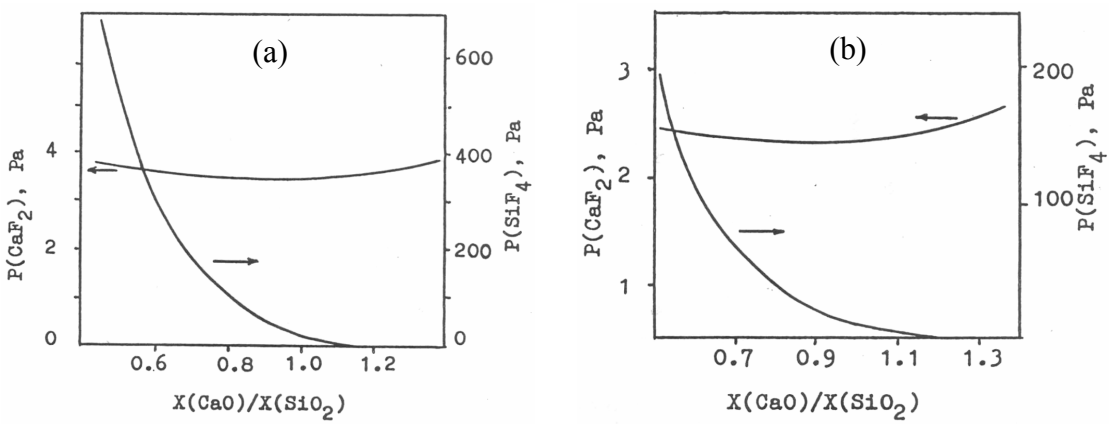

Fig. 2.10 Partial pressure of SiF_4 and CaF_2 over CaO-CaF_2-SiO_2 slags as functions of slag basicity, /28/; (a) $x(CaF_2) = 0.15$, (b) $x(CaF_2) = 0.10$; T=1700 K

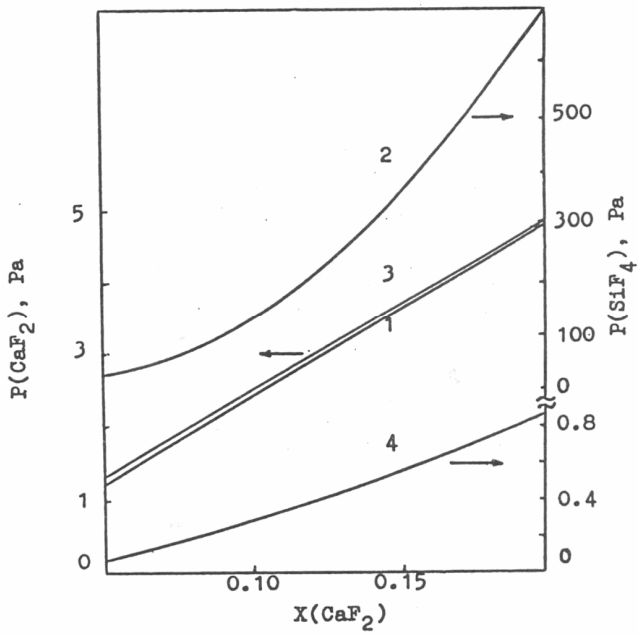

Fig. 2.11 Partial pressure of SiF_4 and CaF_2 over CaO-CaF_2-SiO_2 slags as functions of mole fraction of CaF_2 , /28/; 1 and 2 : $x(CaO)/x(CaF_2) = 0.583$; 3 and 4 : $x(CaO)/x(CaF_2) = 1.25$; T = 1700 K

The range of subjects considered in the study is rather wide. However, a strong emphasis on the problem of atmospheric pollution and recommendations for its minimisation left little space for discussion of experimental technique and procedure and hence, only a rather general survey of mass spectrometric data is given.

2.4 Fluorides in vapour phase

The paper discussed above, /28/, provides a comprehensive analysis of the problem. In other publications more special issues are scrutinized.

Shinmei *et al* /31/ studied equilibria between SiF_4(g) and CaF_2+CaO+SiO_2 melts. Their general aim was a better understanding of chemical bonding and phase relations in the melt, for which purpose SiF_4 gas pressures were measured. The work was carried out by Sievert's method (measurement of the equilibrium vapour pressures over the melts in a vessel of constant volume) at T=1450°C, in dissolution and evolution modes (the results coincided). A mass-spectrometric analysis for the gas phase showed no species other than SiF_4. Therefore, the reaction of CaF_2 and SiO_2, Table 2.6, could formally represent the relationship between the gas and the melt. Experimental and calculated gas pressures superimposed on the phase diagram are reproduced in Fig. 2.12.

The equilibrium pressure of SiF_4 above the melts increases exponentially with the decrease of basicity in calcium silicate constituting the melts. The effects of CaF_2 concentration on $p(SiF_4)$ are practically constant in the CaF_2-rich region.

A similar study was reported in a recent paper of Shimizu et al /32/. The objectives were more industry-oriented: vapour pressures of SiF_4 over CaO+SiO_2+CaF_2 system, temperature dependence of $p(SiF_4)$, effects of Al_2O_3 and MgO additions and equilibrium pressures of the offgas from industrial mould slags. The latter were preliminary sintered in the air at 700°C to remove carbon. Pressures

were measured by Sievert's method in the interval 1280-1500°C. The gas composition was controlled by mass spectrometric analysis taking samples from the reaction tube by gas syringe.

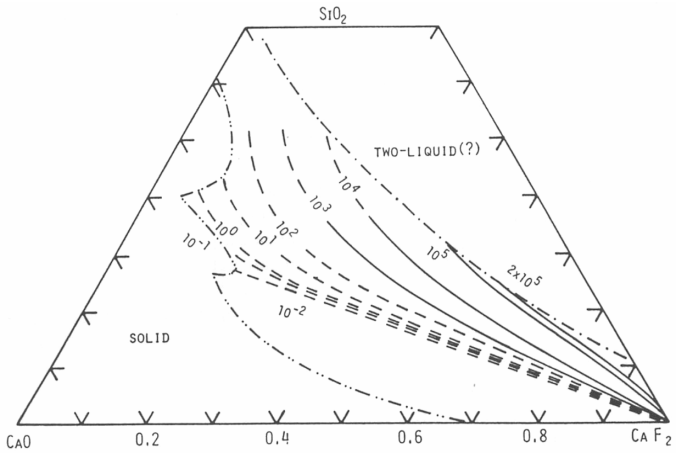

Fig. 2.12 Iso-baric lines of SiF_4(g) [Pa] above CaF_2+CaO+SiO_2 melts at 1450°C, /31/; solid lines are experimental, dashed lines are calculated

Temperature dependence is given in Fig. 2.13. The p(SiF_4) values for 1450°C depicted on the phase diagram confirmed the earlier data /31/ shown above. Linearity with respect to 1/T was taken as evidence that the factor $\{a^2(CaO)\cdot a^{-1}(SiO_2)\cdot a^{-2}(CaF_2)\}$ in the equilibrium constant is independent of temperature. Enthalpy of reaction found from the slope of the lines was in close agreement with the reference data.

Other findings were also consistent with /31/: the pressure grows exponentially with basicity while its dependence on CaF_2-content deviates downward from the linear, Fig. 2.14.

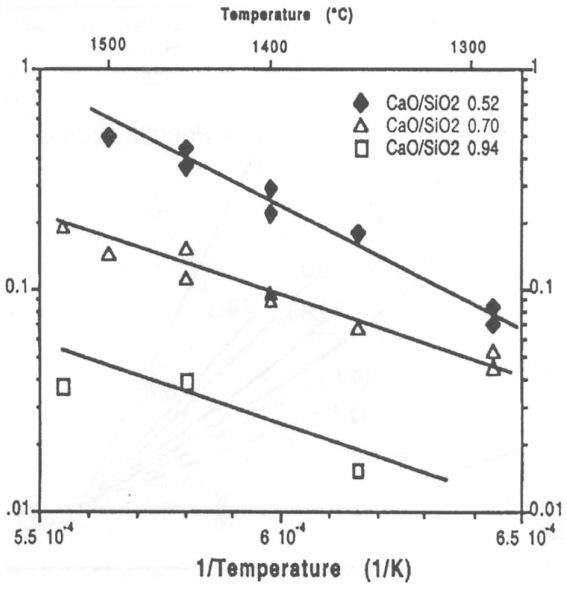

Fig. 2.13 Effect of temperature on the SiF_4 equilibrium pressure /32/

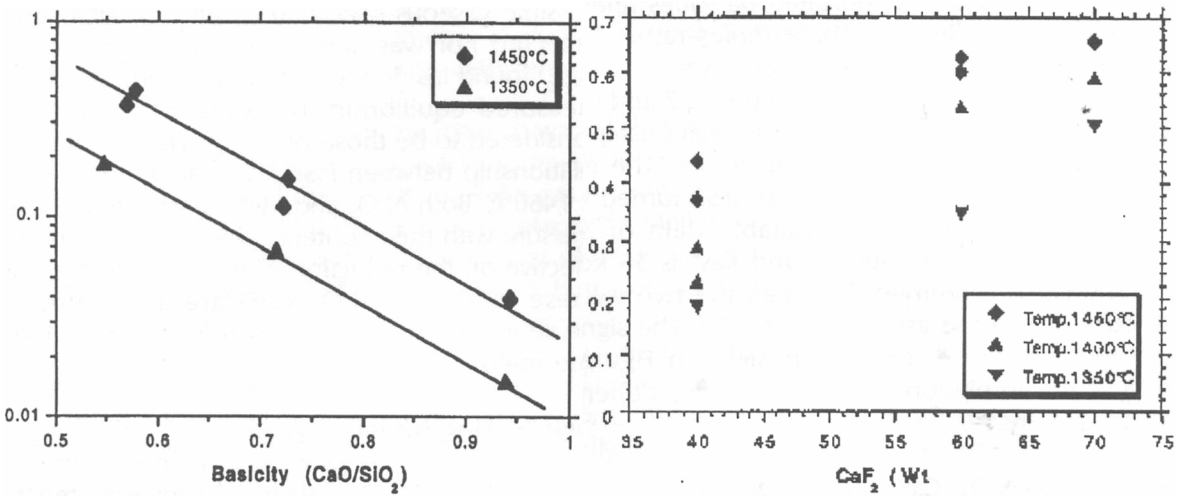

Fig. 2.14 Effects of basicity (CaO wt.% / SiO_2 wt.%) and CaF_2 (wt.%) on the equilibrium pressure of SiF_4 (Y-axis, [atm]) /32/; CaF_2 content and basicity were fixed at 40 wt.% and 0.52 respectively

More complex slags containing Al_2O_3 or MgO were also studied, Fig. 2.15. $CaO\text{-}SiO_2\text{-}CaF_2$ containing 40 wt.% CaF_2 served as a basis (CaO/SiO_2= 0.52), mixtures were examined at 1450°C. Both Al_2O_3 and MgO drastically reduced SiF_4 pressure, MgO being seemingly a more effective additive. These effects were attributed to structural and thermodynamic aspects of the silicate melts.

Mass spectrometric analysis of the gas probes indicated only SiF_4 in the offgas. No other possible gaseous species (e.g. AlF_3, AlOF) were detected nor was any trace of condensation (e.g. MgF_2) found inside the system. It should be noted yet, that the whole range of tested masses was not specified in the article /32/.

Pre-sintered real industrial mould powders were examined in the same way as $CaO\text{-}SiO_2\text{-}CaF_2$ slags. The investigated temperature was 1350°C for slag A and 1400°C for slag B. Equilibrium pressures of the offgas were 0.07 atm and 0.50 atm for slags A and B, respectively. Results of mass spectrometric analysis, Table 2.7, were

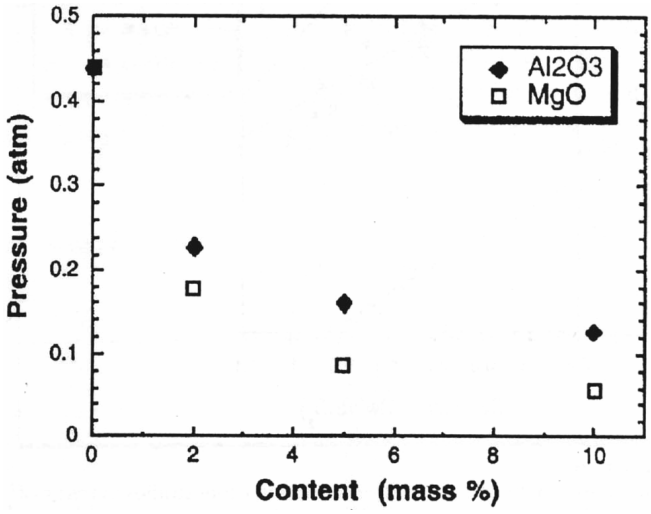

Fig. 2.15 Effect of Al_2O_3 or MgO addition on the equilibrium pressure of SiF_4 /32/ in a slag with 40% CaF_2 and with CaO/SiO_2 ratio =0.52

not so trivial as for synthetic slags. Offgas contained large amounts of CO and CO_2, presumably due to insufficient preliminary decarburisation. A crude calculation of SiF_4 pressure yielded a value of about $2.1 \cdot 10^{-3}$ atm.

In the case of slag A, a significant discrepancy was observed between the actual weight loss of the sample and that estimated from the evolution of the gas. After careful inspection of the inner surface of the reaction tube, an appreciable amount of condensate was found, which was identified by X-ray analysis as NaF. Therefore, formation of NaF(g) takes place in quantities that cannot be ignored from the environmental point of view, though the effect cannot be evaluated by Sievert's method.

Table 2.7 Industrial mould slag samples. Compositions and relative intensities of the gaseous species detected in mass spectrometric analysis (intensities $I^+_{m=28}$ are taken as 100) /32/

	Composition								MS analysis			
	SiO_2	CaO	Al_2O_3	MgO	Fe_2O_3	Na_2O	F	C_{tot}	CO/N_2	O_2	CO_2	SiF_3
Slag A	34.7	35.5	6.6	0.7	0.4	10.7	6.9	4.5	100	17.7	2.01	-
Slag B	37.5	34.7	6.8	5.2	1.5	1.9	8.7	8.7	100	7.89	2.51	0.28

In their next work, Shimizu and Cramb /46/ employed TGA method to investigate the rate-phenomena of fluoride vaporisation. Attention was focused on the development of models of rate-controlling mechanisms and kinetic calculations. The objects of the study were as in the previous work and again part of the analyses was performed by a mass spectrometer (additionally to chemical analysis). The gaseous species evaporated from the CaF_2-SiO_2-CaO system were SiF_4+CaF_2 and from mould fluxes these were NaF+SiF_4. Sodium fluoride was detected only by chemical analysis of condensate, but no explanations are given about CaF_2.

The effects imposed on the vapour phase by NaF/CaF_2 content of a slag were elucidated in /47/. Two samples of synthetic powders of approximately identical compositions were taken (33 wt% CaO, 38% SiO_2, 0.8% Al_2O_3, 14.2% Na_2O, 8.96% F). In one of them F was added in the form of CaF_2 and in the other NaF. Before the experiments, samples were kept for 24h in a drying oven at 150°C.

The experimental procedure included measuring fluorine content after quenching the samples from T=1300°C at different times of exposure, Fig. 2.16. The extent of fluorine emissions was higher when fluorine source was NaF (up to 8% of initial value) in comparison with CaF_2-based slags (up to 5-6% of initial value). From the reference data for NaF and CaF_2 vapour pressures, the authors concluded that the principal volatile species is NaF(g). No explanations were given however, why other volatile species like SiF_4 were ruled out. In fact, in the papers cited above gas phase constitution was not studied. Only well-established vapour species were considered and the processes were described in terms of the simplest reactions compatible with mass balance and slag compositions. However, for mass spectrometric studies any information of less common vapour species is essential since the dynamic range of measurements sometimes exceeds 7-8 orders of magnitude and conclusions are often made judging from the tiniest ion currents. For example, in the work of Kashiwaya /48/ on the vaporisation of hexafluorosilicate, it was proposed, as an option, that Na_2SiF_6 may exist as a gaseous species. If it were so, the interpretation of SiF_4 mass spectra would become a much more difficult task (in their further works /49/ the idea was abandoned).

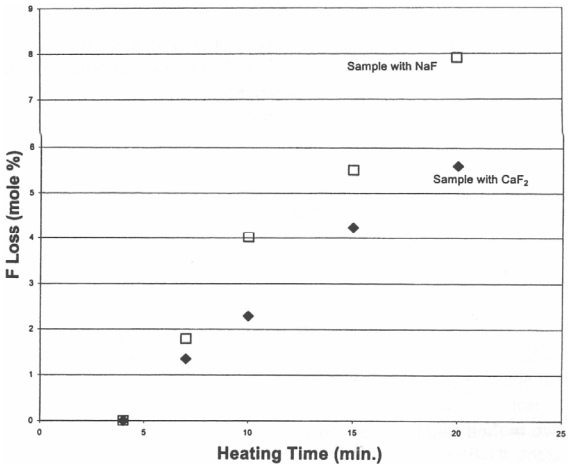

Fig. 2.16 Trend of F^- loss in slags /47/

Nevertheless, speciation of SiF_4(g) in mass spectra of mould powder vapour is not a simple problem. At this point, the results of Farber and Srivastava /50/ may be useful. They studied reaction enthalpies of silicon subfluorides in the temperature range 1317-1509°C by the mass spectrometric Knudsen method. An alumina effusion cell containing pure metallic Si was connected to a separate bulb with SiF_4(g) through a special valve regulating flow inlet to ensure equilibrium conditions within the cell. The standard ionisation voltage, 70 V, was not appropriate, because the coexistence of parent and fragment ions had to be excluded. The ion current of each molecular species in the gas phase (Si, SiF, SiF_2, SiF_3, SiF_4) was recorded at the ionisation voltage of 1-2 V above its appearance potential, i.e. 9-17 V. That is why the relative intensities of these currents for different ions cannot be directly compared with the experimental values obtained at standard parameters (40-90 V). But partial gas pressures calculated from them, Table 2.8, can serve as a reference in some cases.

Table 2.8 Partial gas pressures ($p \times 10^8$, atm) in Si-SiF_4 system /50/

T, K	Si(g)	SiF(g)	SiF_2(g)	SiF_3(g)	SiF_4(g)
1590	6.9	6.9	291	59.8	5.9
1605	10.0	13.7	716	199	25.7
1615	12.6	17.2	1000	305	43.2
1630	16.6	18.9	917	241	28.5
1650	26.3	24.0	803	161	14.1
1670	39.8	44.1	1280	271	24.4
1698	63.1	70.6	1770	358	29.6
1710	66.0	72.2	1750	351	28.3
1750	144.0	140.0	2990	535	37.1
1782	229.0	253.0	6140	1280	98.3

Separate features of vaporisation processes or, on the contrary, general surveys are found in many publications. In the work of Visvanathan et al /51/, as an example, the kinetics of gas transfer in a laboratory apparatus are developed. The data on reactions giving rise to fluorides evolvement from fluxes was taken from other reference sources, however. In the review of mould slags of Feldbauer *et al* /10/ the problem of vapour pressures and their minimisation is also touched upon in brief. The original curve for real mould powders was added to illustrate p(SiF_4) temperature

dependence (obtained by Sievert's method). Hillert /52/ considered, as a by-problem, the formation and partial pressures of SiF_4(g), HF(g) in his dissertation devoted to fluoride-oxide systems and their phase diagrams. In a study of properties and phase relations in the CaO-SiO_2-CaF_2 system /53, 54/ a further developed phase diagram incorporating SiF_4(g) is presented, Fig. 2.17.

Certainly, these scattered data make the present conception of the vaporisation scheme of mould powders more accurate and complete, but do not add very much new to the available data concerning their vapour phase components.

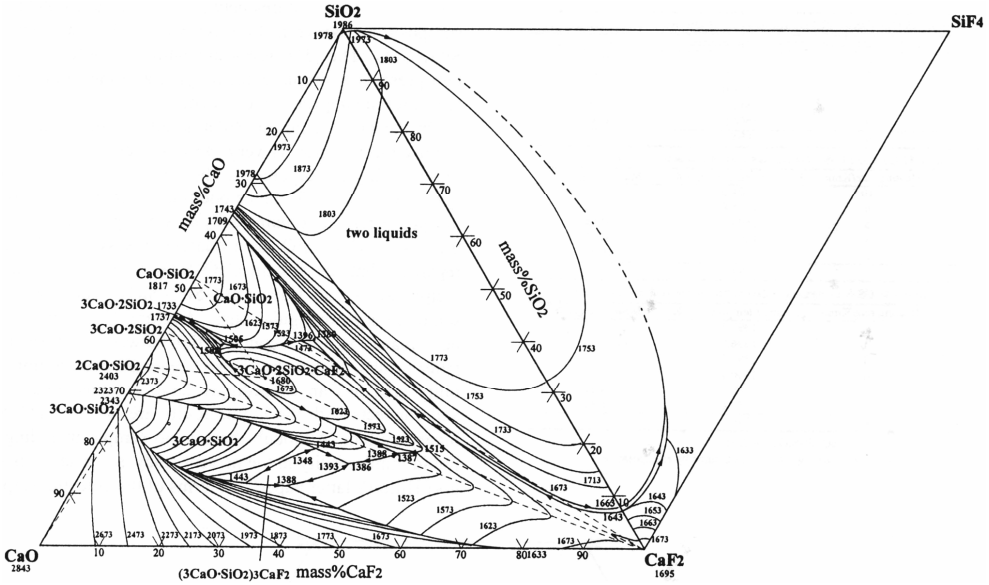

Fig. 2.17 Phase diagram of CaO-SiO_2-SiF_4-CaF_2 system in mass %, /53/

2.5 Partial pressures as auxiliary data

Mass spectrometry is a very sensitive method of measurement of low gas pressures ($p \sim 10^{-15}$ mbar and even lower are measurable), including vapour pressures over the condensed phase (Knudsen and Langmuir methods). Absolute pressures are not determined very accurately by the Knudsen method and in the latter case they are used mostly as the experimental basis for thermodynamic studies, i.e. are considered as auxiliary data. Yet, they comprise quite valuable information about components of the vapour phase, especially when no other relevant experimental data are available.

With regard to systems constituting mould fluxes, considerable mass spectrometric data can be found in the works of A.Zaitsev and co-authors /38-45/ (only papers in English are cited). Through the years of systematic thermodynamic studies in this research group nearly all important systems were investigated, among them CaO-SiO_2, CaO-Al_2O_3-SiO_2, CaF_2-Al_2O_3-CaO, CaF_2-SiO_2-CaO, CaF_2-SiO_2-Al_2O_3, CaF_2-SiO_2-Al_2O_3-CaO, Na_2O-SiO_2, $x$$CaF_2$+$y$$SiO_2$+(1-$x$-$y$)CaO, $x$$CaF_2$+$y$$Al_2O_3$ +(1-x-y)CaO, $CaAl_2Si_2O_8$, $Ca_2Al_2SiO_7$. Attention was focused on phase relations and thermodynamic modelling, but concise summaries of mass spectra of components are also supplied.

For several instances partial pressures were shown in explicit form. Fig. 2.18 and Fig. 2.19, given in /38/ as a proof of equilibrium conditions in effusion cells,

illustrate the effect of basicity and CaF_2 content on the evolvement of different fluorides. They illustrate also the potential of the mass spectrometric effusion method: the gaseous components which in /31, 32, 47/ were either estimated or deduced from supplementary chemical analysis could be determined by direct measurements.

Mass spectrometric data of /38-45/ together with /28/ served as a starting point for the present study and were widely used in mass spectra interpretation. Some of the details will be discussed later, while here some general comments are made, elucidating possible restrictions in borrowing information from theses works.

All measurements were performed as 'reduction' experiments. Equilibria in the systems under study and reactions with the materials of containers were considered jointly, and important conclusions were made on the basis of the relative reducing power of the materials (Mo<Ni<Ta<Nb). The validity of this approach is proven in the paper, but the mass of samples in the cell is never specified. The sensitivity of the employed mass spectrometer seems to be rather high. No information is given, however, about the vacuum conditions attainable in the ion source and evaporation chamber (sketched in /43/). For example, the discrimination of $^{40}Ca^+$, originating from $CaF_2(g)$, from the background of $^{40}Ar^+$ (always present in the residual gas of a vacuum chamber) is easy only for a saturated vapour of pure CaF_2, otherwise a very powerful pumping system is required.

Despite the high performance of the instrument, several ion species that obviously are to be expected in the spectra are missing. For example, ion currents SiF_4^+ and $I(Si^+)$ are comparable to that of SiF^+ according to the reference data (Table 4.5). Double charged ions were not mentioned at all, though for silicon fluoride they must be easily detectable and are not totally negligible in the calculation of partial pressures.

Mass spectra were decoded referring only to isotopic abundance and thermodynamic considerations. It was regarded sufficient for unambiguous interpretation and appearance potentials were not involved.

The ionisation voltage is not given. Supposedly it was within the interval 50-90 V, in which case the data allows comparison with the results of the present study.

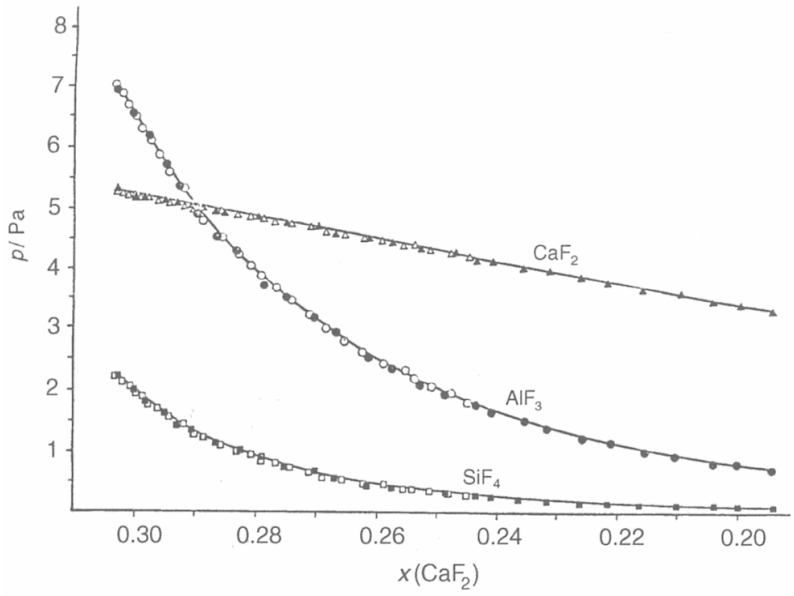

Fig. 2.18 Isothermal vaporisation of CaF_2-CaO-Al_2O_3-SiO_2 system /38/; initial concentrations: CaF_2-0.303, SiO_2-0.242, Al_2O_3-0.147, CaO-0.308; T=1400°C; Nb crucible.

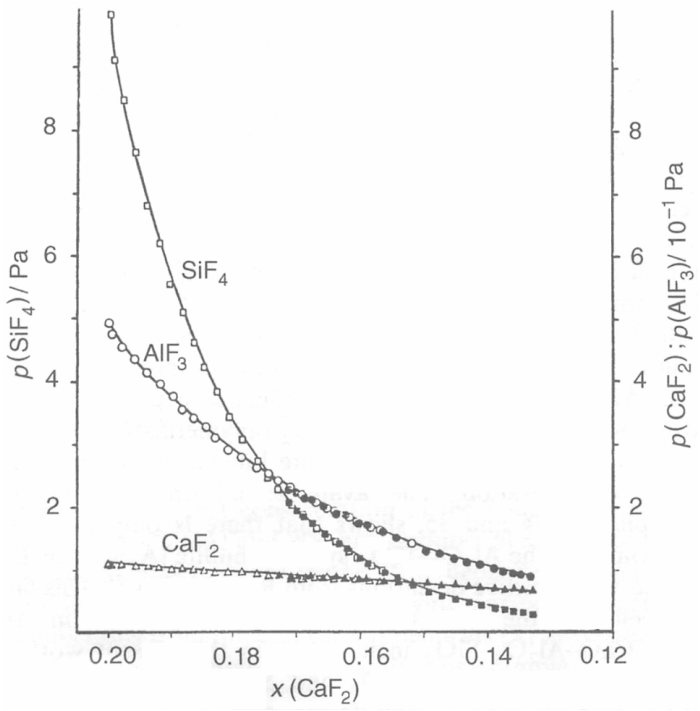

Fig. 2.19 Isothermal vaporisation of CaF_2-CaO-Al_2O_3-SiO_2 system /38/; initial concentrations: CaF_2-0.201, SiO_2-0.400, Al_2O_3-0.095, CaO 0.304; T=1200°C; Mo crucible.

2.6 State of the art

The foregoing review of the results reported in the literature provides an idea of the current advance in the research of mould powder gaseous emissions and allows us to point out the achievements and omissions of these studies:

- Possible components of gas phase over the mould are established, reactions in fluxes leading to their formation are analysed and means to lowering harmful emissions are proposed. Yet, nearly all conclusions are founded on laboratory experiments.
- Separate features of the process are studied in detail in laboratory experiments, but in conditions very different from those of real caster, especially with respect to the time scale.
- Samples for investigations are usually subjected to preliminary heat treatment, like calcination or decarburisation, thus they are not the same as in industrial conditions.
- Chemistries of molten fluxes are analysed more often, whereas the stage of initial heating of 'loose' mould powder is not well studied.
- Additional experiments in the same directions (TGA, Sievert's method) can hardly enrich understanding of processes in the gas phase crucially.

A conclusion can be drawn that two directions of further research are motivated: more sophisticated measurements in plant conditions, or more thorough study of the gas phase constitution. The present work has followed the second approach.

3 RECONSTRUCTION OF EQUIPMENT

Nearly all of the present work was performed by the High Temperature Mass Spectrometric Knudsen Effusion Method. The method, which is a combination of classical effusion method proposed by Knudsen in 1909 and mass spectrometric analysis of the composition of effusing vapour, was initiated by Chupka, Ingram and Honig in a series of their pioneering studies in early 50's. During the next two decades it was extensively developed and became one of the important methods of high temperature chemistry and thermodynamic studies, especially when quadrupole mass spectrometers, cheap and compact compared to magnetic devices, became available. In later years innovations were related mainly to the perfection of computer controle and software.

Very few commercially produced types of mass spectrometers were designed specially for high temperature effusion studies because the method is not widespread and the demand is not high. In most cases researchers themselves equip mass spectrometers with self-made vaporisers, creating set-ups noticeably differing from each other in design and performance as far as they must meet rather contradictory requirements and be suited in every laboratory to a particular field of research.

3.1 Characteristics of the Knudsen method

A general survey of the method may be found in several monographs and reviews /55-60/. Here only a short summary is given, to explain how the measuring procedure was adjusted for the aims of the present work. Typical design of the apparatus is shown in Fig. 3.1. The scheme is similar to all installations based on the quadrupole mass spectrometers but the particular type, design and arrangement of the components drastically affect the quality of experimental results.

The method, in principle, allows for measuring partial pressures of all components in the vapour (usually saturated) above the system under investigation. The key element of the experimental installation is the 'Knudsen effusion cell', i.e. a container with a small orifice into which a sample is loaded. The cell is put in a vacuum furnace, heated to a fixed temperature and the vapour effusing through the orifice is registered by the mass spectrometer. The available temperature range depends on the volatility of the substance. At lower temperatures a limit is set by the sensitivity of the device. At high temperatures the pressure in the cell should not exceed 10^{-4} atm so that the vapour inside can be treated as ideal gas and the flow through the orifice as a molecular flow.

In this case a simple relation exists between the density of molecules in the flow and the vapour pressure in the cell. In the ion source part of the molecules, proportional to the density of a given molecular species, 'i', is converted into ions that are then analysed by quadrupole mass-filter and registered as the ion current corresponding to the selected m_i/z^+_i (m - mass of the i-th ion, z^+ - its charge). A set of screens and apertures cuts off part of the effused flow and forms a molecular beam, which gets into the ion source and is detected by the mass spectrometer. Ion current I_i, corresponding to partial pressure, is the difference between the current measured in open and closed ('background level') positions of the shutter, Fig. 3.1. For pressure measurements some standard is needed as a reference. A cell containing a substance (Ag, CsCl, Au etc) with a well-known pressure of saturated vapour is installed then, in

the same position and the procedure is repeated. Partial pressures are determined by comparison of ion currents:

$$p_i = p_s (I_i T_i \sigma_s \gamma_s a_s)/(I_s T_s \sigma_i \gamma_i a_i) \quad (3.1)$$

where I is the measured ion current, A, T – temperature, K, σ – ionisation cross-section of the selected molecular species, cm^2, γ – coefficient of conversion of secondary electron multiplier, *a* – abundance of the selected isotope, indexes "i" and "s" refer to the sample and the standard, respectively.

When the time dependencies of partial pressures and temperature are established, mass loss of the sample resulting from effusion of 'i' can be determined as (the Hertz-Langmuir formula):

$$m_i = 44.3\ s_{eff} \int \text{sqrt}\,(M_i/T)\ p_i\ dt \quad (3.2)$$

where s_{eff} is the effective area of effusion, cm^2, M_i – molecular mass of species 'i', p_i – pressure, atm, and t – time, s. Precise values of σ are usually unknown /62-64/, especially for molecules, when the additivity rule must be applied /65/, and together with γ they are the main sources of experimental errors. For calibration purposes individual substances are used and experiments are made at T=constant. Then (3.2) becomes $p_i \sim mT^{1/2}/t$, which is the basis of 'the isothermal vaporisation method'.

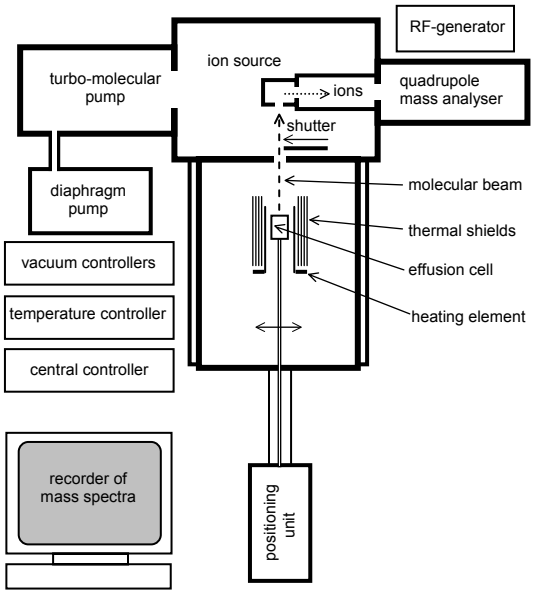

Fig. 3.1 Schematic diagram and components of experimental set-up, /26/

Several half-empirical correction factors were proposed to eliminate or minimise the errors. The universally accepted one is the Klausing factor, always introduced to account for the finite thickness of the orifice edge: the effusion orifice is considered as a channel of the length *l* and diameter *d*. Then, for small *l*-s the Klausing factor is

$$L = (1+l/d)^{-1}, \qquad (3.3)$$

so that the effective area of effusion s_{eff} substituted in formula (3.2) is $L \cdot s$. The conversion factor γ_i for the i-th ion of mass M_i in the expression (3.1) is taken as $\sim(M_i^+)^{-½}$, as a rule. Empirical correction factors for ionisation cross-sections are often introduced /60/, but every time their validity must be justified again. The kinetic effects of evaporation can be taken into account if 'the coefficient of evaporation' (accommodation) is known.

For thermodynamic studies special methods have been developed for the exclusion of device sensitivity needed for application of formula (3.1) (Gibbs-Duhem, monomer/dimer), but in this work they were not used.

More serious mistakes may arise as a result of shortcomings of the effusion method itself. Usually they are caused by a non-equilibrium state in the cell or interaction of the sample with the cell material. When systematic errors of this kind are involved, discrepancy may exceed 2-3 orders of magnitude.

3.2 First modification of the mass spectrometer

The apparatus shown in Fig. 3.1 was constructed in the Laboratory of Metallurgy, originally for the measurement of activities of components in alloys. The experimental device described in /61/ had been taken as a prototype. The shutter shown in the picture was removed and the system was equipped with a triple-cell crucible, the position of which could be regulated. By the successive alignment of cell orifices with the axis of the ion source collimator immediate comparison of ion currents of a sample and a standard was realised. Details can be found in /66, 67/.

For alloy studies the instrument performance proved to be sufficient, but for the aims set in /26/ the experimental part had to be modified. Mould powders, as an object of effusion studies and the problem that had to be solved, set specific requirements. With the knowledge available from the literature and several preliminary experimental tests these requirements were established as follows:

- The furnace must provide high heating rates (100°C per min or more)
- Durable (several hours) data acquisition in the real time scale
- Easy sample manipulation (loading, removal and baking out residuals).

To meet these requirements the following renovations were made:

- The heating element and shields were made of thin (25-50 μm) material with low heat capacity
- The positioning device for the continuous automatic switch of cells was designed and attached to the vaporisation chamber
- The technique of cell sealing was improved (lids in a form of Mo-foil pieces compressed into the crucible).

Some minor improvements were also made. All the mass spectrometric results reported in /26/ were obtained with this installation.

The undertaken refurbishment was justified by the course of further work in all points but one: the attainable heating rate (>500°C/min) was far too excessive, since the breakdown of high-vacuum conditions had already started at 15-20°C/min. The cell switch system proved to be highly beneficial for performance: false ion currents, which are often recorded when the system with a shutter is used, were totally excluded.

Effusion experiments imply stationary conditions in a container with a sample, at least when the pressures are to be evaluated. Mould powders are multi-component mixtures and at constant temperatures measurements give somewhat indefinite results: during the time intervals needed for the scanning of mass spectra the pressures change too much and in some temperature intervals the levelling off of the pressures (ion currents) does not occur at all.

To make possible any comparison, ion currents were recorded at a constant rate of temperature elevation. The parameters chosen for a uniform experimental procedure were:

- Heating rate =100°C/hour
- Orifice diameter =0.29 mm
- Mass of a sample =20 mg.

The resulting vaporisation curves can be found in /26/. The obtained information is not full. Some of the vapour species had to be skipped and not all the data could be interpreted. There were two main reasons for this.

The vacuum system, Fig. 3.1, was pumped by the sole high-vacuum turbo-molecular pump, common for the analytical chamber and the vaporisation chamber (through the holes in the separation wall not shown in the picture). Consequently, the pressure of residual gases forming the background of mass spectra is high, especially during heating. Some of the vapour species under study have masses the same as residual gases and are undecipherable in the mass spectra.

The second reason is a more specific one. SiF_4 effusing from the cell is a gas at ambient temperatures and does not condense on the water-cooled walls of a chamber like other effusates. At a certain moment the pumping speed becomes insufficient and the total pressure of SiF_4(g) in the analytical part is too high compared to the effusion flow, which therefore cannot be discriminated.

At some points the information in the report /26/ is still deficient. For example, no definite conclusions could be drawn about the presence of KF and MgF_2 in the vapour, which are missing on the charts. The curves for silicon fluorides contain some breaks, while CO_2 could be assessed only from its total pressure in vacuum system. Further trials could add only a little towards filling in these blank spaces, because of the limitations set by the performance of the experimental equipment. In view of these problems, the mass spectrometer was once more modified.

3.3 Second modification of the mass spectrometer

The experience gained, /26/, allowed for more accurate formulation of the problem itself and the best methods for its solution. The following were taken into account:

1. Partial pressures above mould powders in effusion experiments are not exactly reproducible. Variation is about ±10% at low temperatures and may be more than 20% at T>1200°C. This is a result of the non-homogeneity of the composition and the uncontrollable behaviour of the melt. In an optimised measuring procedure a comparable uncertainty may be added as a result of experimental errors and statistical fluctuations.

2. There are species among mould powder volatiles, which are gaseous at ambient temperatures (H_2O, CO_2, SiF_4) and are not easily measurable by the mass spectrometric effusion method. Yet, they are inherent constituents of emissions and must be evaluated. The solution may lie in the reduction of the total pressure in the

analytical part, and making it as independent as possible from the vacuum conditions in the vaporiser.

3. Some vapour species cannot be detected because of their small ion currents in the mass spectra compared to that of the residual atmosphere. They can be discriminated by the minimisation of statistical fluctuation, i.e. by increased measuring time, but only if the background level does not change rapidly during heating. Thus, the solution may be the same as in the previous point.

4. A serious drawback, reducing the performance is in the design of the furnace, which was very much like the traditional one found in the prototype, /61/. In the enclosed space formed by the heat shields the pressure of the effused substance may be several times higher than in other parts of the vacuum chamber. This vapour in the form of directed flow gets into the detection unit together with the molecular beam and substantially elevates the background level.

5. The mass spectra for pure substances (NaF, KF, Na_2O etc), helpful for data interpretation, were not reliable, because the molybdenum crucibles are not inert towards these substances. If the position of the crucible is fixed, installation of Pt-inserts into the cells causes no problems.

It is clear that the first priority is the improvement of vacuum conditions. The effect of the residual atmosphere on the detection of different ions can be seen in Fig. 3.2. The spectrum was recorded after several days of pumping (no water-cooling) and provides the idea of an attainable ultimate vacuum when the vaporisation chamber and the analytical chamber are not connected (see Fig. 3.3); during experimental runs the curve goes 2-5 times higher. The feasibility of registration of a particular ion current superimposed on this background is strongly dependent on its m/z^+. For m=23 (ion Na^+) conditions are most favourable, for m=18, 28, 44 (H_2O^+, N_2^+/CO^+, CO_2^+) conditions are least favourable. Masses 39, 41, 42 are intermediate in this respect, but the corresponding ion currents ($^{39}K^+$, $^{41}K^+$, NaF^+) were too small to be detected with the apparatus employed (Fig. 3.1).

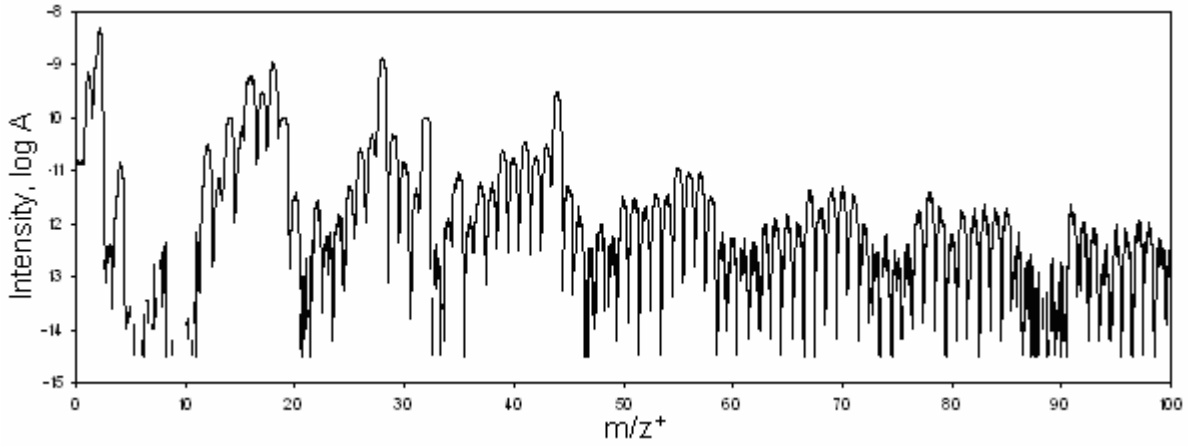

Fig. 3.2 Mass spectrum of residual gases in vacuum chamber; total pressure = $3.5 \cdot 10^{-9}$ mbar

The mass spectrometer modernised according to these guidelines is shown in Fig. 3.3. Test trials with standards and mould powders indicated that its performance has improved in several aspects:

- The analytical chamber is thoroughly separated from the vaporisation chamber; when the vacuum valve is open their volumes are connected only with three holes d = 0.5 mm

- A separate turbo-pump attached directly to the furnace chamber provides a high pumping speed; with all of the studied samples the pressure remains less than $5 \cdot 10^{-6}$ mbar
- A system of slits forms the 'sharp-focused' collimator; the parasitic ion currents that can be registered do not exceed 0.1-0.3 % of the signal
- The position of the crucible is fixed; Pt-cells can be inserted and removed easily, allowing, when needed, mass loss measurements with the accuracy of ±0.1 mg
- The pumping of the quadrupole chamber goes on continuously without air admission for months; it ensures the minimal drift of the parameters of the ion current detector (secondary electron multiplier)
- Measurements may be started from room temperature with no preliminary baking
- The furnace is made transparent to vapour and includes no thermal shields, Fig. 3.4; this is done at the expense of the increased power supply of the heating element and, probably, higher temperature gradients in the crucible; however, for the present task they are considered to remain within tolerable limits.

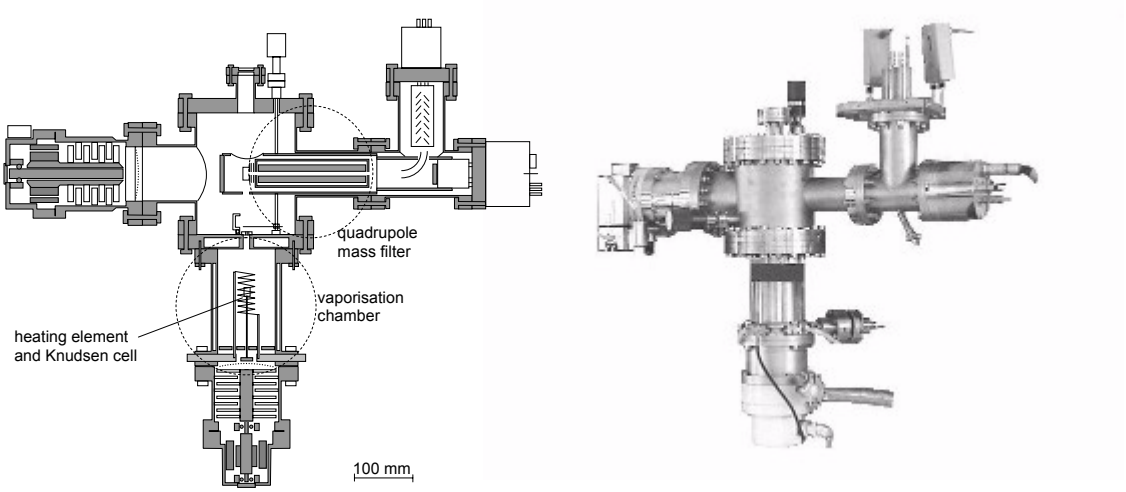

Fig. 3.3. Vacuum system of the experimental setup and its outside view (connections and auxiliary units are not shown)

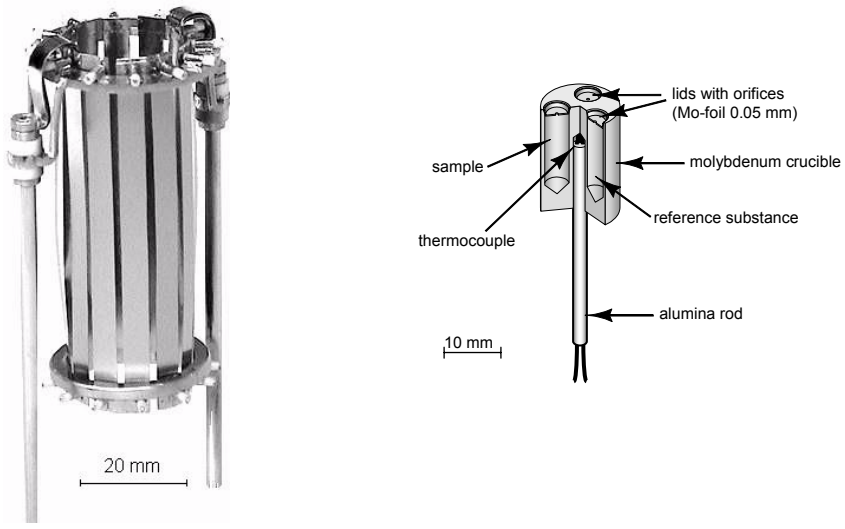

Fig. 3.4. Resistive heating element and cross-section of effusion cell

Characteristics of the vaporization unit:

- Mo-crucible with three cells, d =5 mm, h =12 mm; orifices s_{eff} =0.056 mm^2
- Maximum temperature: 1600°C
- Thermocouple: Pt-Pt10Rh, type S
- Uncertainty of T-measurement: ±5°C at 1000°C (assessed from vaporization of Ag).

Mass spectrometer: Balzers QMG 420; rods d=8 mm; mass range 1÷512; SEM amplifier.

When necessary, additional explanations of some details will be given in the text.

4 EXPERIMENTAL PROCEDURE AND RESULTS

From the review in the earlier section, it is clear that the problem of gas emissions is a rather complex one. Any advanced study implies some limitations in the scope of the studies. As the basic subject of the present work, eight commercial mould powders were chosen and subjected to a mass spectral analysis, uniform to all samples. Within this restricted task the aim was to get as detailed data as possible. Well-developed methods of Knudsen thermodynamic studies are not widely applicable to a study of the sublimation processes. This deficiency had to be compensated for by the abundance of initial experimental data, and at this point a question of feasibility arises. Experimental conditions had to be chosen as an optimum between adequate mass spectrometer performance and such practical factors as time schedules, stability of apparatus characteristics, longevity of high temperature parts etc.

4.1 Measuring procedure and mass spectra

A representative set of mould powders for investigation was selected in co-ordination with the project partners /26/. For convenience they were renamed in the report /26/ and the same notation will be used in further discussion. The compositions are given in Table 4.1.

Table 4.1. Compositions (wt %) of mould powders (SAG-104, SAG-119) and granules (others) studied; SAG-118 with Si_3N_4 additions

Powder	C_{total}	C_{free}	SiO_2	CaO	MgO	Al_2O_3	Fe_2O_3	MnO	Na_2O	K_2O	F
SAG-103	7.30	5.76	38.7	31.6	4.10	5.40	0.54	0.08	4.50	0.28	5.00
SAG-104	6.90	6.09	38.5	30.7	4.50	5.40	1.30	0.04	3.80	0.51	4.90
SAG-113	7.30	6.30	35.5	29.2	2.30	12.50	0.50	0.06	5.10	0.25	3.95
SAG-118	3.40	1.82	42.4	33.9	5.70	4.50	1.50	0.10	0.40	1.00	7.60
SAG-119	-	12.37	31.8	22.2	2.40	14.80	3.60	0.10	3.70	1.00	2.60
SAG-200	6.30	5.00	36.4	29.0	1.60	12.0	0.10	0.10	8.60	1.00	3.70
SAG-201	9.10	5.80	36.0	20.8	1.20	3.60	0.11	0.10	14.30	0.34	5.40
SAG-202	6.70	4.30	37.9	23.7	1.30	4.50	0.10	0.10	11.30	0.36	6.70

All samples were vaporised from molybdenum cells in their ‘as received’ state without any preliminary treatment. For one mould powder (SAG 202) a decarburised sample (1 hour at 750ºC in air) was also examined. The heating rate was set at 100ºC/hour for all samples except one (SAG 202), for which several heating rates in the range 30-3000ºC/hour were tested.

The mass of a sample charged into effusion cell (20 mg) was chosen as a compromise considering sufficient homogeneity of the sample, possible escape of the melt due to creeping and the rate of mass loss of volatile components at the given heating rate.

To facilitate the deciphering of the spectra some individual substances were vaporised in the same conditions (but from platinum cells): NaF, CaF_2, MgF_2, AlF_3, KOH, NaOH, LiOH, $Fe(OH)_n$, Na_2CO_3, K_2CO_3, $NaHCO_3$, LiF, Li_2CO_3, $CaCO_3$, Na_2AlF_6. Isothermal vaporisation of standard substances (Ag and CsCl) was performed periodically to check drifts of sensitivity and temperature inaccuracies.

The measuring procedure should allow for monitoring rapid changes of partial pressures that occur at some moments. Hence, the frequency of data readouts had to be no less than 1 in 10 min. The mass spectrometer parameters were set as follows:

- Dwell time (time of ion current integration) 2-60 s
- Resolution 25
- Number of masses (channels) in one cycle 5-10
- Duration of one cycle 1-4 min

Each vaporisation run lasted about 15 h while the temperature was evenly elevated from 50 to 1550ºC. 2000-3000 values of ion currents $I^+(m/z)$ were recorded in the positions "open" (orifice aligned with the axis of the collimator) and "closed" (background level), the difference being the resulting intensity. One sample of MP required 4-7 runs to check all the ion species that could be expected in the mass spectra, Table 4.2. In every experiment at least one $I^+(m_i)$ common with other runs had to be recorded to serve as the internal standard. Vaporisation curves are given in Appendixes 1, 2, 6. Several other mass numbers were inspected which are not presented on the plots since the results were either negative or not reliable.

Table 4.2 Expected ions and their masses (m/z^+)

12 $^{12}C^+$; Mg^{++}	29 $^{13}C^{16}O^+$; $^{29}Si^+$	46 AlF^+; $^{30}SiO^+$; Na_2^+	66 $^{28}SiF_2^+$
16 $^{16}O^+$	30 $^{12}C^{18}O^+$; $^{30}Si^+$	47 $^{28}SiF^+$	67 $^{29}SiF_2^+$
17 $^{16}OH^+$	33 SiF_2^{++}	48 $^{29}SiF^+$	68 $^{30}SiF_2^+$
18 $H_2{}^{16}O^+$	39 $^{39}K^+$; NaO^+	49 $^{30}SiF^+$	74 $^{55}MnF^+$
19 F^+	40 $^{40}Ca^+$	58 $^{41}KOH^+$; $^{39}KF^+$	75 $^{56}FeF^+$
22 CO_2^{++}; $^{28}SiO^{++}$	41 $^{41}K^+$	59 $^{40}CaF^+$; $^{41}KOH_2^+$	84 $Na_2F_2^+$
23 Na^+; AlF^{++}; $^{30}SiO^+$	42 NaF^+; $^{42}Ca^+$	60 $^{28}Si^{16}O_2^+$; $^{41}KF^+$	85 $^{28}SiF_3^+$
24 $^{24}Mg^+$; $^{29}SiF^{++}$	43 $^{24}MgF^+$; AlO^+	62 $AlOF^+$; $^{30}Si^{16}O_2^+$;	104 $^{28}SiF_4^+$
25 $^{25}Mg^+$	44 $^{12}C^{16}O_2^+$; $^{28}SiO^+$;	$^{28}Si^{16}O^{18}O^+$, Na_2O^+;	107 $Na_3F_2^+$; $^{107}Ag^+$
26 $^{26}Mg^+$	$^{25}MgF^+$; $^{44}Ca^+$	$^{24}MgF_2^+$	
27 Al^+; $^{54}Fe^{++}$	45 $^{13}C^{16}O_2^+$; $^{29}SiO^+$;	63 $^{44}CaF^+$; $^{25}MgF_2^+$	
28 $^{12}C^{16}O^+$; $^{28}Si^+$	$^{26}MgF^+$; $^{12}C^{17}O^{16}O^+$	65 Na_2F^+; AlF_2^+	

With numerous rapidly changing ion currents precise tuning on the mass scale is hardly possible. For this reason the mass scale has been adjusted using the peaks of residual gases and standard substances vaporised in the calibration trials. Then during measurements, mass channels were set on integer values of mass numbers, possible deviation from actual values being assessed as ±0.15.

Quadrupole mass spectrometers are characterised by moderate mass resolution. An $I^+(m_i)$ of small intensity may be disturbed by a contribution from the neighbouring high peaks $I^+(m_i \pm 1)$. This is why the mass numbers adjusting intensive peaks, like CO^+ or CO_2^+, were checked additionally. For example, ion currents at m= 45.25 and 45.75 with the resolution=7 were recorded (not shown on the charts) to find out if $I^+(45)$ is 'a tail' of an intensive peak $I^+(44)$.

4.2 Interpretation of mass spectra

Ion currents must be separated according to their molecular precursors. This can be done, in fact, half-qualitatively and with a degree of uncertainty, by the

collation of ion currents, Appendix 1, while taking into account MP compositions, Table 4.1, abundance of isotopes, Table 4.3, constants of reactions in the gas phase, Table 2.6, and experimental data for individual substances. The reference data for fragmentation patterns of gas molecules, Table 4.4, may also be helpful, though it is used more commonly in gas analysis. The following scheme of treatment was applied:

Ions were assigned to groups originating from or related to the same molecular species: H_2O, CO_2, NaF, KF, SiF_4, SiO_2, AlF_3/AlOF, MgO/MgF_2. If some ions of one group demonstrated similar behaviour of their $I^+(T)$, Appendix 1, i.e. their vaporisation curves were 'parallel' on the logarithmic scale, they were verified by the intensity ratios, Table 4.3. Approximate equality of these ratios to isotope abundances indicates that the ions are formed by different isotopes of the same element and are chemically identical. In case of coincidence of masses, ions from different groups were corroborated by the species that are unique to a group. After the evaluation of gas pressures the initial spectra were analysed once more to make sure that they are compatible with the final results.

Table 4.3 Isotopes important for interpretation of mass spectra (Balzers, reference data)

Element	Mass number	Abundance	Element	Mass number	Abundance
1 Hydrogen	1	100.0	14 Silicon	28	92.2
3 Lithium	6	7.4		29	4.7
	7	92.6		30	3.1
6 Carbon	12	98.9	18 Argon	40	99.6
	13	1.1	19 Potassium	39	93.1
8 Oxygen	16	99.7		41	6.9
	18	0.2	20 Calcium	40	97.0
9 Fluorine	19	100.0		42	0.6
11 Sodium	23	100.0		44	2.1
12 Magnesium	24	78.7	25 Manganese	55	100.0
	25	10.1	26 Iron	54	5.8
	26	11.2		56	91.7
13 Aluminium	27	100.0		57	2.2

Thus, the curves in Appendix 1 were interpreted as follows:

H_2O. Ion currents of m=18 and 17 are in reasonable agreement with the values of Table 4.4 and unambiguously indicate the presence of H_2O(g) in the gas phase. Hence, the partial pressure of water can be immediately determined, though the accuracy is rather low, as can be seen from Fig. 3.3.

CO_2. The problem is to separate the components of spectra originating from CO_2(g), CO(g) and SiO(g). CO_2^+ and SiO^+ can be distinguished by the ratio $I^+(44):I^+(45)$. For silicon monoxide it is nearly five times that of carbon dioxide so that $I^+(44)$ obviously splits in two parts: $I(CO_2^+)$ below 800ºC and $I(SiO^+)$ above 1100ºC. Additional proof for $^{30}SiO^+$ is available with $I^+(46)$ for samples with low alumina content, since $I^+(^{12}C^{16}O^{18}O)$ is negligibly small. Similarly the ratio $I^+(44):I^+(28)$ is different in these temperature regions, which implies that at lower T m=28 originates mainly from CO_2(g) and at higher T supposedly from CO(g). It agrees well with the well-known Boudouard's reaction, but the question is whether $I^+(28)$ stems from $^{28}(CO)^+$ or $^{28}Si^+$ ions. The ion current of $^{12}C^+$ confirms that its major component is $^{28}CO^+$ with a smaller fraction of $^{28}Si^+$which is impossible to separate.

Table 4.4 Fragment ions of H_2O, CO and CO_2 ($U_{ionis.}$=70V); I^+<0.5 are skipped; (Balzers, reference data)

Mass number	H_2O	CO	CO_2
12		6.3	9.7
14		0.8	
16	1.8	2.8	16.0
17	26.0		
18	100.0		
22			2.1
28		100.0	13.0
29		1.2	
44			100.0
45			1.2

NaF. Deciphering is based mainly on experimental data for pure NaF. In saturated vapour over NaF polymers up to Na_4F_4 could be detected, fragment ions being dominant in the mass spectra. In the non-saturated vapour over mould powders monomers, dimers and sometimes trimers were registered as $^{23}Na^+$, $^{65}(Na_2F)^+$ and $^{107}(Na_3F_2)^+$. For half-qualitative interpretation a simplified ionisation scheme was enough, i.e. these ions were considered as fragments of NaF, $(NaF)_2$ and $(NaF)_3$ respectively, though actually about 7% of $I(Na^+)$, for example, is a result of the $(NaF)_2$ fragmentation, /56/. According to crude assessment employing equilibrium constants of polymerisation, Table 2.6, a certain part of $I^+(23)$ has an origin other than sodium fluoride. More exact evaluation in a narrow temperature region was possible using the $I(Na^+)$:$I(NaF^+)$ ratio which should be the same for saturated, and non-saturated vapour. The vaporisation of pure sodium fluoride from Pt-cells showed that this factor equals 36. Then, part of $I(Na^+)$ originating from the fluoride could be taken as $36\times I(NaF^+)$ and this value was substituted in formula 3.1 for the calculation of p(NaF).

KF. An ion current of $^{39}K^+$ corresponds to the same mass as NaO^+, the existence of which is less probable /68/ but cannot be totally excluded from consideration /69/. Possibilities for the identifying of $I^+(39)$ were very limited. Molecular ion $^{58}(KF^+)$ is about 400 times less intensive in the spectra according to the literature data /70/ and could not be found. Partial pressure of $(KF)_2$(g) is also below the registration threshold of the apparatus. With very long integration times $I^+(41)$ produced by another potassium isotope could be detected and gave the proof, Table 4.3, that $I^+(39)$ results from K^+. Following /28/, it may be attributed to KF(g), though the temperature interval in that study was 200ºC lower.

SiF_4. Ion currents related to silicon fluorides obviously have more than one molecular source. In the interval 900-1100ºC the ions are Si^+, SiF^+, SiF_2^+, SiF_3^+ and SiF_4^+ (m=28, 47, 66, 85, 104) and their relative intensities correspond to ionisation pattern of SiF_4(g), Table 4.5. At higher temperatures $I(SiF_3^+)$ drops, $I(SiF_4^+)$ disappears, while $I^+(66)$ and $I^+(47)$ rise concurrently. The ratio of ion currents of m=66, 67 and 68 suggests that they have a common molecular precursor one of the atoms of which is silicon. If these ions are a result of fragmentation the only probable precursor other than SiF_4, is $SiOF_2$(g), but convincing proof of its existence in the vapour was not found. Therefore, these are molecular ions $^{28}SiF_2^+$, $^{28}SiF_2^+$ and $^{30}SiF_2^+$ and SiF_2(g) is predominant in the vapour. Analysis of vaporisation curves in Appendix 1 and the data of Table 2.8 bring to a conclusion that above 1100ºC silicon fluorides are represented mainly by SiF_2(g) with an admixture of SiF(g), plus some amount of SiF_4(g) decreasing on the time/temperature scale.

Table 4.5 Mass spectrum of SiF_4 ;$U_{ionis.}$=70V (Balzers, reference data for quadrupole m.s.)

Mass	14	19	28	33	47	66	85	86	87	104
Ion	Si^{++}	F^+	Si^+	SiF_2^{++}	SiF^+	SiF_2^+	SiF_3^+	SiF_3^+	SiF_3^+	SiF_4^+
Intensity	0.6	1.9	4.0	3.7	3.2	0.5	100	5.2	3.4	1.5

Mg. Ion currents of $^{43}(MgF)^+$, $^{62}(MgF_2)^+$ and $^{24}Mg^+$ in the mass spectrum of saturated vapour over MgF_2 are related as 100:5:3. The curves $I^+(43)$ and $I^+(62)$ in Appendix 1 are common to magnesium fluorides and aluminium oxifluorides, for which reason they could not be used for decoding directly. But m=24, 25 and 26 definitely represent Mg^+ since the ratio I(24):I(25):I(26) closely corresponds to the abundance of magnesium isotopes, Table 4.3. If $I^+(24)$ were a result of the fragmentation of $MgF_2(g)$, it should be 30-100 times smaller, hence this ion current is a combined result of the ionisation of Mg(g) and MgF(g), the ionisation scheme for which is unknown. Reactions governing the vaporisation process are given in Table 4.6. From these values it can be concluded only that Mg, MgF and MgF_2 may coexist in the vapour their relative amount being dependent on the temperature and slag composition. For SAG 202, as an example, vaporisation curves $I^+(24)$, $I^+(43)$ and $I^+(62)$ are largely uncorrelated. Analysing also their relative intensities, it was assumed that they originate from Mg(g), MgF(g) and AlOF(g) respectively. It is clear that such ascription is to some extent arbitrary and is fraught with large mistakes, but these are compensated for by the simplicity of further analysis.

Table 4.6 Equilibrium constants /71/regulating the amount of Mg and MgF in the vapour

Reaction	Equilibrium constants			
	1200°C	1300°C	1400°C	1500°C
MgO+C=Mg(g)+CO(g)	2.29E-7	5.70E-6	9.56E-5	1.16E-3
$MgF_2(g)$+Mg(g)=2 MgF(g)	1.06E-2	1.80E-2	2.86E-2	4.31E-2

SiO_2. Ions with the mass numbers 44, 45 and 46 indicate that above 1100°C they are products of SiO(g) ionisation. Dimers of silicon monoxide should also be present in the vapour as follows from the experimental data for the (SiO_2+Si) system known from the literature, /72/. Thus, there are some grounds to attribute the observed $I^+(60)$, i.e., SiO_2^+, to $(SiO)_2$, though neither the ionisation pattern nor intensity of this ion current are in agreement with the works, rendered in /72/. It is at least 1-2 orders of magnitude higher than could be expected, but $I^+(60)$ for SAG 104 is anomalously high even in comparison to other samples. Yet, the only other conceivable molecule is $SiO_2(g)$ the reported pressure of which, /72/, is still several orders of magnitude lower. Probably, the observed vapour composition is a result of the high carbon content in the melt.

AlF_3. The expected Al-containing species in the vapours are AlF_3, AlF_2, AlF, Al and AlOF. The ion currents related to this group of ions were recorded at m= 27, 43, 46, 62, 65 and 84. The mass spectrometric data, including pure AlF_3, is too scarce and inaccurate to make any stringent analysis. The curve for $I^+(27)$ had to be abandoned, because despite all efforts could not be definitely separated from the neighbouring $I(CO^+)$. $I(AlF^+)$ can be taken only as a difference $I^+(46)$-$I(^{30}SiO^+)$. The second term is calculated from $I(^{29}SiO^+)$ and is aggravated with great uncertainties. Consequently, the experimental data was classified in the simplest possible way. The ion current m=62, as it was mentioned above, was attributed wholly to AlOF. All others were regarded as having the same origin, that is $AlF_3(g)$, though at T>1400°C its partial pressure should be much lower than $AlF_2(g)$ and AlF(g). Thus, $p(AlF_3)$ was

determined from $I^+(65)$. However, this ion current is a sum of $I(AlF_2^+)$ and $I(Na_2F^+)$. The latter could be accounted for only in the T-interval where NaF^+ was detectable.

Fe, Mn. Iron and manganese were expected to evaporate as fluorides, /28/. In the earlier part of the work /29/ when 'CSM' types of mould powders (provided by Centro Sviluppo Materiali, Rome, Italy) were studied FeF^+ and MnF^+ ions were easily detectable in the mass spectra. The manganese content in the SAG-samples was too small, Table 4.1, so Mn-containing species were not examined thoroughly. No vapour species containing Fe were found either.

Low temperature interval. In search of the expectable but missing vapour species (Fe, K, HF), and for an assessment of the water content in MP, the lower limit of the temperature interval of the measurements was set at 50°C. It was supposed that some elements could be present in MP in the form of hydroxides, carbonates or more complex compounds. Accordingly, the masses to be recorded were selected. Mass spectra, Appendix 1, allowed identification only of H_2O and CO_2 resulting from desorbtion/decomposition. A number of vaporisation curves lying in the temperature range 100-450°C below 10^{-12}-10^{-11}A could not be deciphered. Individual substances start to evaporate at higher T: KOH – 350, NaOH – 420, Li_2CO_3 – 550°C, K_2CO_3 – 750, Na_2CO_3 – 750 (the samples usually had considerable admixtures of H_2O and CO_2 which evaporate below 150°C). At the given experimental conditions, full calcination of $CaCO_3$ occurs between 470 and 600°C and this may probably explain the decarburisation curves $I(CO_2^+)$ observed for mould powders below 700-800°C, Appendix 1. Only KOH and maybe $(KOH)_2$ yield some contribution to this group of small ion currents. However, these unidentified vaporisation curves are well reproducible, do not disappear after decarburisation, Appendix 6, or higher heating rates, Appendix 2. Probably they are binders or some other technological admixtures, but most likely not organic substances judging from the low intensity of $I(C^+)$. The important findings in the lower temperature range are: (i) HF(g), if it is present, is below the detectable limit; (ii) maxima on the curves for SAG 201 at T=380°C (among which $I(Na^+)$ is identified) prove that components volatile below 400°C may be present in mould powders. Total mass loss corresponding to these low intensity ion currents may be assessed as 10^{-2}-10^{-1} mg, therefore they will be not considered further.

The mass spectral data sorted out for the calculation of partial vapour pressures are given in Appendix 3.

A note about fragment ions. The relative intensity of different fragment ions measured with the apparatus in Fig. 3.4, was found to be considerably different from the reference data used in the gas analysis, Table 4.4. The ratio $I(CO_2^+)/I(C^+)$ measured for a number of carbonates indicated that this is a regular feature. To some extent it can be explained by different experimental conditions: in gas analysis the analysed gas uniformly fills the ionisation box of ion source, while in the last modification of our mass spectrometer the molecular beam passing through the ion source was 0.8-0.9 mm in diameter. Extraction potential and other parameters of ion optics may cause noticeable discrimination effects for different ions /73/, depending on the molecular mass and the point of ionisation.

4.3 Partial vapour pressures

Partial pressures calculated from ion currents (formula 3.1) are given in Appendix 4. In the principle, time/temperature dependence of the weight loss of all

components and flux composition can be calculated by the integration of the curves, but the results may be confusing and misleading due to low accuracy.

It is interesting, however, to assess the reduction of weight of the samples at the first stage of heating runs when the vapour phase composition is simple. In a series of experimental trials the samples of mould powders were loaded into the effusion cell in special containers with thin walls allowing the easy extraction of residues and precise determination of their weight. After the standard procedure of heating (100°C/h) up to 600°C the samples were rapidly cooled down and weighed. The results are presented in Fig. 4.1. The measured weight losses are in quite acceptable agreement with the values derived from the mass spectrometric data. It is hardly possible to perform the same procedure at higher temperatures (above the melting point) because of the difficulties connected with the extraction of small amounts of residues from the cells without altering their weights.

The precision of the assessments of weight changes by the integration of vaporisation curves can be judged also from the results concerning different heating rates, Appendix 2. Though in this case the removed mass of different slag components should depend on the heating rate, the curves for some of the vapour species are in satisfactory agreement (coefficients accounting for different times of effusion were introduced).

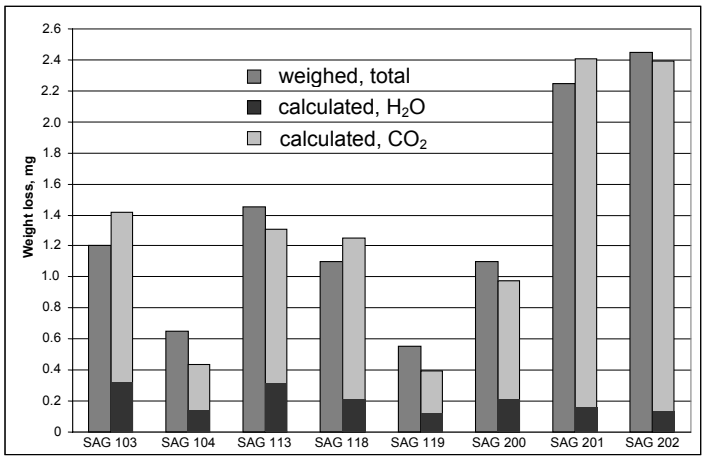

Fig. 4.1 Weight loss of mould powder samples (m=20 mg) after heating up to 600ºC calculated from vaporisation curves and measured directly.

4.4 Reliability of the results

Major results are deduced from the vaporisation curves. Their reliability and possible mistakes are connected with:

- Systematic errors. These include misinterpretation of the mass spectra or omission of important ions, approximate values of the constants used for assessment of the device sensitivity, the unknown effects of the interaction of the samples with the material of the cells and the deviation of the effusing gas flow from the Hertz-Knudsen law when the partial pressures of CO_2 or CO exceed the limits of validity of the method.
- Malfunctioning of equipment. In the present work it included the imperfect initial positioning of the crucible and its displacement in the course of heating, possible small variations in the shape of the effusion orifice, occasional escape of molten

samples out of the cells due to creeping and other factors reducing reproducibility. Total errors could be assessed as ±20%. Results of the experimental runs, which did not fit these limits, were discarded as a rule.

- Statistical fluctuations. Usually these can be reduced by an increase of measuring time, but in the present work it was not always feasible. At best (Na^+) mean root square deviation of the ion current was about 3%. For less intensive currents and/or amore 'dirty' background it was 5-10%, and for the ion currents measured only to get some evidence of the existence of molecular species in the vapour, like $^{104}SiF_4^+$ or $^{41}K^+$, only the order of magnitude may be correct. High precision was not the main priority of the work and in most cases it was unachievable, since the ion currents were always obtained as a difference between two fluctuating values. Hence, DWELL time in the mass spectrometer was usually set at a minimum determined by the possibility of further correct interpretation of the curve.

The reliability of the results was proved by the agreement of the vapour pressures of the standard substances measured in calibration trials with the reference data, general consistence of the results and their compatibility with the information found in the literature.

4.5 Fluorine-free mixtures

As a part of project /26/, this work was aimed at the properties of modified and newly developed fluxes. Though later the focus of attention shifted slightly, the results concerning pre-fused and Li-substituted powders still have some value and may be interesting. The measurements were performed with the previous, less discriminative modification of the evaporation chamber. However, no great errors have been found in the results since.

Tests with fluorine-free synthetic mixtures were performed to support further studies of Li-containing samples, i.e. to facilitate the interpretation of their mass spectra. The main problems of decoding were the separation of the components of $I(Li^+)$ originating from Li(g), LiF(g) and Li_2O(g) and the distinguishing of $^{23}(LiO)^+$ from $^{23}Na^+$. Vaporisation curves of pure Li_2O were recorded several times but for some ions essential for interpretation, for example $^{30}Li_2O^+$, reliable data could not be obtained because of the deficiency of pumping system and unfavourable position of the lithium-containing ions (both $^7Li^+$ and $^6Li^+$) on the mass scale. The data for fluorine- and carbon-free synthetic compositions could provide additional means for the deciphering of the mass spectra.

Compositions of the samples prepared by IIST in Freiberg /20/ are given in Table 4.7 with corrections for the decomposition of $CaCO_3$ and $SrCO_3$ (in effusion cell it is completed at T<650°C and has little effect on further vaporisation process). Samples denoted 'CX' and 'VLS' form two series with the stepwise substitution of Na_2CO_3 by Li_2CO_3 and of Li_2CO_3 by $SrCO_3$.

Table 4.7 Fluorine-free mixtures containing oxide fluxing components Li_2O, Na_2O, SrO; compositions in wt%

Type	No.	SiO_2	CaO	MgO	Al_2O_3	Fe_2O_3	MnO_2	Na_2CO_3	Li_2CO_3	SrO
CX	2	35.86	29.51	2.32	12.63	0.50	0.06	9.15	9.97	0
	5	35.50	29.22	2.30	12.50	0.50	0.06	6.84	13.08	0
	8	35.24	29.00	2.28	12.41	0.50	0.06	5.09	15.43	0
	11	34.98	28.78	2.27	12.32	0.49	0.06	3.37	17.74	0
	14	34.72	28.57	2.25	12.22	0.49	0.06	1.67	20.02	0
	19	34.46	28.36	2.23	12.13	0.49	0.06	0	22.27	0
VLS	5	39.19	31.26	4.85	3.92	1.31	0.28	1.90	17.30	0
	6	40.87	32.60	5.06	4.09	1.36	0.29	1.98	10.83	2.92
	7	41.77	33.32	5.17	4.18	1.39	0.30	2.03	7.38	4.48
	8	42.71	34.06	5.29	4.27	1.42	0.31	2.07	3.77	6.10

The mass spectra of the samples consisted of Li^+, Na^+, LiO^+, Mn^+ and Fe^+. The vaporisation curves, Appendix 5, were recorded in experimental conditions uniform for all the present study, $I(Mn^+)$ and $I(Fe^+)$ are skipped for simplicity as having minor importance. Deciphering was based on the assumptions:

- Li^+ originates from $Li_2O(g)$; such a conclusion can be made from the literature analysis, e.g. /72/, and from the similarity in the behaviour of ion currents $I^+(7)$ and $I^+(23)$ at T>1400°C: $I(LiO^+) = (0.22\text{-}0.25)\cdot I(Li^+)$ for all samples.
- The ion current $I^+(23)$ at T>1400°C is formed mostly by LiO^+(previous point);
- At T<1400°C the ion current $I^+(23)$ is formed mostly by Na^+.

The last statement may be illustrated by comparison of the curves, Appendix 5 and Fig. 4.2. Below 800°C Na(g) is a result of the decomposition of Na_2CO_3, the formation of silicates and oxidation of Mo, whereas at higher temperatures silicates are the main source of gaseous sodium. Probably, the small maxima on the curves $I(Li^+)$ can be explained similarly.

The mixture CX-19 exhibits irregularity: $I^+(23)$ has a big maximum at T=800°C though this mixture contains no Na. In the vaporisation tests of pure lithium carbonate, LiO^+ and Li_2O^+ were detected at 650°C and 1200°C. At high temperature they refer to $Li_2O\text{-}MoO_3$. At 650°C the data is not reliable since Li_2CO_3 decomposition and emission of CO_2 spoils the mass spectra. According to the reference data /74, 75/ the pressure $p(Li_2CO_3)$ at 650°C is about $2\cdot10^{-5}$ atm. If LiO^+ and $Li_2O^+$are fragments of $Li_2CO_3(g)$ this may explain the curve for the CX-19 and should be taken into account for other samples as well.

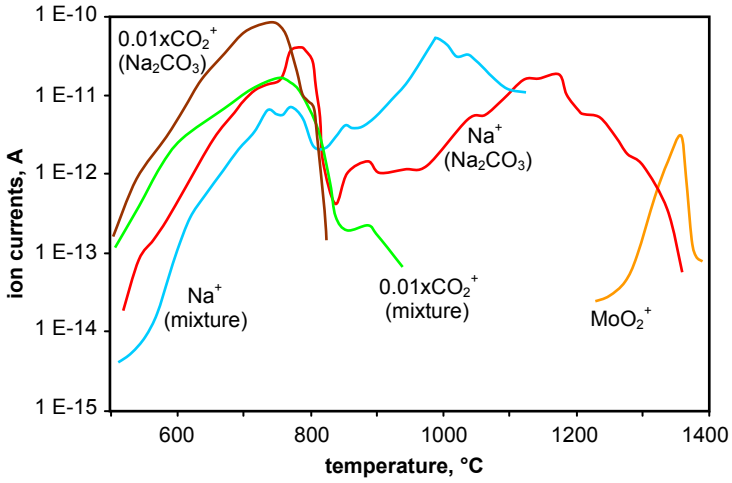

Fig. 4.2 Vaporisation of $(Na_2CO_3+SiO_2+C)$-mixture compared to pure Na_2CO_3

Vaporisation curves converted to vapour pressures are shown in the figures. Applying the Hertz-Langmuir formula to them, the emission of alkaline metals can be assessed, Table 4.8 (T=1400°C is chosen as the point when the evaporation of sodium drops to a negligible rate).

Table 4.8 Mass loss of Li, wt% to initial content, during elevation of temperature up to 1400°C; heating rate 100°°C/h, orifice diameter =0.29 mm, initial mass 20 mg.

Type	CX						VLS			
No.	2	5	8	11	14	19	5	6	7	8
Mass-loss	41.3	39.8	46.4	46.7	41.8	39.2	8.2	5.5	2.5	2.9

For the VLS series the correlation of vaporisation curves with compositions and mass loss is quite regular: the higher the concentration of a component, the greater is the area under the corresponding curve and the mass loss. For the CX series relative values are nearly the same, so that absolute emissions are proportional to Li_2O contents in first approximation.

The total substitution of fluxes with SrO (not revealed in gas phase) would give perfect 'environmentally friendly' mould powders.

4.6 Pre-melted mould powders

Preliminary separate melting of oxides and subsequent addition of fluorspar is supposed to reduce the amount of emission of fluorides. Measurements of weight loss in air conditions carried out at Centro Sviluppo Materiali (CSM), as well as reported in /28/, confirm this idea. However, no mass spectrometric data on pre-melted samples are given in this article. It is interesting to compare the results in these two cases to get hints of the applicability of vacuum measurements to real processes.

CSM 3 mould powder and modified compositions prepared on its basis at CSM were taken as a trial object. In its initial state (the 'reference powder') it contains, wt%:

SiO_2	35%;	(Na_2O+K_2O)	15.7%;	MnO	2.0%;
(CaO+MgO)	28.5%;	Fe_2O_3	<1.0%;	F	8.5%;
Al_2O_3	2.7%;	CO_2	7.5%.		

The phases revealed by X-ray analysis /20/ in the initial compositions were: CaF_2, Na_3AlF_6, SiO_2, $Ca_3Al_2Si_3O_{12}$. The experimental procedure and conditions were the same as the previous.

Cryolite content is a specific feature of CSM 3. No data concerning composition of the vapour above pure Na_3AlF_6 were found in the literature. Some of the mould powders studied in /28/ contained cryolite. Mass spectra of their vapour phase included $NaAlF_3^+$ and $Na_2AlF_4^+$. Decoding of the spectra led the authors to the conclusion that $Na_2AlF_5(g)$ and $NaAlF_4(g)$ were among the main vapour species. In the present work the mass spectra of CSM 3 could not be interpreted so definitely. The data obtained for pure Na_3AlF_6 were of little help because ion currents corresponding to m=107 ($NaAlF_3^+$) and m=149 ($Na_2AlF_4^+$) were too small. These masses coincide with those of $Na_3F_2^+$ and $Na_4F_3^+$, which are found in the mass spectrum of pure NaF(s,l). Thus, mass spectra of cryolite and sodium fluoride is not easy to distinguish, especially taking into account that according to /28/ cryolite dissociates in the vapour yielding NaF(g) and $Na_2F_2(g)$. Moreover, there is another source of NaF(g) in mould powder and hence the equilibrium may be shifted. Smallness of $I^+(107)$ and $I^+(149)$

and the relation between Na^+ and Na_2F^+ ion currents lead to an assumption that below 1100°C the vapour is formed predominantly by NaF(g) and its dimer while the partial pressures of cryolite molecular species are relatively small.

Vapour pressure curves derived from the mass spectra are given in Fig. 4.3. Pre-melting seems to have no great impact on their general character:

- Intensity of more volatile components (NaF, Na_2F_2) decreases, less volatile increases;
- Na practically disappears from the vapour phase at T<600°C;
- SiF_4 curve shifts toward higher temperatures.

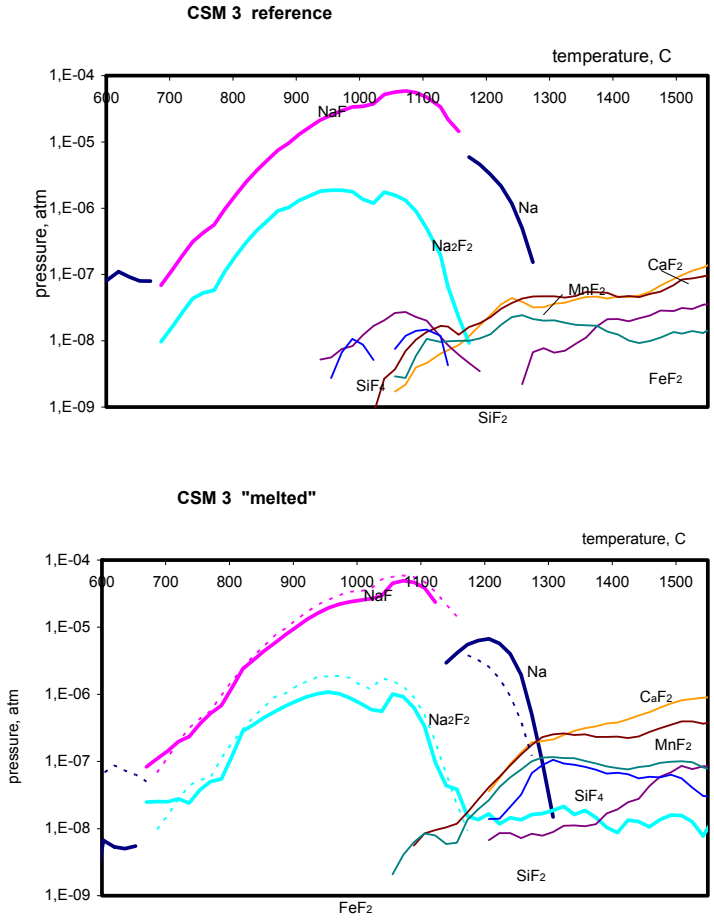

Fig. 4.3 Effect of preliminary melting on the vapour pressure; dotted curves are copied from the upper plot for comparison.

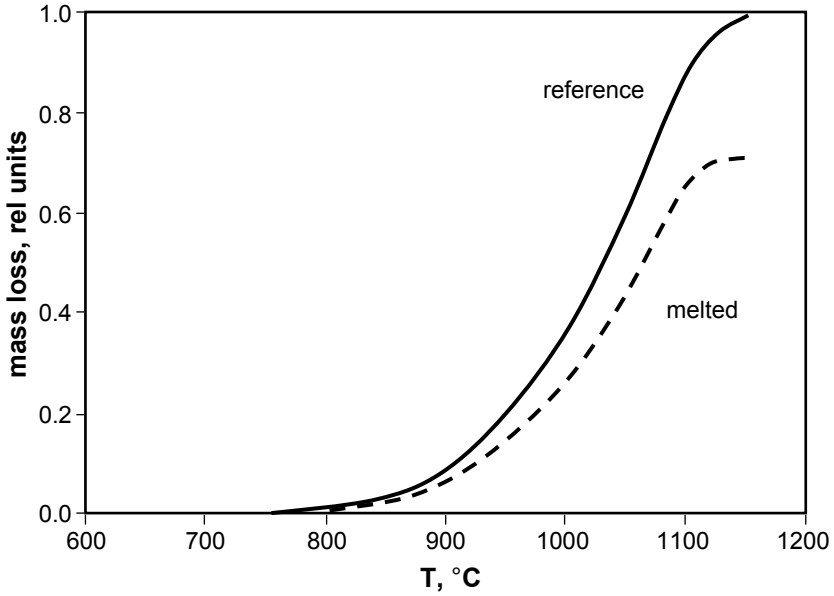

Fig. 4.4 Relative evolution of fluorides $NaF+Na_2F_2$ from mould powder CSM 3 (reference and pre-melted); heating rate 100°C/h; the ordinate value 1.0 approximately equal to 1.7 mg.

Thus, during slow heating in vacuum conditions vaporisation of fluorides occurs at higher temperatures for pre-melted compositions. Fig. 4.4 illustrates to what extent emission is reduced by pre-melting if heating is stopped at some temperature below 1100°C (assessment was made by Formula 3.2).

4.7 Lithium substitution

In the samples prepared at CSM, lithium was introduced into mould powders in the form of Li_2CO_3. For the mass spectrometric study of the vapour phase mixture CSM-3 with an index of fluorine substitution equal to 0.28 was chosen, /26/.

Standard methods of mass spectra deciphering (measurement of the appearance potentials of ions, isothermal vaporisation etc.) are not applicable to mould powders. That is why interpretation of vaporisation curves was based on a more complex approach than previous and included:

- Special, more accurate measurements (with increased integration times) intended to detect molecular ions like NaF and Li_2O;
- Experiments at reduced ionisation voltage (20V) providing better signal/background/noise ratio in some ranges of mass spectra;
- Analysis of monomer, dimer, and trimer ion currents and their compliance with constants of reactions of polymerisation;
- Comparison with the vaporisation processes of CX fluorine-free mixtures.

The vapour pressure curves obtained as a result are given in Fig. 4.5. The diminishing of the fluorine content dramatically modifies the vapour phase:

- New components, LiF and Li_2O, appear in the vapour;
- Total amount of evaporated fluorides is much smaller;
- Less volatile fluorides CaF_2, MnF_2, FeF_2 are completely exterminated;
- A greater part of the sodium evaporates in the form of Na(g).

The origin of two maxima on the Na-curve is not clear. The first one, at T=1160°C, repeats the peak of p(Na) for the CX-2 mixture, Appendix 5. The sharp maximum at

T=1330°C has no analogues. The smoothness of the p(Li_2O) curve implies that it is not misinterpreted, I(LiO^+) having the same mass number m=23. At the ionisation voltage 20 V the second maximum is not clearly distinguished but p(Na) is also extended to T>1300°C.

Other Li-containing samples that were examined vaporise in a similar way. Above 1100°C only a small amount of SiF_2 was found in the vapour additionally to Na and Li_2O.

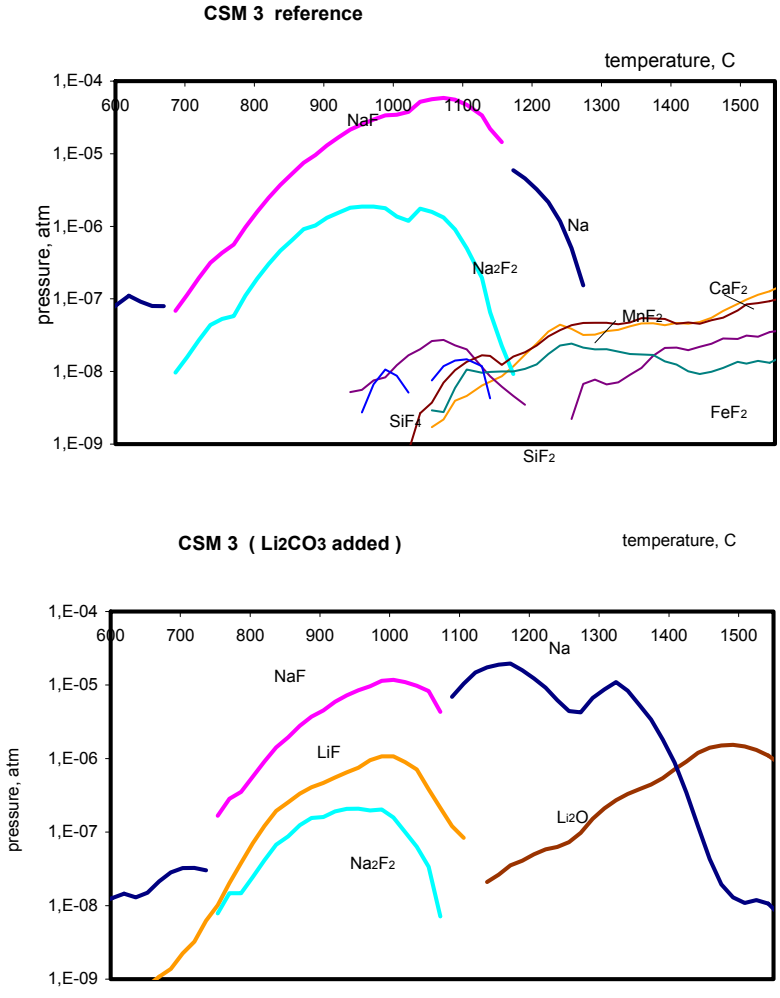

Fig. 4.5 Effect of partial substitution of CaF_2 with Li_2CO_3 in mould powder CSM 3

5 DISCUSSION

5.1 Gas emissions in effusion experiments

All laboratory trials were based on the same principles and methods of partial pressure determination, but had some variations conditioned by practical aims motivating the whole study. The most essential departure from the traditional Knudsen method was the permanent temperature elevation during the experimental runs dictated by the multi-phase nature of the mould powders.

As a first step, /29/, the effect of the heating rate was examined in order to determine the experimental conditions: high heating rates comparable to those of a real caster were supposed achievable in the mass spectrometer and relevant trials had to show if the method remains valid. The upper limit of validity was found to be much lower and the heating rate was set as low as 100°C/hour, primarily with regard to the device sensitivity. During further investigations, especially when the temperature range was broadened, the optimum was found to be 150-200°C/hour, but the initially adopted heating rate had to be retained for compatibility. With sufficient knowledge of the mass spectra and improved equipment these tests were repeated, several curves are given in Appendix 2. Their implications are very important:

- The principal features of mould powder sublimation are uniform for the rates of temperature elevation in the interval 30-3000°C/h. The vapour phase components and their relative amount remain largely the same. Precise calculations of the mass balance by the Hertz-Knudsen formula were not possible because the curves could not be easily calibrated, but assessments provide quite reasonable values. The evaporated mass of components is scattered within ±(20-30)% for different temperatures.
- I(SiF_3^+) undergoes a certain modification: a maximum at 1000°C (30°C/h) gradually transforms into another maximum at 1300°C (3000°C/h).
- Sharp peaks on the curves cannot be attributed in all cases to melting points since their position on the T-scale is not fixed. For 30 and 3000°C/h the observed shift on the plots is more than 200°C.

Comments about higher heating rates should be made: (i) the temperature gradients in the crucible are expected to be much higher than in other experiments, (ii) the smoother shape of the curves is partly due to the scarcity of experimental points, 2-3 recorded values per 100°, (iii) the measured partial pressures of CO_2 and CO approach 10^{-4}atm already at the heating rate 100°C/h, at higher pressures the method is usually considered to have limited applicability.Thus, the chemical reactions and their sequences in the effusion cell may be not very different from those in the mould.

The variety of the investigated mould powders (17 in all) gives an idea of both the regularities and peculiarities of evaporation processes. The samples were selected to cover a wide range of compositions and types. However, the volatile properties of MPs are diverse and other types may exhibit different features. It is interesting to compare the curves in Appendix 4 with the results of Zaitsev and co-workers /28/ as far as the present study closely follows their work in its mass spectrometric part. The mould powder supplier was not specified there, but at least some of their samples, Table 2.4, were not similar to ours, Table 4.1. Which SAG-powder is the closest analogue of No.2 sample presented in Fig. 2.9 is not obvious, therefore SAG 202 was taken for comparison, since it was more thoroughly examined. The partial pressures of the main components plotted against the temperatures are reproduced in Fig. 5.1

(curved from Appendix 4, refined). Small partial pressures disappear on the linear scale, but the contribution of different vapour species to gas emission can be seen more explicitly.

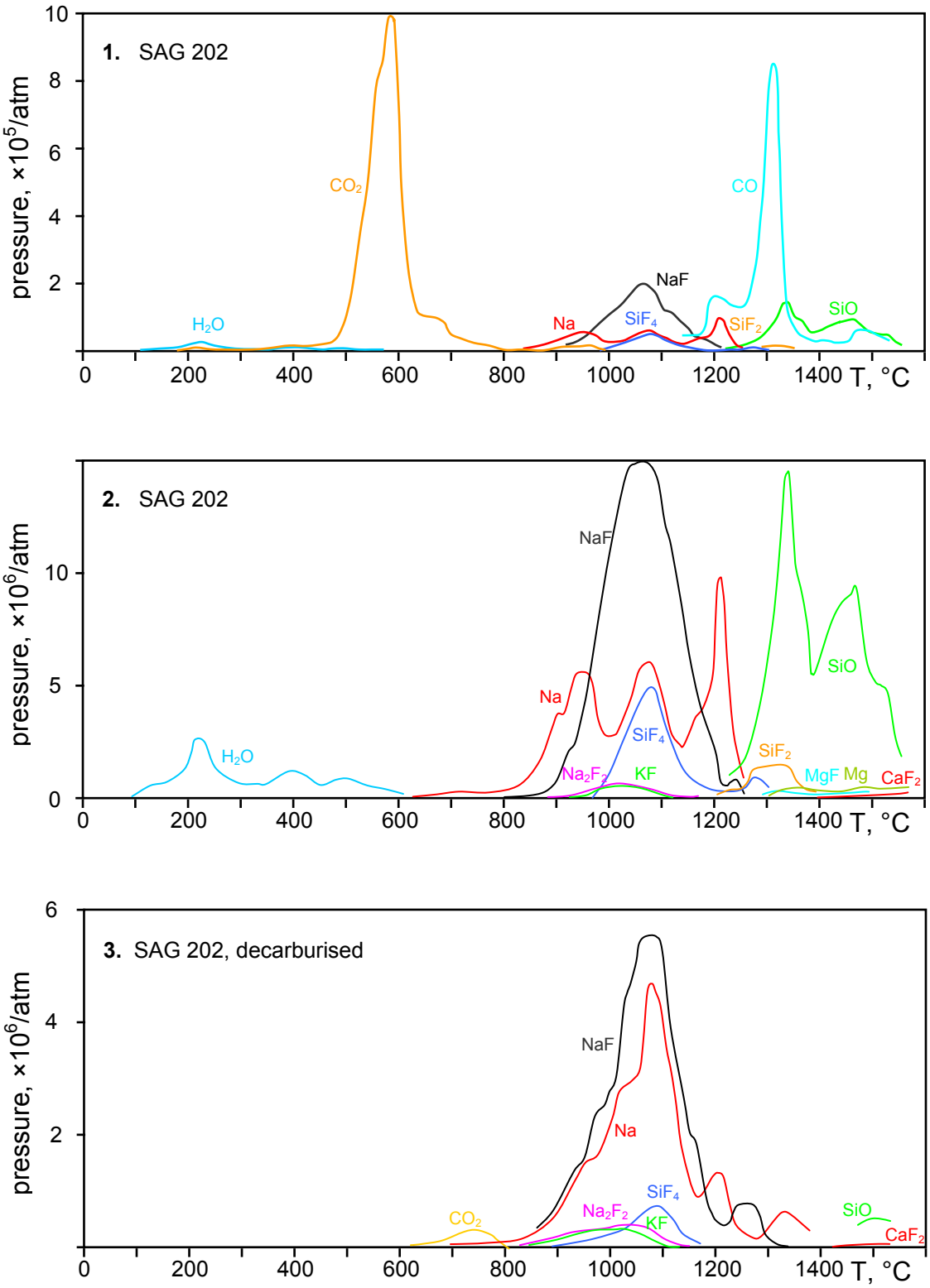

Fig. 5.1 Partial vapour pressures over mould powder SAG 202. 1- sample not subjected to preliminary heat treatment (contains carbon and carbonates); 2 – the same curves given on enlarged scale; 3 - decarburised sample. Heating rate 100°C/h.

A closer inspection of Fig. 2.9 and Fig. 5.1 reveals more differences than similarities (it is worth noting, however, that the objectives in /28/ were strictly reserved and their mass spectrometric results were not intended for detailed scrutiny). Certainly, the experimental parameters were not the same and the compositions of mould powders could be very different. Nevertheless, some points are arguable. The essential objections are:

- Only fluorides are mentioned as constituents of the vapour phase. The highest peak is NaF(g) and its maximum corresponds to a rather low temperature. The absence of $Na_2F_2(g)$ dimer on the plot is unexplainable in these conditions, the more so that its ion mass is the same as AlF^+_2 and therefore it could not be overlooked.
- The possibility of the formation of carbides in flux melts is discussed, but the role of carbonates and reactions of carbon with oxygen were neglected.
- Despite the fact that mould powder fluxes have melting points lying usually above 1000°C, NaF and KF on Fig. 2.9 were regarded as evaporating from molten powders, probably because the investigation widely refers to the previous data on the slags.

Nevertheless, the main conclusion of /28/ is confirmed by Fig. 5.1: the greater part of fluoride emissions is formed by NaF, KF and SiF_4.

In general, the vaporisation curves in Appendix 4 are in satisfactory agreement with the brutto-compositions of the mould powders, Table 4.1. For example, the curves for SAG 103 and 104 of nearly identical compositions are very similar. Even the small difference in their C_{free}/C_{tot} ratio clearly shows itself in the temperature dependence of $p(CO_2)$ and $p(CO)$. Yet the chemical compositions are not sufficient for analysis when discrepancies are found, knowledge of the phase composition is required. For this purpose, structural analysis of the mould powders was carried out by Centro Sviluppo Materiali, /26/. Samples were analysed in their initial states without heat treatment, the results are given in Table 5.1. The phases found in the table have very little in common with those in Table 2.2, only $CaO \cdot SiO_2$ is the same.

Table 5.1 Mineralogical phases of mould powders and granules (/26/, CSM contribution)

Phase	SAG103	SAG104	SAG113	SAG118	SAG119	SAG200	SAG202
CaF_2	+	+	+	+	+	+	+
C(carbon black)	+	+	+	+	+	+	+
SiO_2	+	+	+	+	+	+	+
$CaSiO_3$	+		+	+		+	+
Ca_3SiO_5		+			+		
$CaAl_2SiO_6$	+		+	+		+	+
$CaAl_2Si_2O_8$			+			+	+
$(Al,Mn)_2(SiO_4)O$	+		+	+		+	+
$NaAlSi_3O_8$	+		+	+		+	+
K_2SiO_3			+			+	+

Moreover, in the two samples no phases containing sodium were found and in four samples potassium is missing, including SAG 118 and 200 with the highest K concentration. This means that routine measurements cannot provide adequate accuracy to make possible the detailed analysis of the reactions responsible for the formation of the vapour phase. Important for further discussion is that alkali metals are present in the mould powders only as components of the oxide systems, probably,

including carbonates, the amount of NaF is negligible (found only in one sample in Table 2.2).

In the vapour phase above the SAG-mould powders the following vapour species were detected: NaF, Na_2F_2, Na, KF, SiF_4, SiF_2, CaF_2, AlF_3, MgF, Mg, AlOF, SiO, Si_2O_2, CO_2, CO and H_2O. Some of the vapour components could not be distinguished from each other and for simplicity are referred to as one entity. Thus,'KF' in Appendix 4 indicates gaseous KF and/or K, 'SiF_2' - SiF_2, SiF and Si, 'AlF_3' - AlF_3, AlF_2, AlF and Al, 'MgF' - MgF_2 and MgF. The relative abundance of the species in these groups depends on the temperature and composition of the condensed phase, the experimental data alone does not allow us to point out the predominant ones. The vaporisation process obviously proceeds in three stages.

- Below 600-800°C H_2O and CO_2 are found in the vapour with minor additions of other volatile components like KOH.
- In the interval 600-1200°C alkali metals are evaporated, along with SiF_4 and AlF_3 at higher temperatures. The formation of CO(g) starts at the same time. Supposedly, sodium and potassium are present in the vapour in the form of Na(g)+NaF(g) and K(g) +KF(g). The presence of NaF(g) was proven in two ways: by the detection of the molecular ion $(NaF)^+$ and by the determination of Na_2F_2(g). The partial pressure of Na(g) could be derived from them only with great uncertainties, but in both cases the same trident-shaped curve was obtained, Fig. 5.1, 2.
- Above 1200°C p(CO) reaches its maximum and then drops. The main constituents of the vapour phase are SiF_2, SiO, Mg, MgF, AlF_3 and CaF_2.

At higher heating rates, Appendix 2, vaporisation curves of the two stages above 600°C tend to merge.

Decarburised powders, Appendix 6, are volatile only in one relatively narrow interval 600-1400°C.

There is clear evidence of the prevailing role of Na(g) compared to NaF(g) for some of the mould powder samples. At T<800°C half of the compositions studied demonstrate the values of the ion current $I(Na^+)$ one or two orders of magnitude higher than the saturated vapour of pure sodium fluoride. Probably, the mechanism of sublimation cannot be fully described only in terms of the reactions of fluoride formation, Table 2.6, the evaporation of the oxides themselves must also be taken into account. For example, the following sequence of reactions may be proposed in which Na(g) and NaF(g) coexist:

$$Na_2O = 2\ Na(g) + ½\ O_2(g) \quad (5.1)$$

$$CaF_2 + 2\ Na(g) + ½\ O_2(g) = CaO + 2\ NaF(g) \quad (5.2)$$

At 600°C partial pressure of Na(g) is about 10^{-7}atm according to the literature data /72/ (sublimation of Na_2O in BeO- or MgO-containers), which is high enough to explain the curves in Appendix 4. Similar reactions can be written for K_2O, but as potassium has a stronger affinity to fluorine than sodium, one more exchange reaction must be added:

$$NaF(g) + K(g) = KF(g) + Na(g) \quad (5.3)$$

As a result, the relative amount of K(g) in the vapour must be lower. Phases which can serve as the source of Na_2O(s), can be anticipated. It may be that Na_2CO_3 is a source referring to the publications concerning the decomposition of carbonates cited in

chapter 2. Below 700-800°C the $I(CO_2^+)/I(Na^+)$ ratio is big enough to support this idea. Above 1000-1100°C the rapid increase of p(CO) is observed and hence Na(g) may be a result of the direct reduction of Na_2O in the melt:

$$Na_2O + C = 2\ Na(g) + CO(g) \qquad (5.4)$$

It is clear, that the role of carbon may be important, but in the vapour of the decarburised powder, Fig. 5.1, the partial pressure of Na(g) remains quite noticeable.

In the temperature range 1400-1550°C, the data are less reliable, especially concerning the accuracy of the experiments. However, inasmuch as mould fluxes reach these high temperatures only at the points of contact with liquid steel, for the evaluation of gaseous emissions they are less significant.

Reduction of the weights of the samples inflicted by the evolving components can be obtained by the integration of the vaporisation curves in Appendix 4 (formula 3.2). Mass losses resulting from the vaporisation of fluorides during heating from 100 to1400°C at the rate 100°C/hour are given in Table 5.2. Also the amounts of sodium in the samples before heating (calculated from the start compositions, Table 4.1) and carried away by the gas flow are compared.

Table 5.2 Calculated total mass of vapour components evaporated during heating up to T=1400°; m=20 mg

	Sample							
Mass loss, mg	103	104	113	118	119	200	201	202
NaF+ Na_2F_2	0.093	0.078	0.142	0.000	0.051	0.444	0.759	0.781
KF	0.017	0.059	0.025	0.005	0.078	0.02	0.019	0.025
CaF_2	0.004	0.014	0.007	0.004	0.014	0.002	0.001	0.002
SiF_4+ SF_2	0.132	0.102	0.071	0.393	0.051	0.024	0.021	0.301
Fluorides total	0.246	0.253	0.245	0.402	0.194	0.492	0.801	1.109
Na	0.312	0.352	0.433	0.032	0.343	0.596	0.935	0.766
Na, chem. analysis	0.690	0.583	0.782	0.061	0.567	1.319	2.193	1.723
SiO	0.196	0.130	0.290	0.099	0.119	0.320	0.184	0.305
Basicity, CaO/SiO_2	0.93	0.80	0.82	0.80	0.70	0.80	0.58	0.63
Fluorine content, wt%	5.00	4.90	3.95	7.60	2.60	3.70	5.40	6.70

At the given experimental conditions a high accuracy of mass balance calculations cannot be expected. The agreement found in Fig. 4.1 may be regarded as good. Mass losses due to the effusion of CO(g) are about 20-40% less than those assessed from the carbon content of the mould powders and this is also reasonable in view of the relatively high uncertainties of p(CO) measurements. On the other hand, components containing Na could be measured quite accurately and systematic errors introduced by approximations (ionisation cross-sections, the conversion factor of the electron multiplier, application of the additivity rule) should not exceed 30-40%. Wrong determination of the molecular precursor of Na^+ could not lead to crucial mistakes in estimations of the removed Na either. Nevertheless, the values for evaporated Na in Table 5.2 differ considerably from the initial amount of Na in the compositions. Consequently, the evaporation of sodium from the samples is not complete: more than half of its total amount remains in the slag above 1400°C and the abrupt drop on the vaporisation curves $I(Na^+)$ does not mean that the concentration of

sodium becomes negligibly small, but most likely is connected with the melting of the powders and low activities of Na_2O in the fluxes, /76/.

Potassium demonstrates the same behaviour. Approximately half of its initial content is preserved in the melt and above 1200°C it could not be detected in the vapour, which indicates its low activity in the melt. Mass losses in SAG 118 and 200 are anomalously small. A possible explanation is that a bigger part of potassium of these powders evolves in the low temperature region in some unidentified form. Erroneous decoding of the mass spectral data cannot be totally ruled out also, but alternative explanations of ion mass 39, e.g. as NaO^+, AlC^+, CaF_2^{++}, are far less probable.

Partial pressures of $CaF_2(g)$ are considerable, but not so high as it was considered before, /29/. HF(g) could not be found despite the well detectable amount of water in the MPs.

In all of the reported studies the key factor effecting fluoride emissions is considered to be the basicity of the slags. In Table 5.2 the index of basicity is given simply as the CaO/SiO_2 ratio. More adequate value would probably be an average between its starting value and the one that corresponds to T=1400°C when part of CaF_2 is transformed into CaO and a fraction of SiO is vaporised. However, the limited number of samples with randomly varying concentrations of fluorine (fluorspar) can demonstrate only the most general tendency; so approximate values are enough. In graphic form it is presented in Fig. 5.2. The diminishing of fluoride emissions with the increase of basicity can be stated definitely. If a correction is made for a small concentration of fluorine in SAG 119 it becomes even more obvious.

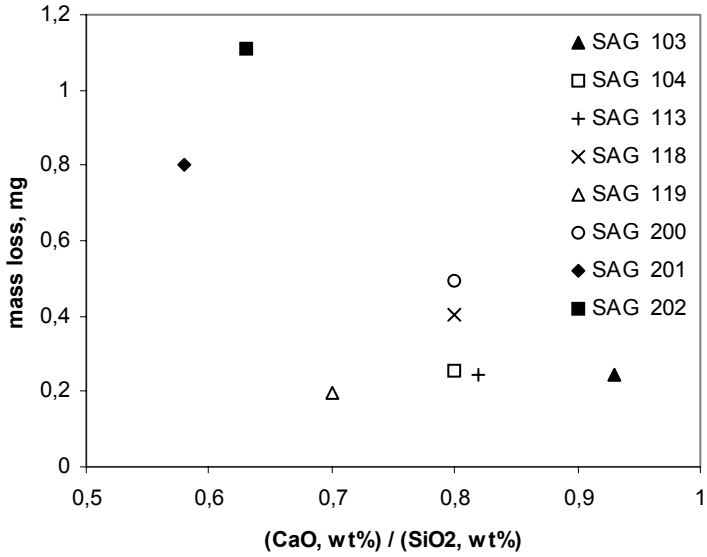

Fig. 5.2 Total mass of fluoride components evaporated below 1400°C vs basicity index.

But it should be noted, that this trend is imposed mainly by NaF and Na_2F_2, while other fluorides, including SiF_4, do not exhibit similar regularities. Thus, the results are noticeably different from the literature data. It seems reasonable since in all the experiments summarised in Table 5.2 different components are evolved in succession, unlike in the static experiments described in the literature. During the vaporisation of NaF and KF, fluorine is consumed, so when the formation of SiF_4 starts, the composition is impoverished with fluorspar.

At higher temperatures the role of carbon and carbon monoxide is significant. SiO(g), Mg(g) and probably Al(g) become the dominating vapour species. In a mould of real caster, such conditions are hardly ever found.

5.2 Gaseous emissions in a caster

The primary goal of the study was the evaluation of the hazardous effects of fluorine content in plant conditions and air pollution in particular. The values in Table 5.2 have to be translated in some way into concentrations of fluorides in the air of the working grounds of a plant. Zaitsev and co-workers /28/ made use of the data collected by the health surveillance research group. The available data was not quite discriminative being given only as concentrations of HF and the total of other fluorides in the air (g/m^3). To make possible the comparison the concentrations were assessed in the study /28/ by computation for typical plant conditions. The agreement was found to be reasonable. The concentration of fluorides coincided within a factor of 1.5-3, for HF the difference was larger.

These conclusions refer to the data on the mass loss of fluorides in effusion experiments reproduced partly in Table 5.3. The data of the present work (Table 5.2) are essentially similar, except AlF_3, which could not be exactly specified and hence is not given. Thus, it is possible to use them for the simulation of air pollution by a caster. Nevertheless, additional experiments in industrial conditions are of great value and the problem is to choose the suitable and informative ones.

Table 5.3 Results of effusion determination of various fluorides evolution from the mould powder during heating and isothermal exposure at 1262°C /28/; m is the amount of fluorides evolved, mg, per 20 mg of initial sample of mould powder

	Mould powder No. (from Table 2.4)				
Fluoride	1	2	4	5	7
NaF+KF	0.250	1.110	0.328	0.298	0.230
CaF_2	0.006	0.040	0.002	0.002	0.006
SiF_4	0.124	0.850	0.136	0.142	0.200
AlF_3	0.154	0.600	0.174	0.184	0.114

Most explicit information can be obtained by direct measurements of the gas composition above the mould powder layer in plant conditions. Conventional mass spectrometric equipment for gas analysis requires some kind of attenuator reducing gas pressure so that the probe could be attached to the high vacuum system. This is usually a capillary tube combined with a system of diaphragms. It is impossible to study substances like NaF(g) or CaF_2 in this way since they condense on the walls and do not reach the analytical chamber, only substances gaseous at normal conditions are available.

A series of such *in situ* experiments were performed in Saarstahl AG, /26/. An inlet tube was attached to the mould, 2 cm above the meniscus. The sucked gases passed through the filters and then the concentrations of O_2, CO_2 and CO were determined. The filters were also subjected to chemical analysis to know the deposits and condensates they had accepted.

One of the results of the gas analysis is reproduced in Fig. 5.3. It may serve as a practical illustration of the theoretical model considered in the work /33/. The concentrations of CO are about ten times lower than CO_2, as a result of the reactions taking place in the mould powder layers above the layer contacting the liquid steel.

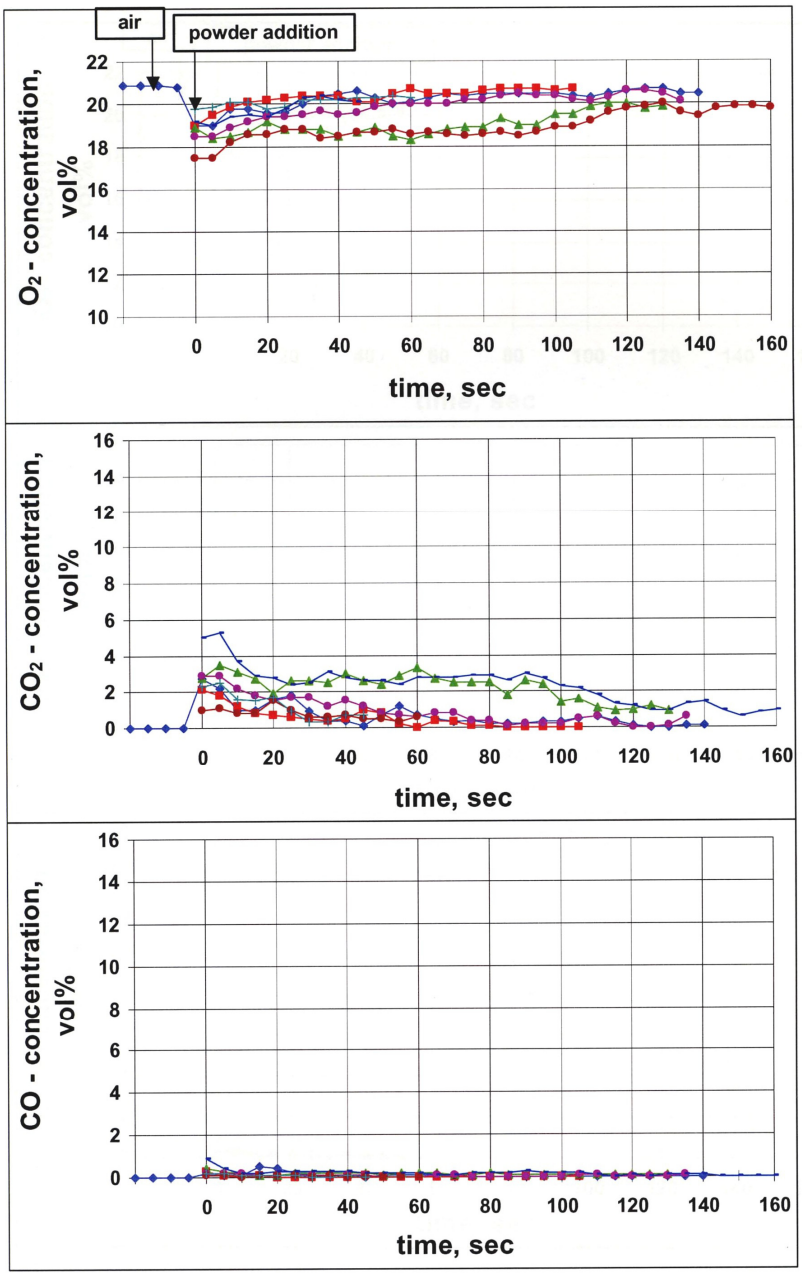

Fig. 5.3 Changes in the mould atmosphere after an addition of SAG 104 powder; probe is 2 cm above the meniscus

The chart also gives an idea of the time limits of the reactions involving carbon and carbonates.

Solid emissions absorbed by the filters were analysed by SEM, the results are given in Table 5.4. It is difficult to draw any conclusions about the process of formation of the analysed particles and about the role of the gaseous components in their formation. Compositions of some of these were not far from the original powders, others were located in other domains of the phase diagram. It was suggested that a high content of Na_2O and F might be a result of the condensation of NaF(g).

Supposedly, these phases are formed by both condensed gaseous components and microparticles, dispersed and transferred by the gas flow. According to the mass spectrometric data SiO_2, MgO and Al_2O_3 can be explained by the evaporation of

SiO(g), Mg(g) and Al(g). But calcium was present in the vapour only in the form of CaF_2(g), no Ca(g) was detected.

Thus, the results of the plant experiments need additional assumptions to account for the emissions of fluorides or oxides. Mass spectrometry provides more detailed and well-established data. The question is: To what extent are the obtained results applicable to real casting conditions?

The approach may be similar to the modelling of CO and CO_2 distributions in the mould powder layer in the investigation /33/. The mass spectrometric data (Appendix 4) can be directly used for the simulation of fluoride emissions if the following scheme is applied:

Consider Fig. 2.3. Through the powder layer a certain temperature gradient is established. The temperature of the upper surface of the loose powder layer is <600°C, the surface of the sintered layer in contact with the liquid flux pool may be at T=1400-1500°C, depending on the caster parameters. The most intensive chemical processes accompanying the melting of the powder and descent of the layers downwards are the combustion of carbon and formation of carbon monoxide from CO_2. The second process proceeds with the increase of volume and hence there is a gas flow of $CO+CO_2$ in the direction of the powder surface.

Table 5.4 Analyses of the phases of emissions from mould powder SAG 104; sampling 2 cm above meniscus; SEM analysis /26/; SAG contribution

Assay No.	SiO_2	CaO	MgO	Al_2O_3	F	Na_2O	K_2O
1	64	30	1	2		1	
	7	58	1	1	13	18	
	100						
	6	9		83		1	
	5	7	2				1
2	49	46	1			3	
	32	14	4	1	22	24	1
	39	41	2	16		2	
	100						
	31	64	2	2		1	
3		65			35		
	74	22	2	1		2	
	100						
	74	20	50	15		1	

The volatile components start to evaporate noticeably at 700-800°C i.e. in the sintered layer where the atmosphere is reducing. Since the pressure of oxygen is small the same vapour components as in vacuum effusion experiments can be expected: NaF, Na, KF and K.

The ascending $CO+CO_2$ gas carries them to the less heated loose powder layer. The specific surface area of the mould powders is about 2 m^2/g and for granules it is also considerable. Thus, the loose powder layer should act as an effective absorber of these components. It is enriched therefore with alkali metals, their fluorides and oxides. The result of this permanent re-vaporisation is the diminishing of the escape of these fluorides and the facilitation of mould powder sintering.

In the vicinity of the liquid pool less volatile components start to evaporate: SiF_4, AlF_3, SiO, MgF_2. In the upper layers they must also be retarded to some extent as a result of condensation and reactions. Silicon fluoride, which remains gaseous at low temperatures and does not condense, escapes into the atmosphere most easily from this point of view.

It may be concluded, that if this scheme of gas circulation and transfer of components is correct, than the vapour phase species identified by the mass spectrometric experiments actually exist in the mould, but the problem of emissions must be separated into two: a) the formation of volatiles in the mould powder layer and b) their escape into the atmosphere.

The principal environmentally hazardous component under these conditions is SiF_4. Therefore, substitution of Li_2O for fluorspar, totally eliminating SiF_4 from the vapour may be far more effective in practice than in the laboratory experiments (paragraph 4.6).

6 CONCLUSIONS

The aim of the study was to characterise the volatile properties of conventional mould powders for the continuous casting of steel and to assess the amount of environmentally hazardous and corrosive components in the mould atmosphere. The next objective was to evaluate the effect of the modifications of mould powder composition intended to minimise the harmful effect of their fluorine and alkali metals content.

The measurements were performed by the mass spectrometric high temperature effusion method in vacuum conditions in the temperature range of 100-1550°C. Eight industrial mould powders with precisely determined chemical compositions were heated at the rate of 100°C/hour while their mass spectra were recorded. The spectra were decoded and transformed into the time/temperature dependence of partial pressures of the vapour components, which served as a basis for all conclusions. Pre-melted and lithium-substituted compositions were studied in the same way.

By contrast to the usual practice when molten decarburised fluxes are analysed in the present work 'as received' mould powders were investigated. As a result, the study has demonstrated the critical influence of carbon on the formation of the gas phase and great differences in the processes of vaporisation below and above the melting point.

The results can be summarised in the following conclusions.

General characteristics of the vapour phase over the mould powders:

- The vaporisation process splits into three distinct stages on the temperature scale with slightly differing limits for different powders.
  1. 100-600°C. H_2O and CO_2 are the main gaseous components. The maximum of H_2O evolution is at 200°C and the peak of CO_2 partial pressure is between 450 and 500°C. Some unidentified vapour species with small partial pressures were registered in the range 100-450°C. HF(g) has not been detected
  2. 600-1200°C. CO_2 disappears and formation of CO starts. The main vapour components are NF, Na_2F_2, Na_3F_3 (negligibly small), Na, KF and K. At 900-1000°C, depending on the powder composition, formation of SiF_4 and AlF_3 starts, the pressure of the latter being always much lower. Separation of Na from NaF could be done only approximately, K and KF were indistinguishable
  3. 1200-1550°C. Partial pressure of CO reaches its maximum and drops. Vapour phase is formed by SiF_2, SiO, CaF_2, Mg, MgF, AlF_3, AlOF. Additionally SiF, Si, MgF_2, AlF_2, AlF, Al and $(SiO)_2$ may occur in this temperature range
- The main vapour species and succession of their appearance during temperature elevation remain unchanged with heating rates up to 3000°C/hour
- Decarburisation noticeably affects the vaporisation mode eliminating low and high temperature stages
- The greater part of fluorine evolves in the form of sodium fluoride
- The role of basicity as the key factor in the estimation of fluoride emissions was confirmed. Emissions of SiF_4 and KF did not exhibit a strong correlation with basicity
- The second important factor for fluoride emissions is the concentration of sodium, and the third is the concentration of fluorspar. The relation between these two, in

addition to the basicity index, determines the ratio of Na and NaF concentrations in the vapour and their partial pressures

Modified compositions indicated the following tendencies:

- Pre-melting of the powders reduced emissions of NaF by 30% as a result of the low activities of SiO_2 and Na_2O in oxide melts
- Partial substitution of CaF_2 with Li_2O in mould powders resulted in a crucial change in vapour composition. SiF_4 and CaF_2 disappeared from the vapour phase and LiF and Li_2O emerged. The total of evaporated fluorides is diminished.

Possible further development:

- As an immediate continuation of the present work several issues may be added:
  - Determination of the vapour species, like SiF_2, MgF_2 or AlOF, for which unambiguous data was not acquired, with higher accuracy
  - Vaporisation of the mixtures (SiO_2+CaF_2+C and etc) simulating chemical processes in mould powders
  - Chemical analysis of the flux melts quenched in effusion cell from different temperatures
  - Measurement of partial vapour pressures over decarburised samples of all mould powders studied (in addition to SAG 202)
  - Investigation of the vaporisation processes of mould powders from other suppliers
- When reliable and sufficiently complete data on vaporisation processes in effusion experiments are acquired the work may proceed with simulation of formation of gaseous components in the mould powder layer in the mould of a caster and the resulting emissions into the atmosphere.

REFERENCES

1. Mills, K.C., Physical properties of casting powders: Part 1 Scheme to represent chemical compositions of powders. Ironmaking and Steelmaking, vol. 15, no. 4, 1988, p. 175-180.

2. Grieveson, P., Bagha, S., Machingawuta, N., Liddell, K. and Mills, K.C., Physical properties of casting powders: Part 2 Mineralogical constitution of slags formed by powders. Ironmaking and Steelmaking, vol.15, no. 4, 1988, p. 181-186.

3. Taylor, R. and Mills, K.C., Physical properties of casting powders: Part 3 Thermal conductivities of casting powders. Ironmaking and Steelmaking, vol.15, no. 4, 1988, p. 187-192.

4. Mills, K.C., Olusanya, A., Brooks, R., Morrell, R. and Bagha, S., Physical properties of casting powders: Part 4 Physical properties relevant to fluid and thermal flow. Ironmaking and Steelmaking, vol.15, no. 5, 1988, p. 257-264.

5. Mills, K.C., Continuous Casting Powders and Their Effect on Surface Quality and Stiker Breakouts. Proceedings of the 5th International Conference on Molten Slags, Fluxes and Salts '97, January 5-7, 1997, Sydney, Australia, p. 675-682.

6. Mills, K.C., The performance of casting powders and their effect on surface quality. Steelmaking Conference Proceedings, vol. 74, 1991, p. 121-129.

7. Mills, K.C., Billany, T.J.H., Normanton, A.S., Walker, B. and Grieveson, P., Causes of sticker breakout during continuous casting. Ironmaking and Steelmaking, vol. 18, no. 4, 1991, p. 253-265.

8. Pinheiro, C.A., Samarasekera, I.V., Brimacombe, J.K., Mold Flux for Continuous Casting of Steel. I&SM, vol. 21, no. 11-12, 1994, vol. 22, no. 1-12, 1995, vol. 23, no. 1-3, 1996.

9. Nakamura, Y., Ando, T., Kurata, K. and Ikeda, M., Effect of Chemical Composition of Mold Powder on the Erosion of Submerged Nozzles for Continuous Casting of Steel. Continuous Casting, vol. 6, 1992, p. 33-39.

10. Feldbauer, S., Jimbo, I., Sharan, A., Shimizu, K., King, W., Stepanek, J., Harman, J. and Cramb, A.W., Physical Properties of Mold Slags That are Relevant to Clean Steel Manufacture. Steelmaking Conference Proceedings, vol. 78, 1995, p. 655-667.

11. Kawamoto, M., Nakajima, K., Kanazawa, T. and Nakai, K., Design Principles of Mold Powder for High Speed Continuous Casting. ISIJ International, vol. 34, no. 7, 1994, p. 593-598.

12. Cho, J., Shibata, H., Emi, T. and Suzuki, M., Thermal Resistance at the Interface between Mold Flux Film and Mold for Continuous Casting of Steels. ISIJ International, vol. 38, no. 5, 1998, p. 440-446.

13. Moore, J.A., Phillips, R.J. and Gibbs, T.R., An overview for the requirements of continuous casting mold fluxes. Steelmaking Conference Proceedings, vol. 74, 1991, p. 615-621.

14. Fukuda, Y., Kawai, H., Okimori, M., Hojo, M. and Tanaka, D., Development of Mold flux for Continuous Casting of Type-304 Stainless Steel. Proceedings of the 5th International Conference on Molten Slags, Fluxes and Salts '97, January 5-7, 1997, Sydney, Australia, p. 791-796.

15. Nakato, H., Takeuchi, S., Fujii, T., Nozaki, T. and Washio, M., Characteristics of new mold fluxes for strand casting of low and ultra low carbon steel slabs. Steelmaking Conference Proceedings, vol. 74, 1991, p. 639-646.

16. Mahapatra, R.B., Brimacombe, J.K. and Samarasekera, I.V., Mold Behavior and Its Influence on Quality in the Continuous Casting of Steel Slabs: Part II. Mold Heat Transfer, Mold Flux Behavior, Formation of Oscillation Marks, Longitudinal Off-Corner Depressions, and Subsurface Cracks. Metallurgical Transactions B, vol. 22B, 1991, p.875-888.

17. Mills, K.C. and Fox A.B., The Role of Mould Fluxes in Continuous Casting – So Simple Yet So Complex. ISIJ International, vol. 43, no. 10, 2003, p. 1479-1486.

18. Mills, K.C. and Lahiri, A.K., Metal Separation Problems in the Continuous Casting of Steel: A Review. Metal Separation Technologies III, Proceedings of the Symposium in Honour of Professor Lauri E. Holappa of the Helsinki University of Technology. Copper Mountain, Colorado, June 20-24, 2004, p. 249-255.

19. Hiraki, S., Nakajima, K., Murakami, T. and Kanazawa, T., Influence of mold heat fluxes on longitudinal surface cracks during high speed continuous casting of steel slab. Steelmaking Conference Proceedings, vol 77, 1994, p. 397-403.

20. Emi, M., The mechanisms for sticking type break-outs and new developments in continuous casting mold fluxes. Steelmaking Conference Proceedings, vol. 74, 1991, p. 623-630.

21. Dick, A.F., Yu, X., Pomfret, R.J. and Coley, K.S., Attack of Submerged Entry Nozzles by Mould Flux and Dissolution of Refractory Oxides in the Flux. ISIJ International, vol. 37, no. 2, 1997, p. 102-108.

22. Shibata, H., Cho, J.-W., Emi, T. and Suzuki, M., Optical and Thermal Properties of Continuous Casting Mold Fluxes at Elevated Temperatures. Proceedings of the 5th International Conference on Molten Slags, Fluxes and Salts '97, January 5-7, 1997, Sydney, Australia, p. 771-776.

23. Kusano, A., Sato, N., Okimori, M., Fukunaga, S., Nishihara, R., Sato, M. and Minagawa, Y., Improvement of mold fluxes for stainless and titanium bearing steels. Steelmaking Conference Proceedings, vol. 74, 1991, p. 147-151.

24. Kawamoto, M., Tsukaguchi, Y., Nishida, N., Kanazawa, T. and Hiraki, S., Improvement of the Initial Stage of Solidification by Using Mild Cooling Mold Powder. ISIJ International, vol. 37, no. 2, 1997, p. 134-139.

25. Hammerschmid, P. and Janke, D., Experiments on the development of non-oxidizing fluxes for continuous steel casting. Steel Research, vol. 62, no. 9, 1991, p. 395-404.

26. Janke, D., Schulz, T., Tonelli, M., Cimarelli, T., Holappa, L., Shilov, A., Havette, E., Viguet-Carrin, C., Valentin, P., Bruch, C., Improvement of casting fluxes and slags by minimisation of environment-polluting and corrosive constituents (fluorine, alkali components). European Commission, Report EUR 20645 EN, 2003, 137 p.

27. Chavez, J.F., Rodriguez, A., Morales, R. and Tapia, V., Laboratory and plant studies on thermal properties of mold powders. Steelmaking Conference Proceedings, vol. 78, 1995, p. 679-686.

28. Zaitsev, A.I., Leites, A.V., Litvina, A.D. and Mogutnov, B.M., Investigation of mould powder volatiles during continuous casting. Steel Research, vol. 65, no. 9, 1994, p. 368-374.

29. Holappa, L., Shilov, A., Improvement of casting fluxes and slags by minimisation of environment-polluting and corrosive constituents (fluorine, alkali components). European Commission, Technical Report No.3, 1999, 26 p.

30. Holappa, L., Shilov, A., Improvement of casting fluxes and slags by minimisation of environment-polluting and corrosive constituents (fluorine, alkali components). European Commission, Technical Report No.5, 2000, p. 27-33.

31. Shinmei, M., Uematsu, H., Maekawa,T. and Yokokawa, T., The equilibria between $SiF_4(g)$ and $CaF_2 + CaO + SiO_2$ melts at 1450°C. Canadian Metallurgical Quarterly, vol. 22, no. 1, 1983, p. 53-59.

32. Shimizu, K., Suzuki, T, Jimbo, I. and Cramb, A.W., An Investigation on the Vaporization of Fluorides from Slag Melts. I&SM, vol. 28, no. 7, 2001, p. 87-93.

33. Supradist, M., Cramb, A.W. and Schwerdtfeger, K., Combustion of Carbon in Casting Powder in a Temperature Gradient. ISIJ International, vol. 44, no. 5, 2004, p.817-826.

34. Kim, J.-W. and Lee, H.-G., Thermal and Carbothermic Decomposition of Na_2CO_3 and Li_2CO_3. Metallurgical and Materials Transactions B, vol. 32B, 2001, p. 17-24.

35. Kim, J.-W., Lee, Y.-D. and Lee, H.-G., Decomposition of Na_2CO_3 by Interaction with SiO_2 in Mold Flux of Steel Continuous Casting. ISIJ International, vol. 41, no. 2, 2001, p. 116-123.

36. Kim, J.-W., Lee, Y.-D. and Lee, H.-G., Decomposition of Li_2CO_3 by Interaction with SiO_2 in Mold Flux of Steel Continuous Casting. ISIJ International, vol. 44, no. 2, 2004, p. 334-341.

37. Motzfeldt, K., The thermal decomposition of sodium carbonate by the effusion method. J. Phys. Chem., vol. 59, no. 2, 1955, p. 139-147.

38. Zaitsev, A.I., Litvina, A.D., Lyakishev, N.P. and Mogutnov, B.M., Thermodynamics of $CaO-Al_2O_3-SiO_2$ and $CaF_2-CaO-Al_2O_3-SiO_2$ melts. J. Chem. Soc. Far. Trans., vol. 93, no. 17, 1997, p. 3089-3098.

39. Zaitsev, A.I., Korolyov, N.V. and Mogutnov, B.M, Thermodynamic properties of $\{xCaF_2 + yAl_2O_3 + (1-x-y)CaO\}$ (I) I. Experimental investigation. J. Chem.Thermodynamics, vol. 22, 1990, p. 513-530.

40. Zaitsev, A.I., Korolyov, N.V. and Mogutnov, B.M, Thermodynamic properties of $\{xCaF_2 + yAl_2O_3 + (1-x-y)CaO\}$ (I) II. Model description. J. Chem. Thermodynamics, vol. 22, 1990, p. 531-543.

41. Zaitsev, A.I., Litvina, A.D. and Mogutnov, B.M, Thermodynamic properties of the intermediate phases of $\{xCaF_2 + ySiO_2 + (1-x-y)\ CaO\}$. J. Chem. Thermodynamics, vol. 24, 1992, p. 737-750.

42. Zaitsev, A.I., Litvina, A.D. and Mogutnov, B.M, Thermodynamic properties of the intermediate phases of $\{xCaF_2 + ySiO_2 + (1-x-y)CaO\}$ (I) 1. Experimental. J. Chem. Thermodynamics, vol. 24, 1992, p. 1039-1055.

43. Zaitsev, A.I., Korolyov, N.V. and Mogutnov, B.M, Vapor Pressure and Heats of Sublimation of CaF_2 and SrF_2. High Temperature Science, vol. 28, 1990, p. 341-350.

44. Zaitsev, A.I., Shelkova, N.E., Lyakishev, N.P. and Mogutnov, B.M., Thermodynamic properties and phase equilibria in the Na_2O-SiO_2 system. Phys. Chem. Chem. Phys., vol. 1, 1999, 1899-1907.

45. Zaitsev, A.I., Litvina, A.D. and Mogutnov, B.M., Thermochemistry of Oxide-Fuoride Flux Systems. High Temperature Science, vol 28, 1990, p. 351-377.

46. Shimizu, K. and Cramb, A.W., The Kinetics of Fluoride Evaporation from CaF_2-SiO_2- CaO Slags and Mold Fluxes in Dry Atmospheres. I&SM, vol. 29, no. 6, 2002, p. 43-53.

47. Carli, R., Righi, C. and Giacobbe, A., Mold fluxes fluoride content. Some technological considerations. 85th Steelmaking Conference Proceedings, vol. 85, 2002, p. 157-163.

48. Kashiwaya, Y. NaF vaporization. Center for Iron and Steelmaking Research, Carnegie Mellon University, Technical report 1996, http://cisr-mac.mems.cmu.edu/kashiwy/naf

49. Kashiwaya, Y. and Cramb, A.W., Kinetics of Formation and Dissociation of Na_2SiF_6. Metallurgical and Materials Transactions B, vol. 33B, 2002, p. 129-136.

50. Farber, M. and Srivastava, R.D., Mass Spectrometric Determination of the Heats of Formation of the Silicon Fluorides SiF(g), SiF_2(g) and SiF_3(g). J. Chem. Soc. Far. Trans. I. vol. 74, 1978, p. 1089-1095.

51. Viswanathan, N.N., Fatemeh, S., Sichen, D. and Seetharaman, S., Estimation of escape rate of volatile components from slags containing CaF_2 during viscosity measurement. Steel Research, vol. 70, no. 2, 1999, p. 53-58.

52. Hillert, L.H., The effect of alkaline earth fluorides on some oxides of technical importance. Acta Polytech. Scand. Ch.90, 1970, 210 p.

53. Nagata, K. and Fukuyama, H., Physicochemical Properties of CaO-SiO_2-CaF_2-NaF Slag system as a Mold Flux of Continuous Casting. Steel Research, vol. 74, no. 1, 2003, p. 31-35.

54. Watanabe, T., Fukuyama, H. and Nagata, K., Stability of Cuspidine ($3CaO{\cdot}2SiO_2{\cdot}CaF_2$) and Phase Relations in the CaO-SiO_2-CaF_2 System. ISIJ International, vol. 42, no. 5, 2002, p. 489-497.

55. Semenov, G.A., Nikolayev, E.N. and Frantseva, K.E., Primeneniye mass-spektrometrii v neorganicheskoi himii. 1976, 152 p. (Application of mass-spectrometry in inorganic chemistry, in Russian)

56. Sidorov, L.N., Korobov, M.V. and Zuravleva, L.V., Mass-spektralniye termodinamicheskiye issledovaniya. 1985, 208 p. (Mass-spectrometric thermodynamic studies, in Russian)

57. Stolyarova, V.L. and Semenov, G.A., Mass Spectrometric Study of the Vaporization of Oxide Systems. J.H.Beynon (Ed.), John Wiley, 1994, 434 p.

58. Kato, E., Thermodynamic Studies of Metallurgical Systems by Mass Spectrometry. J. Mass Spectrom. Soc. Jpn., vol. 41, no. 6, 1993, p. 297-316.

59. Asano, M., Kato, E. and Sata, T., Mass Spectrometry Applied to High Temperature Chemistry. Mass Spectrometry, vol. 28, no. 2, 1980, p. 107-132.

60. Drowart, J. and Goldfinger, P., Die Massenspektrometrie anorganischer Systeme bei hohen Temperaturen. Angew. Chem., vol. 79, no.13, 1967, p. 389-604.

61. Lee, M. and Adams A., A Combination Compact Knudsen Cell – Mass Spectrometer Apparatus for Alloy Studies, High Temp. Sci., vol. 25, 1988, p. 103-116.

62. Mann, J.B., Ionization Cross Sections of the Elements Calculated from Mean-Square Radii of Atomic Orbitals. J. Chem. Phys., vol. 46, no. 5, 1967, p. 1646-1651.

63. Lennon, M.A., Bell, K.L., Gilbody, H.B., Hughes, A.E., Kingston, M.J., Murray, M.J. and Smith, F.J., Recommended Data on the Electron Impact Ionization of Atoms and Ions: Fluorine to Nickel. J. Phys. Chem. Ref. Data, vol.17, no. 3, 1988, p. 1285-1363.

64. Bell, K.L., Gilbody, H.B., Hughes, A.E., Kingston, M.J. and Smith, F.J., Recommended Data on the Electron Impact Ionization of Light Atoms and Ions. J. Phys. Chem. Ref. Data, vol.12, no. 4, 1983, p. 891-916.

65. Otwos, J.W. and Stevenson, D.P., Cross-sections of Molecules for Ionization by Electrons. J. Amer. Chem. Soc., vol. 78, no. 3, 1956, p.546-551.

66. Shilov, A., Holappa, L., Stolyarova, V., A High Temperature Mass Spectrometric Study of the Thermodynamic Properties of Cu-Mg Solid Alloys. Rapid Communications in Mass Spectrometry, vol. 12, 1998, p. 1133-1136.

67. Shilov, A., Holappa, L., Stolyarova V., A Knudsen Effusion High Temperature Assembly for a Quadrupole QMG-420 Mass Spectrometer. Rapid Communications in Mass Spectrometry, vol. 11, 1997, p.1425-1429.

68. Hildebrand, D.L., Murad, E., Dissociation Energy of NaO(g) and the Heat of Atomisation of Na_2O(g). J. Chem.Phys., vol. 53, 1970, no. 9, pp. 3403-34013.

69. Steinberg, M. and Schofield, K., A reevaluation behavior of sodium oxide and the bond strengths of NaO and Na_2O: Implictions for the mass spectrometric analysis of alkali/oxygen systems. J. Chem. Phys., vol. 94, p. 3901-3907.

70. Shol'ts, V.B. and Sidorov, L.N., Entalpii dissotsiatsii, mass-spektri I structuri nekotorih kompleksnih ftoridov. Vestnik Moskovskogo Universiteta, no. 2, 1972, p. 371-382. (Enthalpies of dissociation, mass-spectra and structures of some complex fluorides, in Russian)

71. Barin, I., Thermochemical Data of Pure Substances. VCH, 1993, 1739 p.

72. Kazenas, E.K. and Tsvetkov, Yu.V., Isparenie oksidov. Nauka, 1997, 543 p. (Vaporisation of oxides, in Russian)

73. Poll, H.U., Winkler, C., Margreiter, D., Grill, V. and Märk, T.D., Discrimination effects for ions with high initial kinetic energy in a Nier-type ion source and partial and total electron ionisation cross-sections of CF_4. Int. J. Mass Spectrom. Ion Process., vol. 112, 1992, p. 1-17.

74. Gurvich, L.V, Veits, I.V. and Alcock, C.B. (editors), Thermodynamic Properties of Individual Substances, vol. 1-5. Hemisphere Publishing Corporation, 1989.

75. Knacke, O., Kubaschewski, O. and Hesselmann, K. (editors), Thermochemical Properties of Inorganic Substances, 2-nd ed. Springer-Verlag, 1991, 2412 p.

76. Slag Atlas, 2nd Edition, Verlag Stahlesen GmbH, Dusseldorf, 1995, p.245.

APPENDIX 1

Complete mass spectra of mould power samples

a. SAG 103

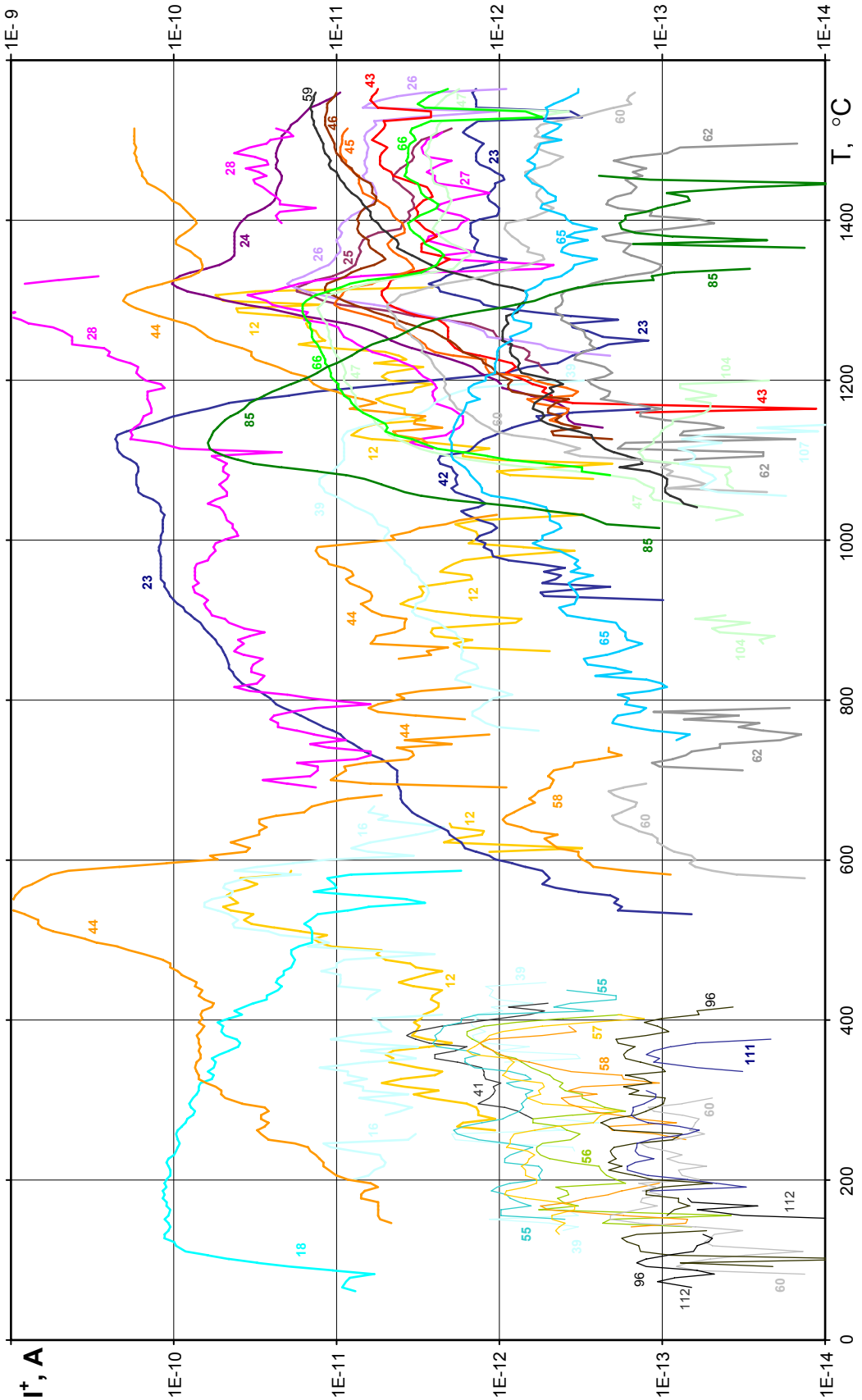

APPENDIX 1

b. SAG 104

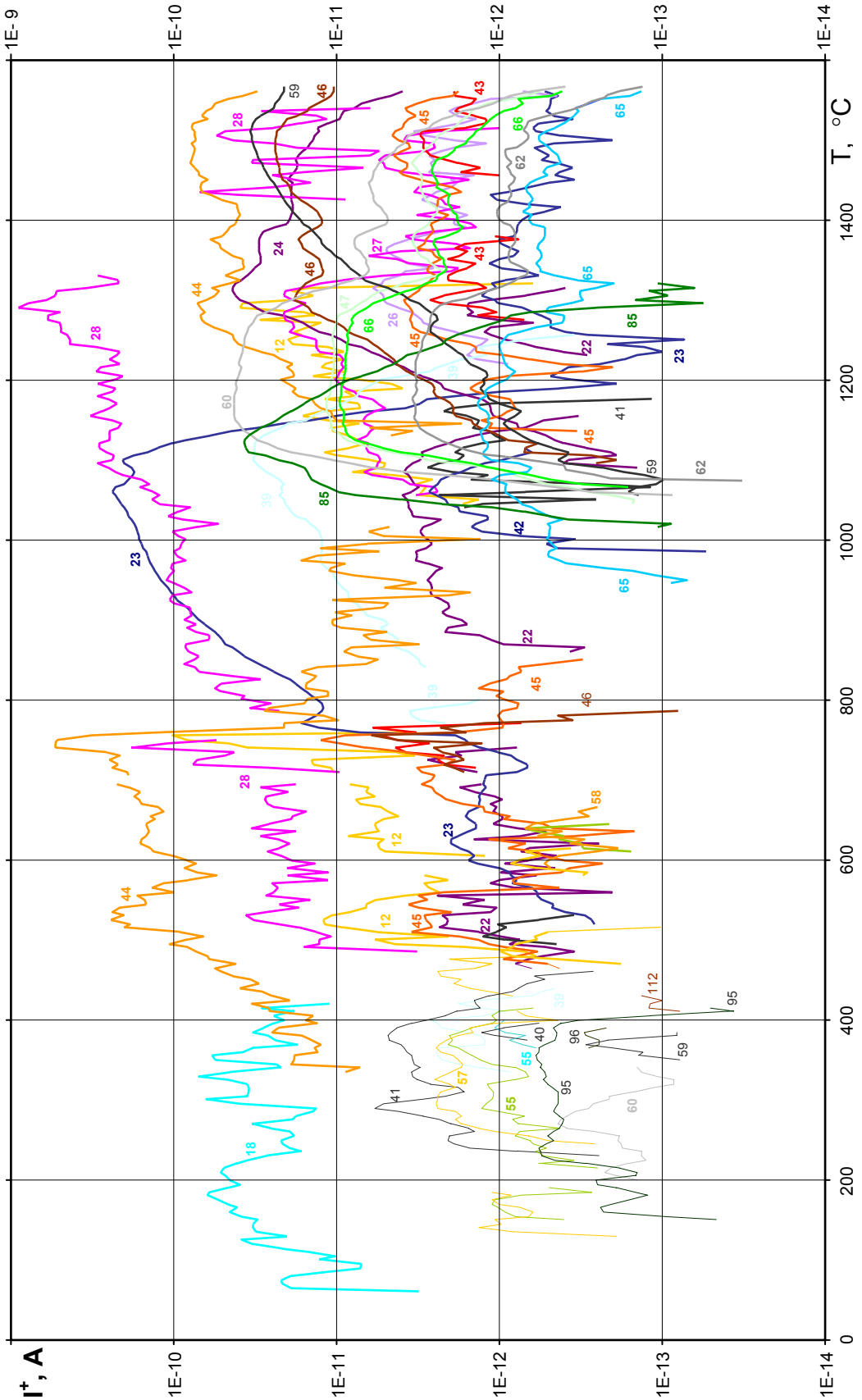

APPENDIX 1

c. SAG 113

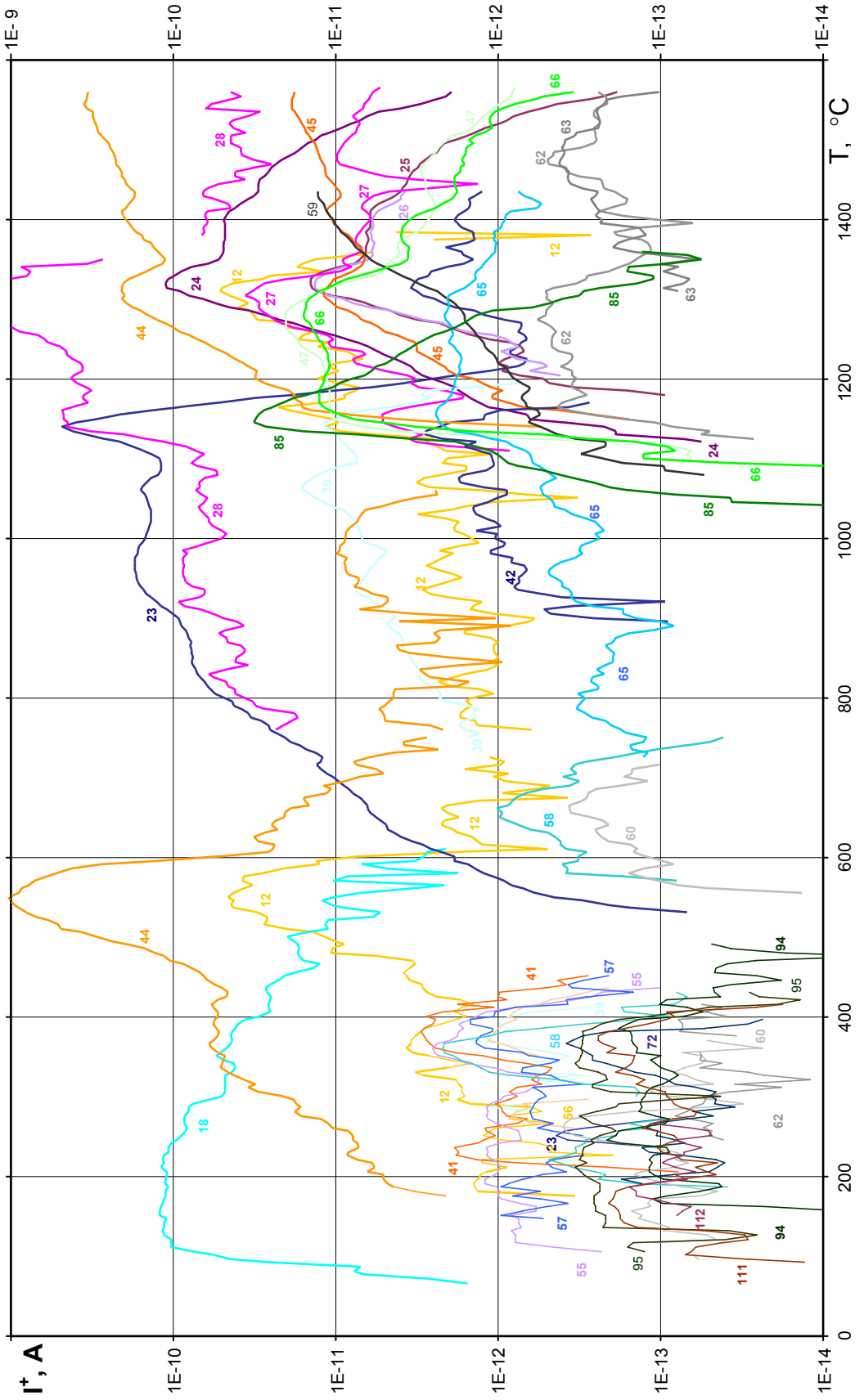

APPENDIX 1

d. SAG 118

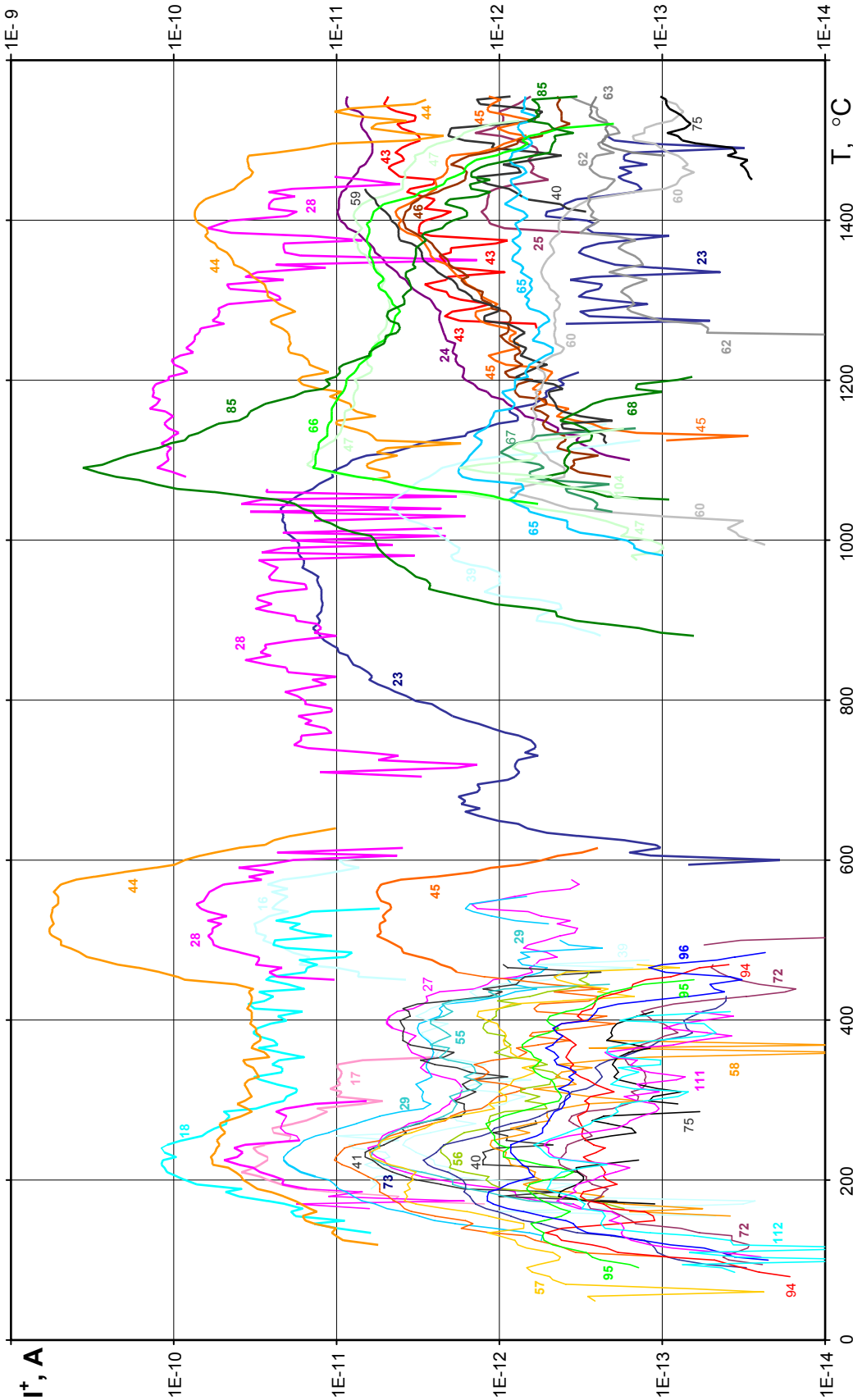

APPENDIX 1

e. SAG 119

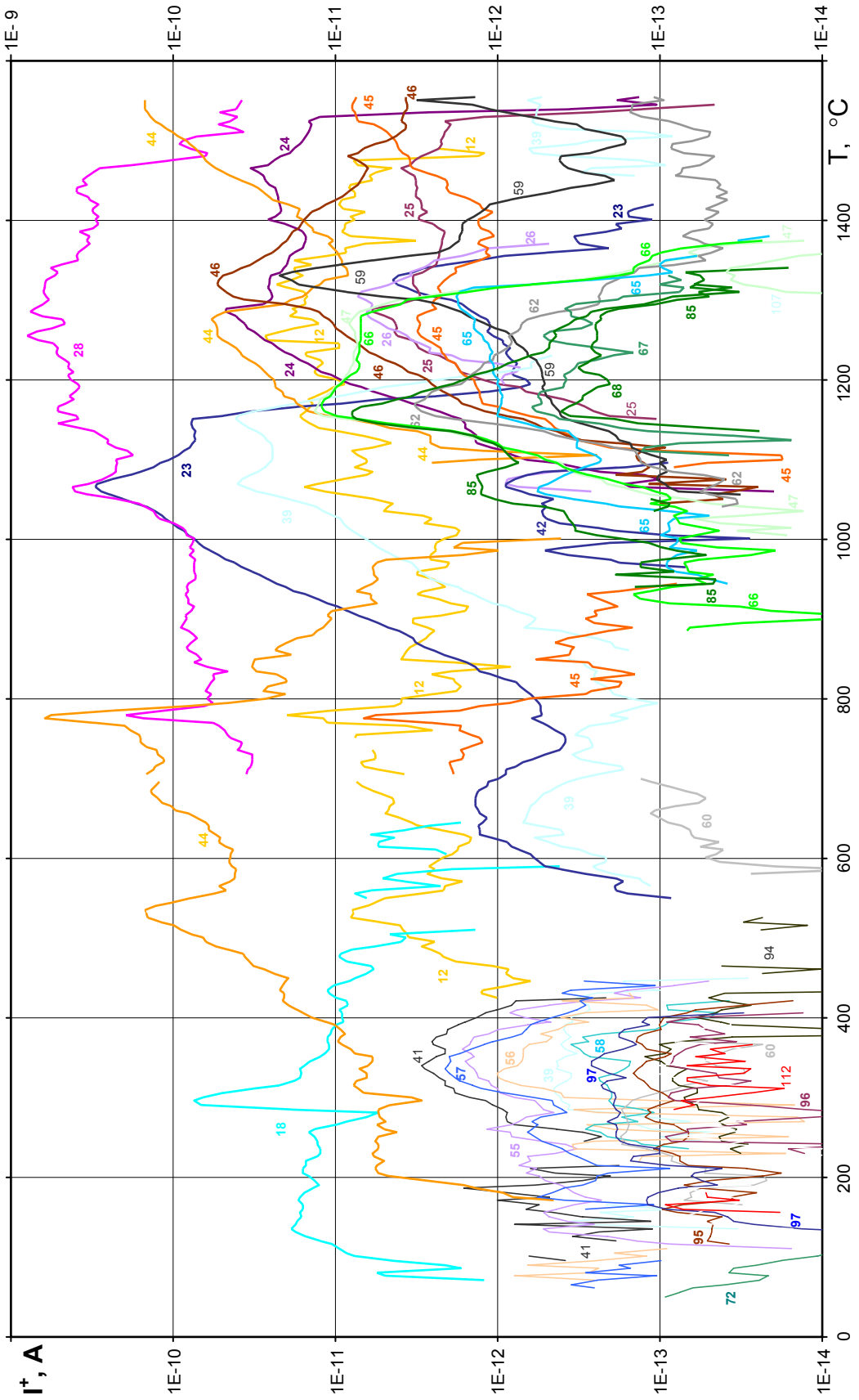

APPENDIX 1

f. SAG 200

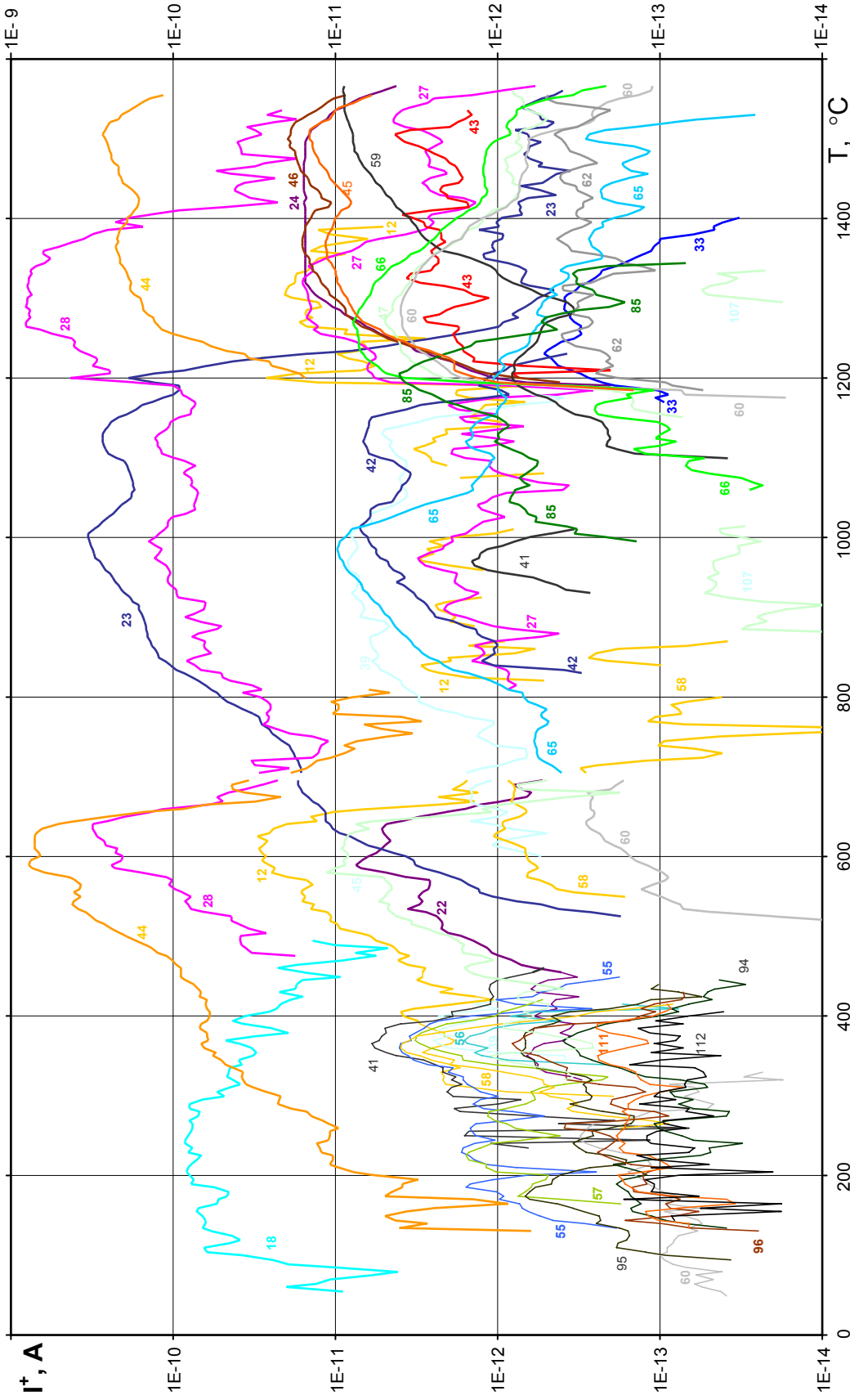

APPENDIX 1

g. SAG 201

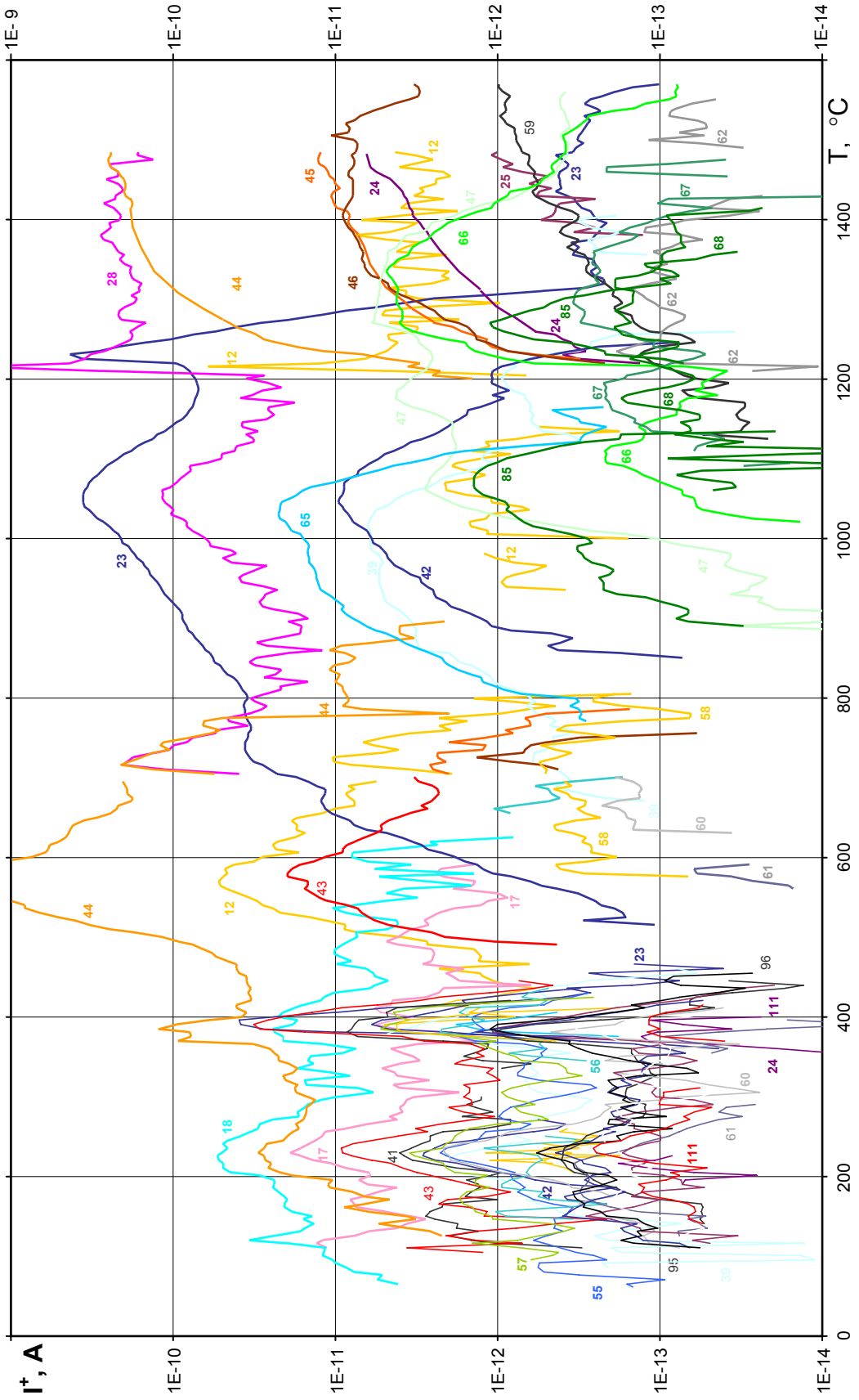

APPENDIX 1

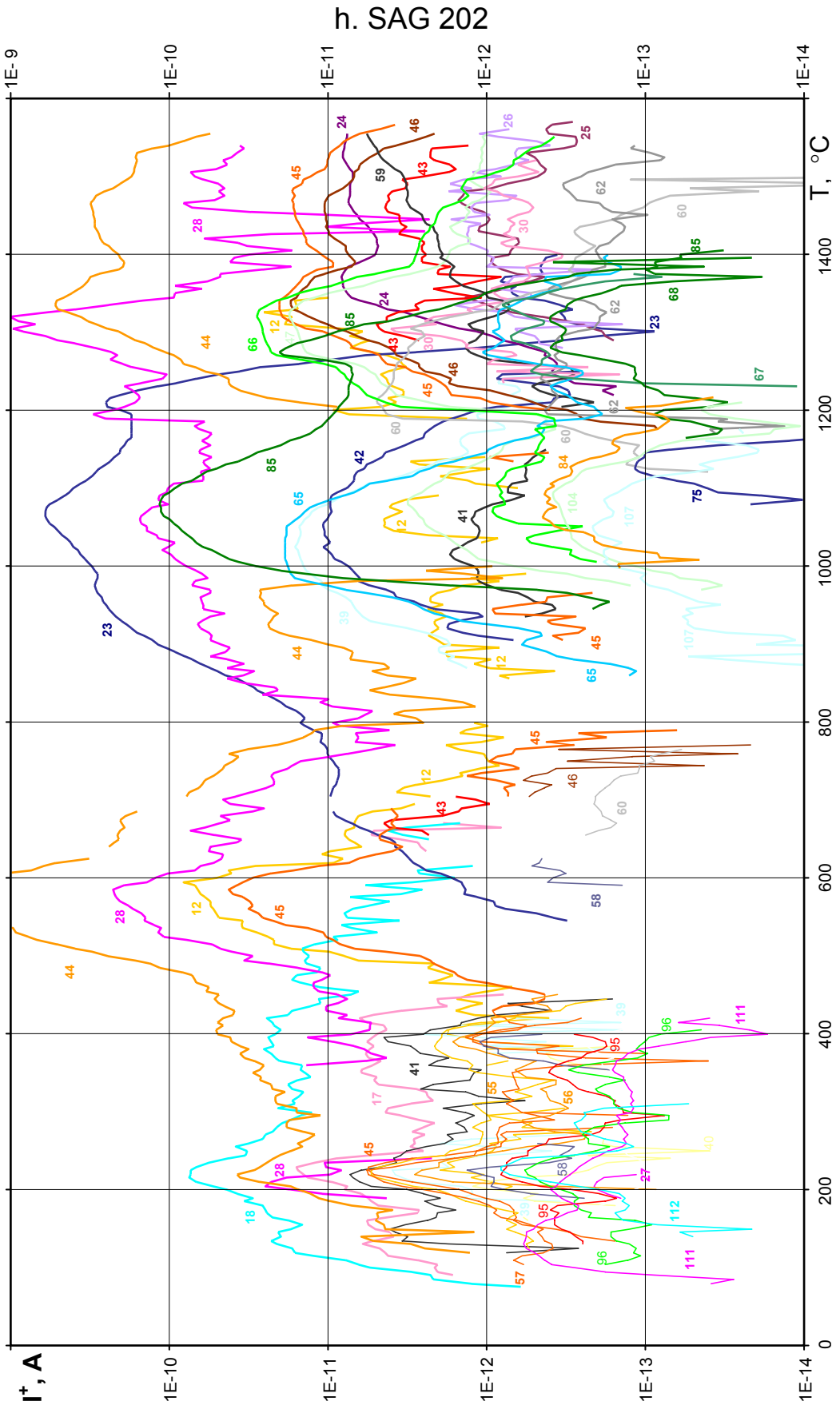
h. SAG 202
1E- 9
1E-10
1E-11
1E-12
1E-13
1E-14
T, °C
0
200
400
600
800
1000
1200
1400
I+, A

APPENDIX 2

Effect of heating rates: 30, 100, 300, 1000, 3000°C/hour. Mould powder SAG 202

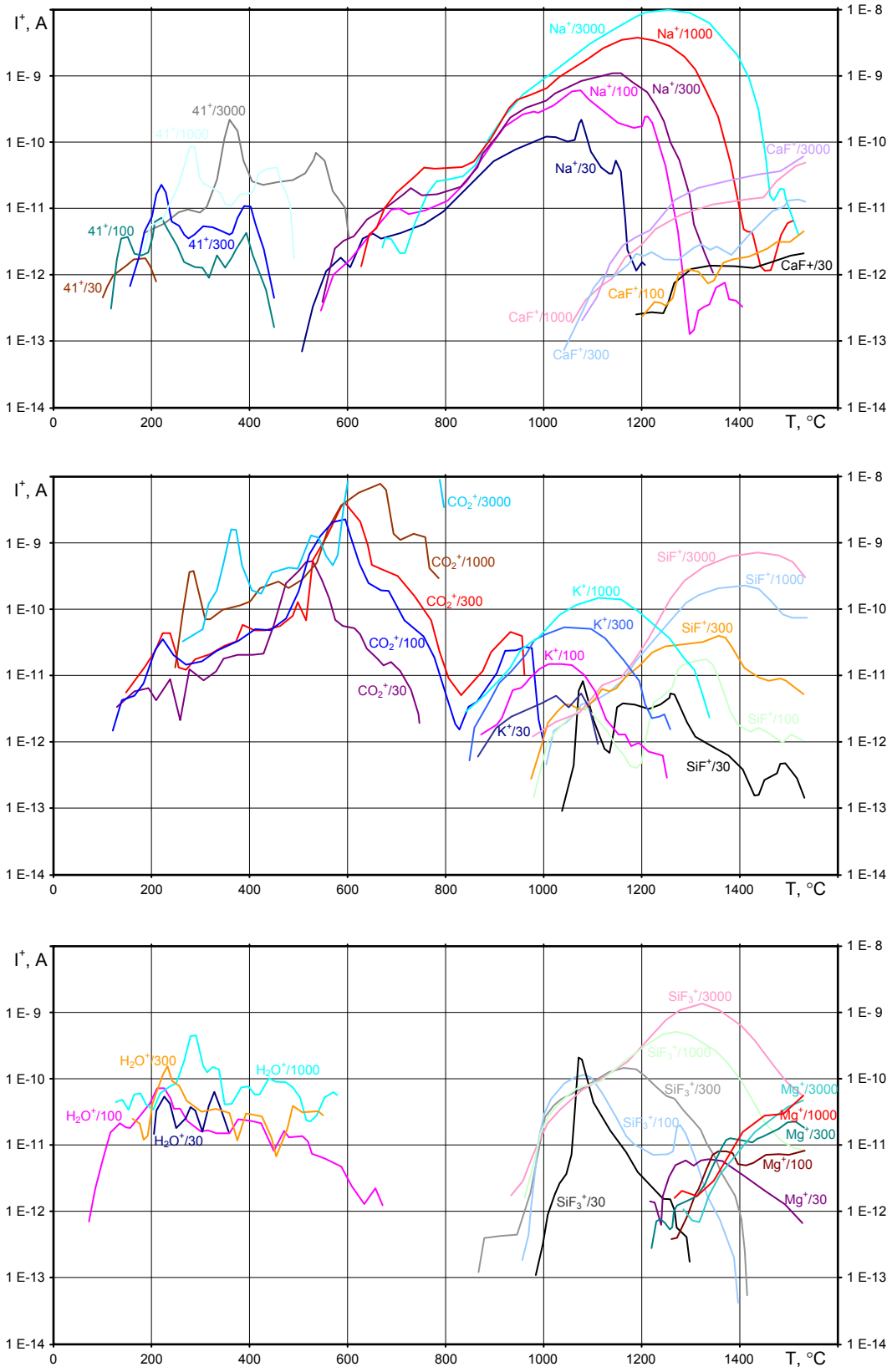

APPENDIX 3

Decoded mass spectra

a. SAG 103

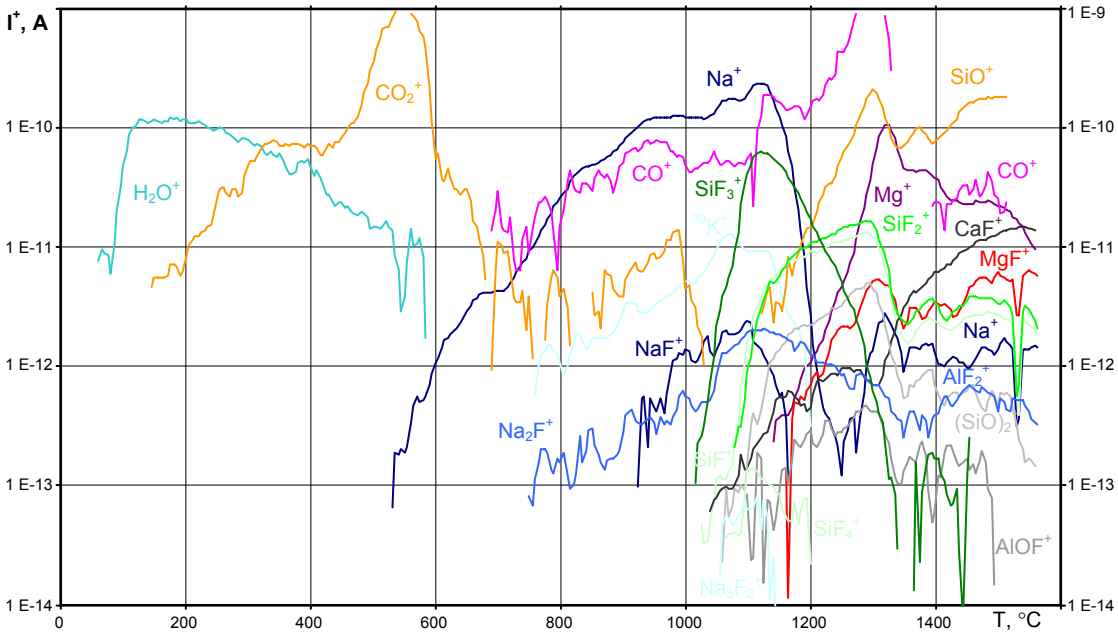

b. SAG 104

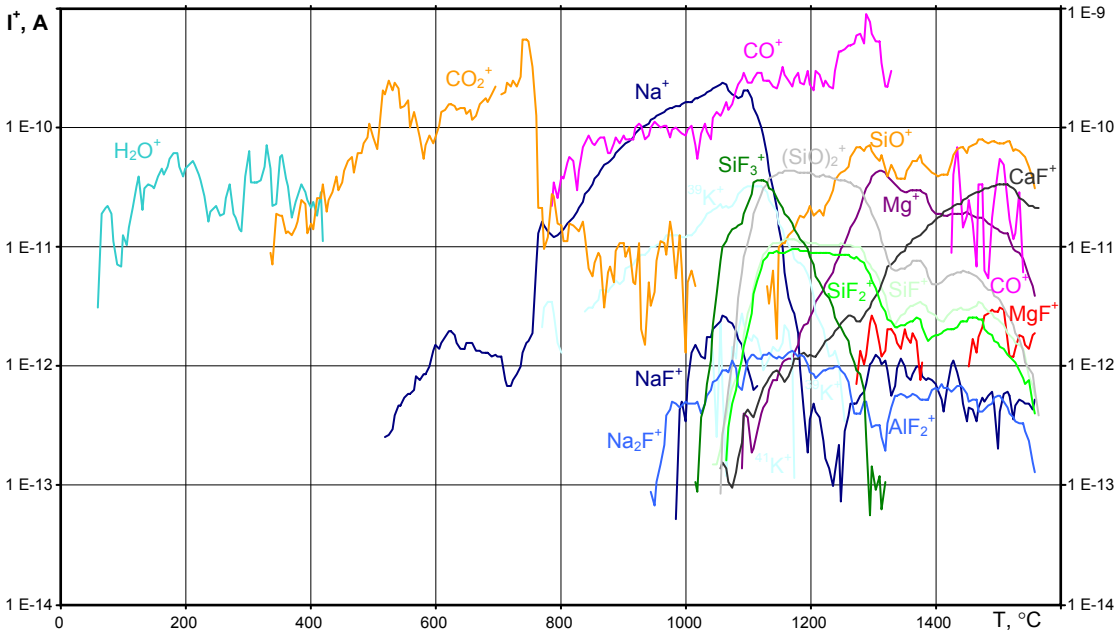

APPENDIX 3

Decoded mass spectra

c. SAG 113

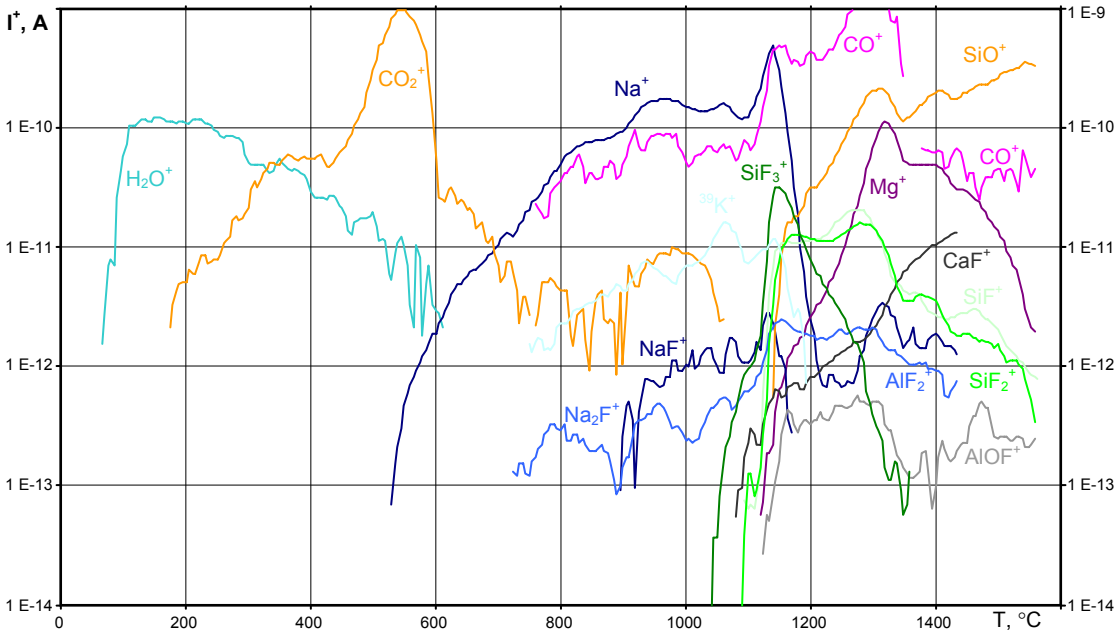

d. SAG 118

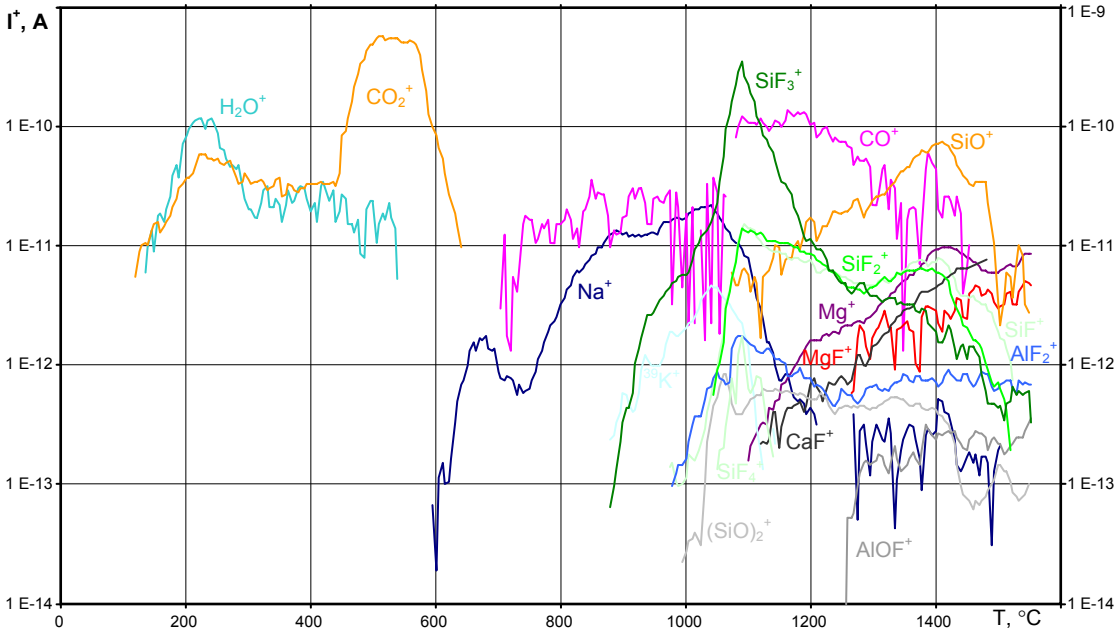

APPENDIX 3

Decoded mass spectra

e. SAG 119

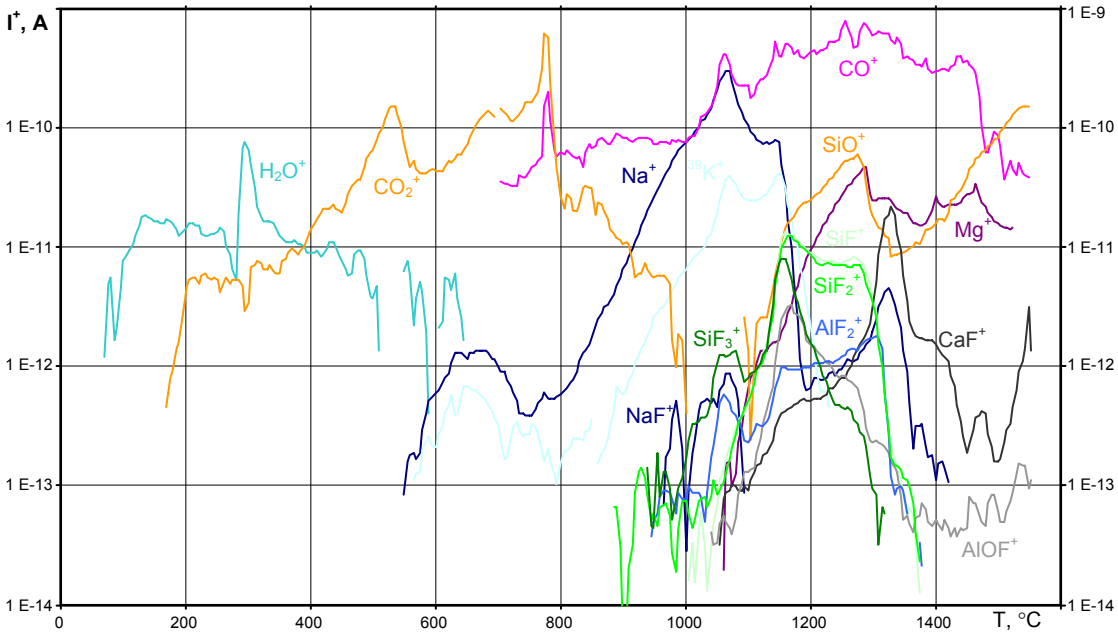

f. SAG 200

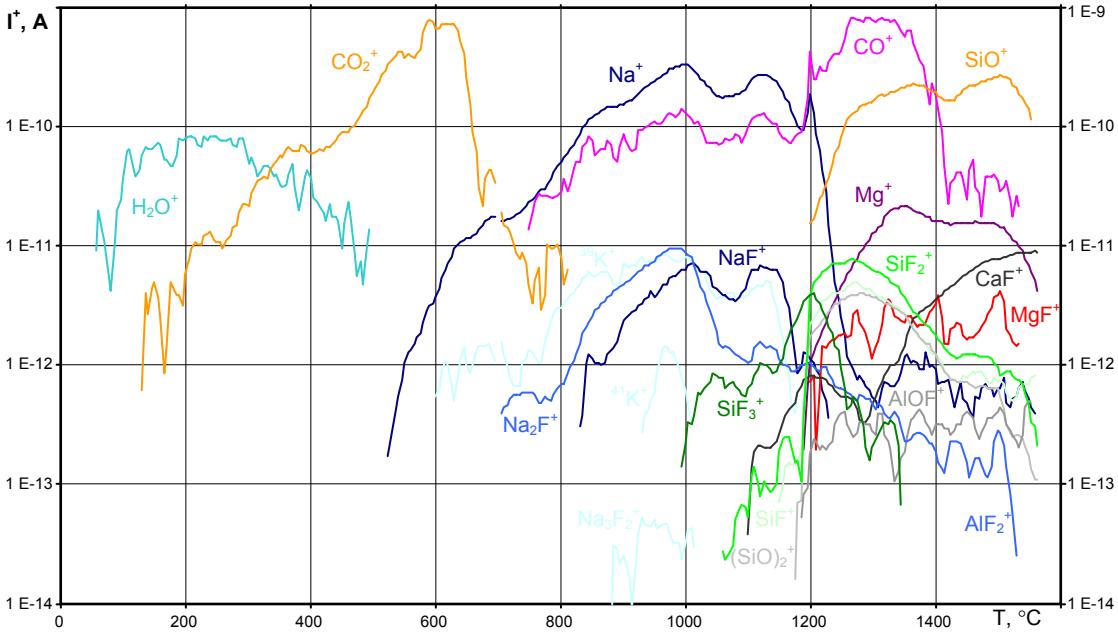

APPENDIX 3

Decoded mass spectra

g. SAG 201

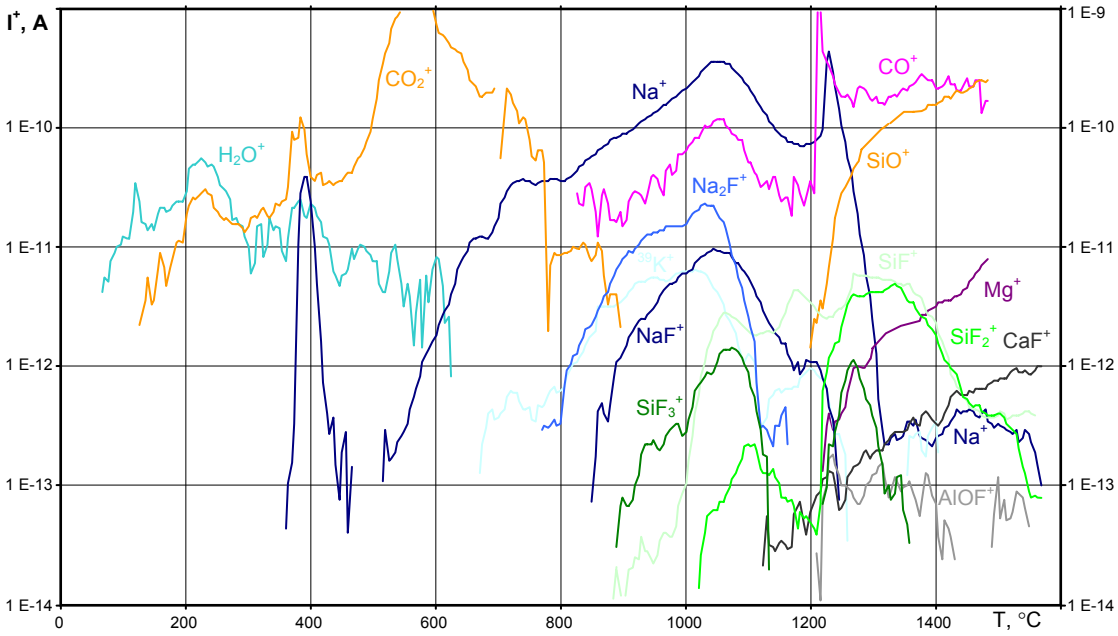

h. SAG 202

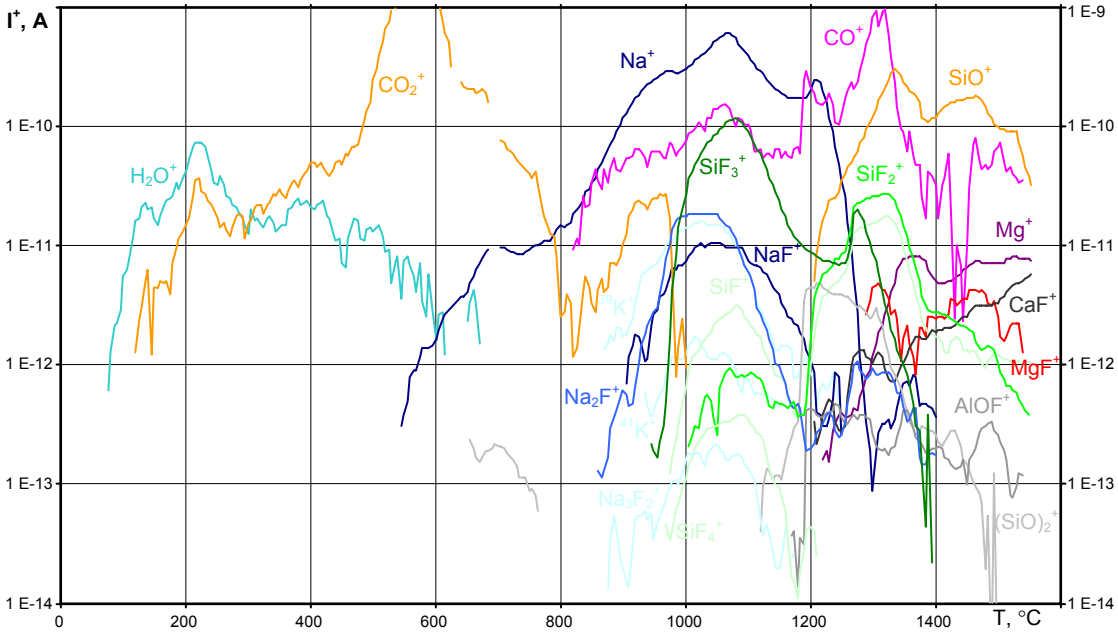

APPENDIX 4

Partial vapour pressures over mould powders

a. SAG 103

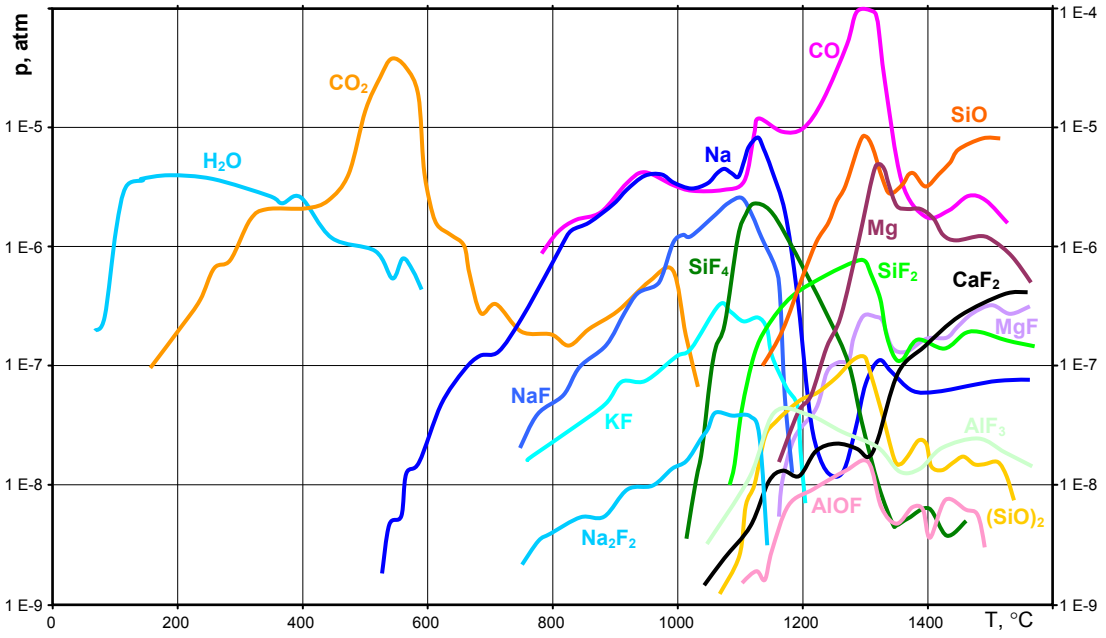

b. SAG 104

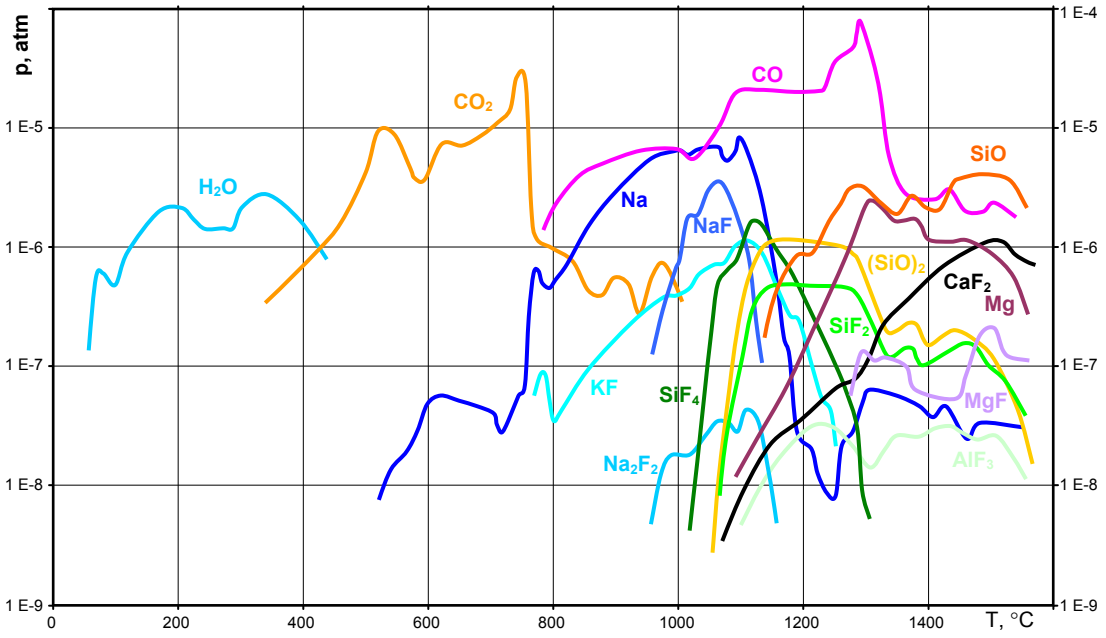

APPENDIX 4

c. SAG 113

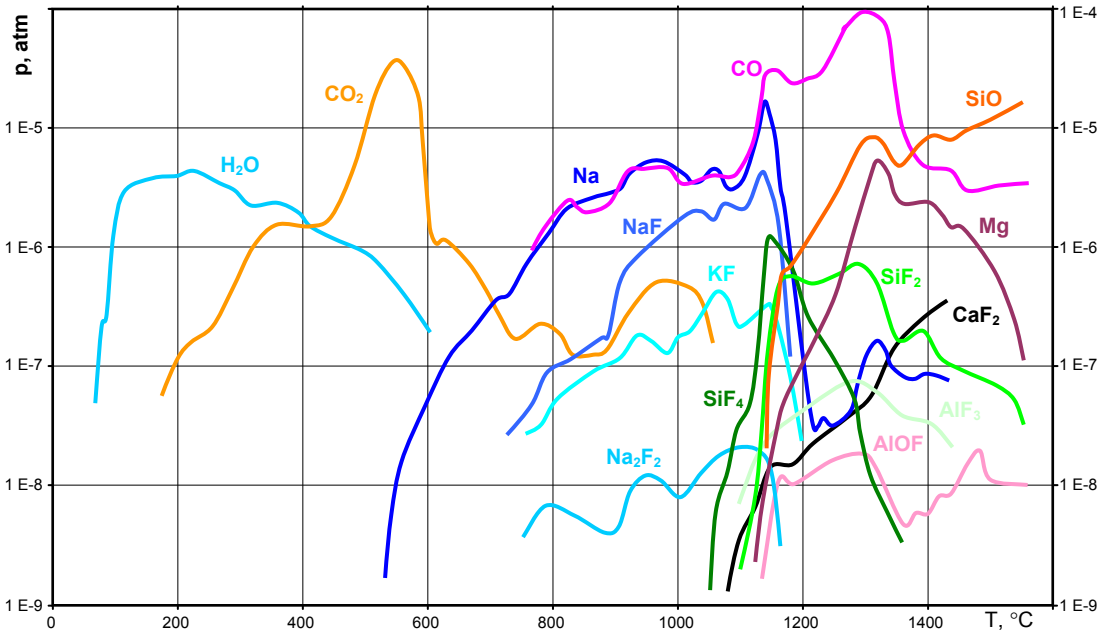

d. SAG 118

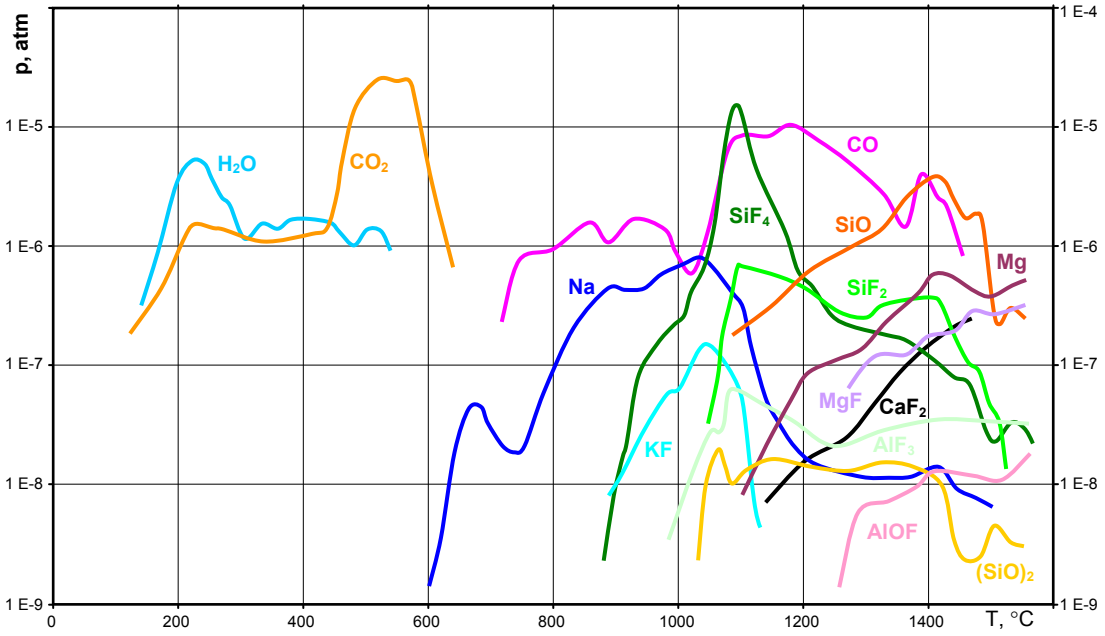

APPENDIX 4

e. SAG 119

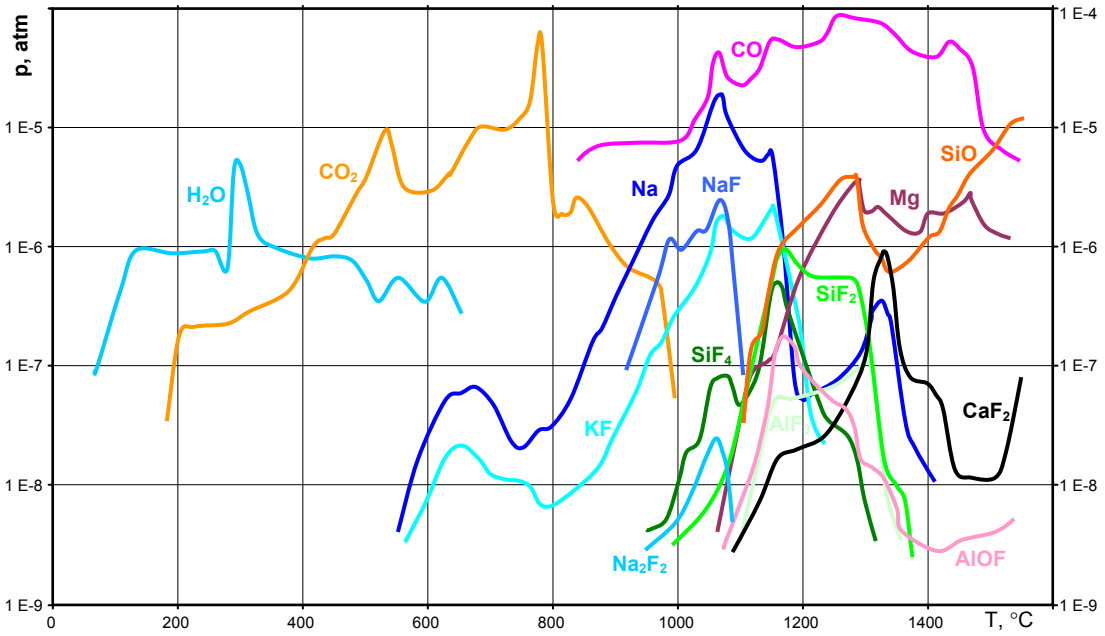

f. SAG 200

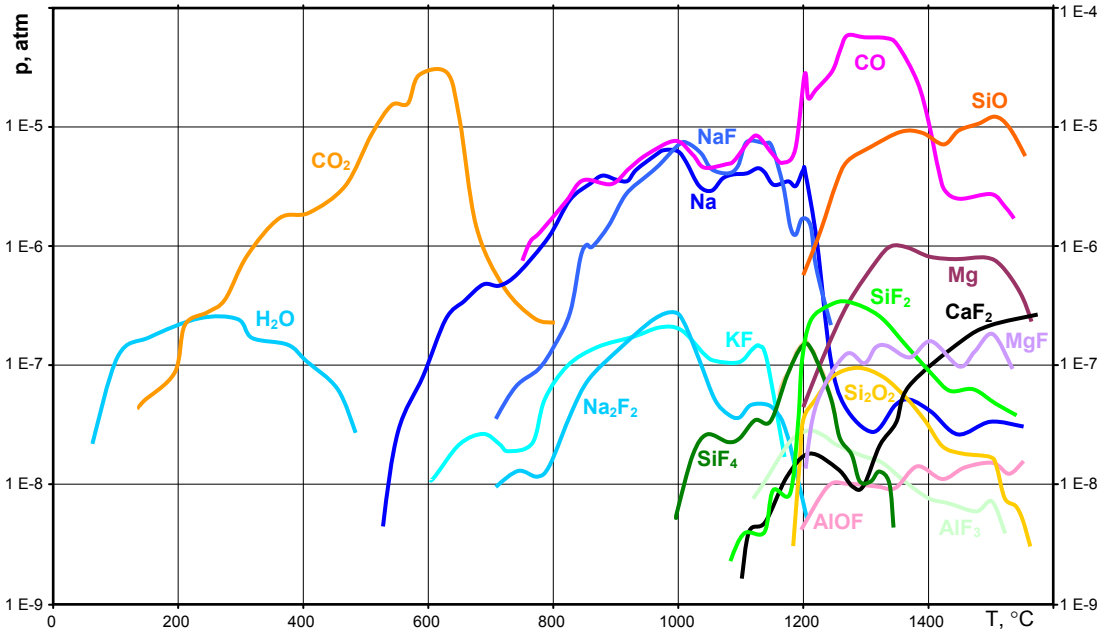

APPENDIX 4

g. SAG 201

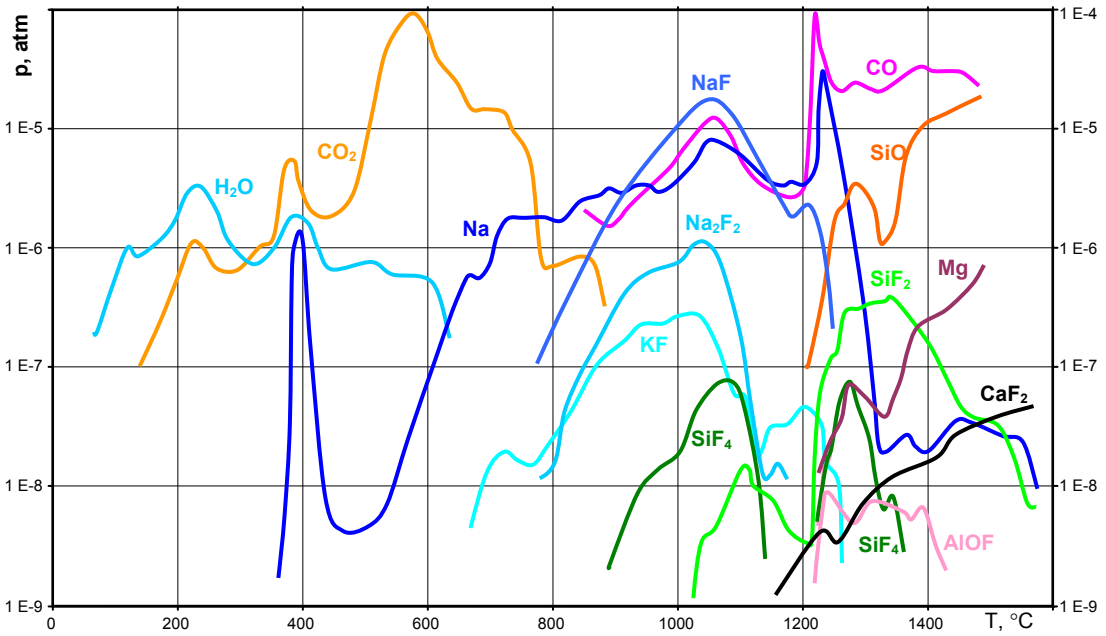

h. SAG 202

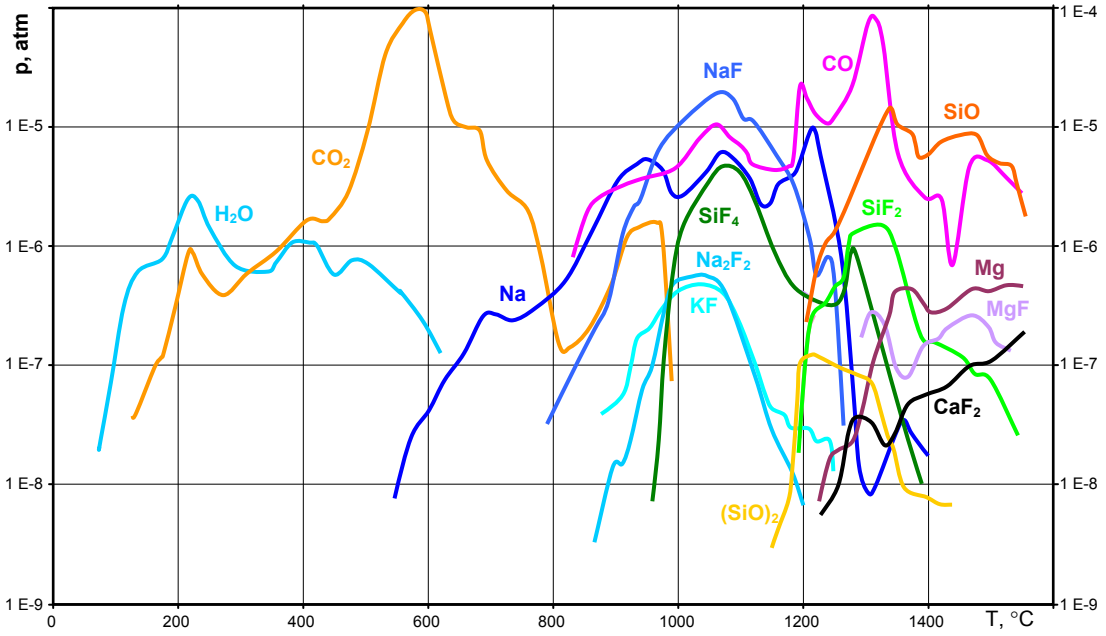

APPENDIX 5

a. Vaporisation of CX fluorine-free mixtures

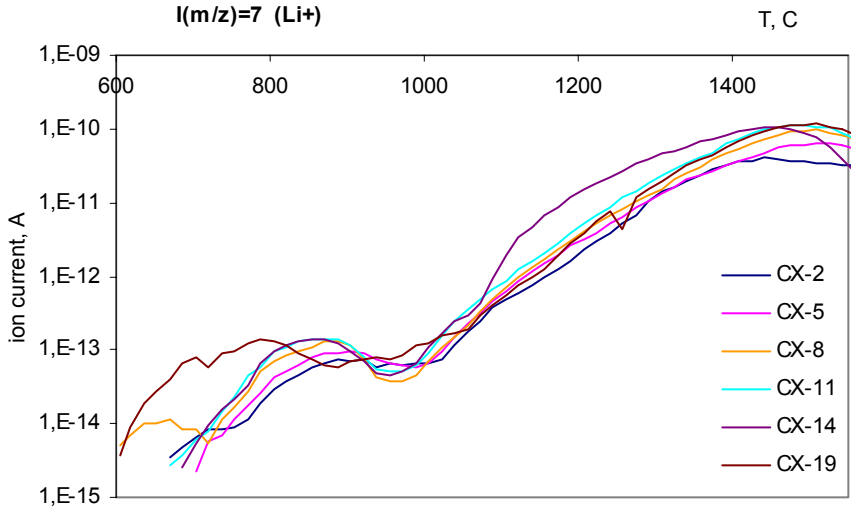

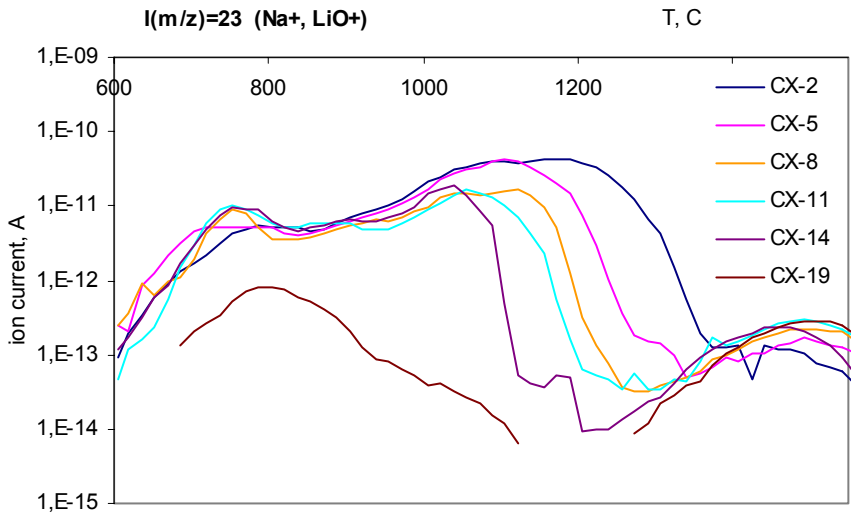

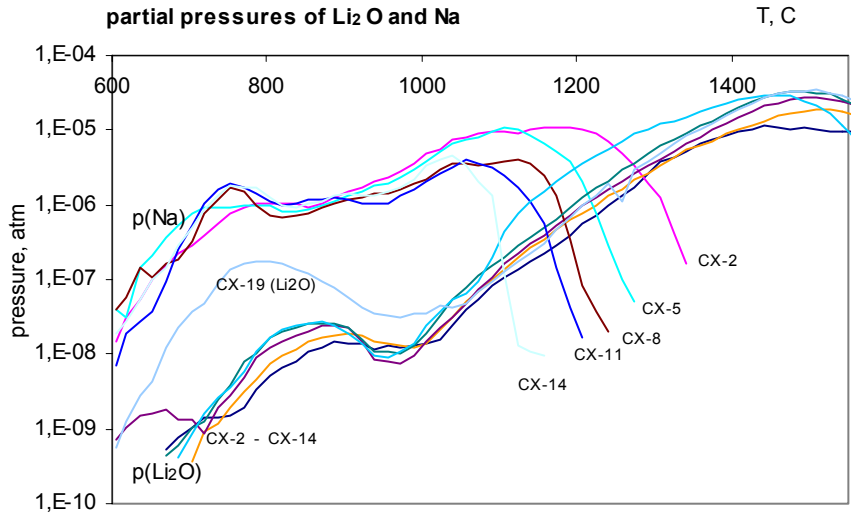

APPENDIX 5

b. Vaporisation of VLS fluorine-free mixtures

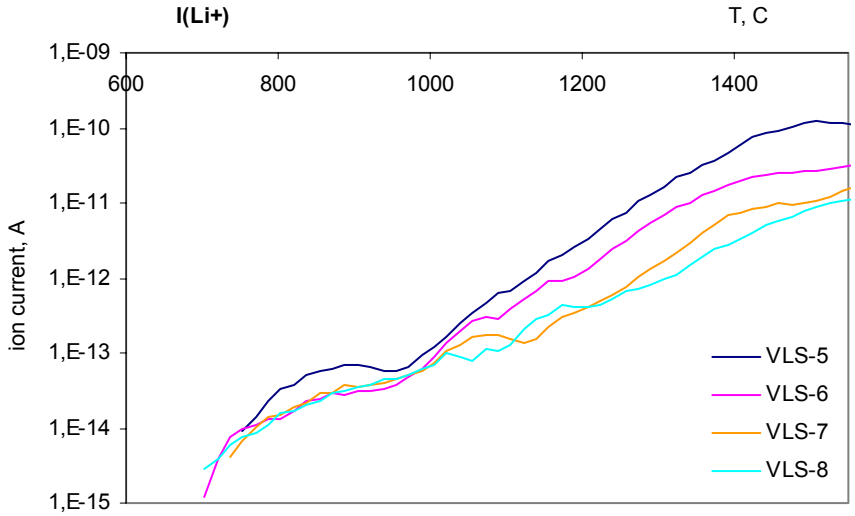

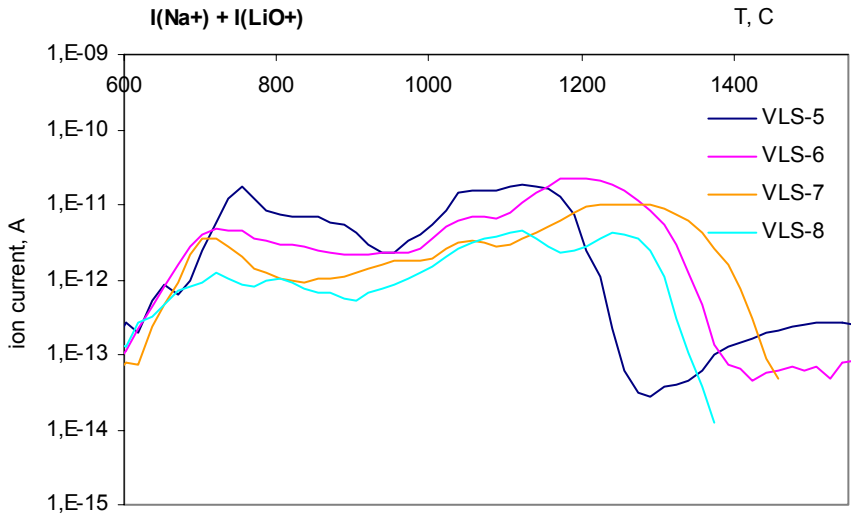

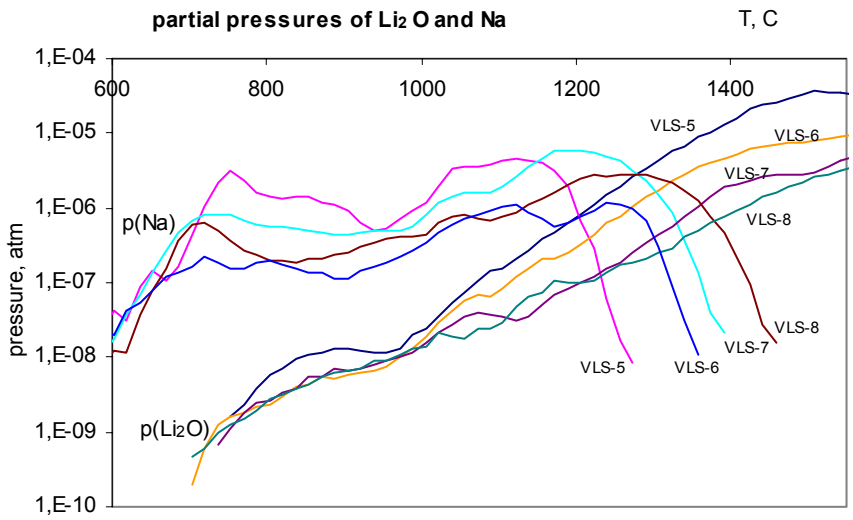

APPENDIX 6

Mass spectrum of decarburised mould powder SAG 202; heating rate 100°C/hour

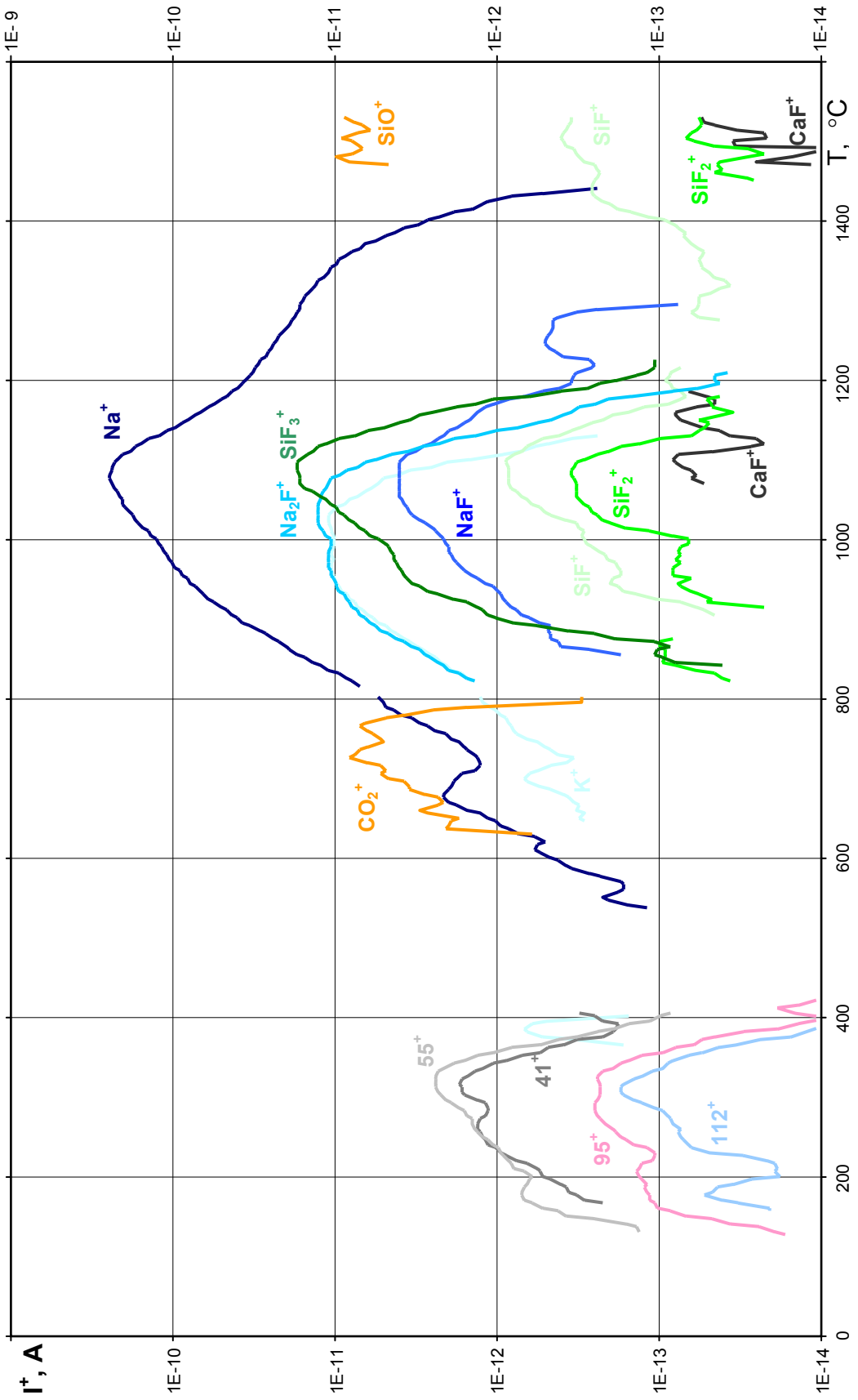

HELSINKI UNIVERSITY OF TECHNOLOGY PUBLICATIONS IN MATERIALS SCIENCE AND METALLURGY

TKK-MK-149 Forsen, M., Holappa, L.,
Mahdollisuudet alentaa CO2-päästöjä terästeollisuudessa. 2003.

TKK-MK-150 Wang, S., Holappa,L.,
Evaluation and prospects for novel casting technologies. 2003.

TKK-MK-151 Raipala, K.,
On Hearth Phenomena and Hot Metal Carbon Content in Blast Furnace. 2003.

TKK-MK-152 Kekkonen, M. (ed.),
Seminar Course on Advanced Metallurgical Processes / 2003. Mak-37.145. 2003.

TKK-MK-153 Erola, H., Nurmi, S., Holappa, L.,
Radiosteel. 2004.

TKK-MK-154 Anttonen, K., Kaskiala, T.,
Liuosfaasien matemaattisia malleja. 2004.

TKK-MK-155 Aromaa, J. (ed.),
4th Kurt Schwabe Corrosion Symposium. Mechanisms of Corrosion and Corrosion Prevention. 2004

TKK-MK-156 Seppänen, E.,
Kallionäytekairaus. 2004.

TKK-MK-157 Oghbasilasie, H., Jalkanen, H., Holappa, L.,
Study on Radust and Other Processes for Dust Treatment. 2004.

TKK-MK-158 Jormalainen, T., Louhenkilpi, S.,
Lämmönsiirron ja virtauksen mallintaminen senkassa ja välialtaassa valun aikana – osa 4
Loppuraraportti. 2004.

TKK-MK-159 Kekkonen, M. (ed.),
Seminar Course on Advanced Metallurgical Processes / 2004 Mak-37.145. 2004.

TKK-MK-160 Korpiola, K.,
High Temperature Oxidation of Metal, Alloy and Cermet Powders in HVOF Spraying Process. 2004.

TKK-MK-161 Miettinen, J.,
Simulation of Solidification and Calculation of Thermophysical Properties for Binary Copper Alloys. 2004.

TKK-MK-162 Miettinen, J.,
CAS2 – Solidification Analysis Package for Binary Copper Alloys, User Manual of Dos Version 2.0.0. 2004.

ISBN 951-22-7311-X
ISBN 951-22-7327-6 (electronic)
ISSN 1455-2329